UNIVERSITY OF BERGAMO
Faculty of Engineering
Department of Industrial Engineering

PH.D. THESIS
IN
ENERGY AND ENVIRONMENTAL TECHNOLOGIES
Cycle XXIII

Year 2011

Cogeneration of cooling energy and fresh water

Author: Alberto Picinardi

Supervisor: Prof. Antonio Perdichizzi

Co-Examiner: Prof. Giuseppe Franchini

Bergamo, Dipartimento di Ingegneria Industriale - Università di Bergamo, 2011

Acknowledgements

I would like to thank Prof. Antonio Perdichizzi, Prof. Giuseppe Franchini and Prof. Gianpietro Cossali for their support in my activity, Vittorio, Daniele, Alessandro and Paolo for their relevant contribution during this study, David Bradley for his help with TRNSYS problem, Davide, Giorgio and Francesco for their availability.

Furthermore, I would like to thank my parents, my friends, and all the people I met during three last years.

Contents

List of Figures

List of Tables

Introduction

"Thousands of years ago, prosperous conditions in fertile river locations throughout the world motivated nomadic people to form sedentary, agrarian communities. The inhabitants of these areas built cities, earned to fabricate pottery and to use metals, invented writing systems, domesticated animals and created complex social structures. In short, civilization was born when hunters and gatherers became settlers and farmers.

Except for energy: today's civilization is still based on gathering different forms of fossil energy, just like our ancestors, that collected berries and hunted animals until resources were depleted and they had to move elsewhere. Today, fossil energy resources are still sought and gathered until the last drop is spent. It becomes more and more evident that this is not a civilized behaviour, and certainly not a sustainable one, because there is no other planet in view to move to after resources are depleted and the atmosphere is spoiled.

However, our hunting and gathering ancestors found a solution to that dilemma: they became farmers, sowing seeds in springtime and harvesting corn and fruits in autumn, making use of technical know-how and the abundance of solar energy for their survival. That's exactly what is overdue in the energy sector: we must become farmers for energy, sow wind farms, wave and hydropower stations, biomass- and geothermal co-generation plants, photovoltaic arrays, solar collectors and concentrating solar power plants and harvest energy for our demand.

The same is true for freshwater: if the freely collectable natural resources become too scarce because the number of people becomes too large, we have to sow rainwater-reservoirs, wastewater reuse systems and solar powered desalination plants, and harvest freshwater from them for our daily consumption. Maybe as a side-effect of this more "civilized" form of producing energy and water, we will also – like our ancestors – find another, more developed social structure, maybe a more cooperative and peaceful one."

This is what Franz Trieb wrote in the introduction of the AQUA-CSP final report of November 2007 [1]. He has fully grasped one of the key points of the future energy strategy: "growing energy" by renewable sources, in contrast to the current exploitation of natural resources.

Considering the amount of solar energy incident on earth surface in one year, we could evaluate a mean power of 117.000TW (230W/m^2), while the primary energy used by human beings in the XXI century correspond to a mean annual power of 12TW (Figure 1). Comparing the conventional energy resources with the solar radiation, we can understand how big is the potential of solar

energy. The main problems related to the solar energy harvesting are two: this energy source is really widespread, so it's necessary a large surface to intercept a huge amount of energy. Moreover it's not feasible everywhere: the map in Figure 2 shows the amount of solar radiation on different areas . The dark red shows the areas with the most solar radiation (express in kWh/m^2 each day) and the light color shows the areas with the least solar radiation. The most favorable areas for the solar energy utilization are the tropical regions, in particular, Latin America, Africa, South Asia and Australia.

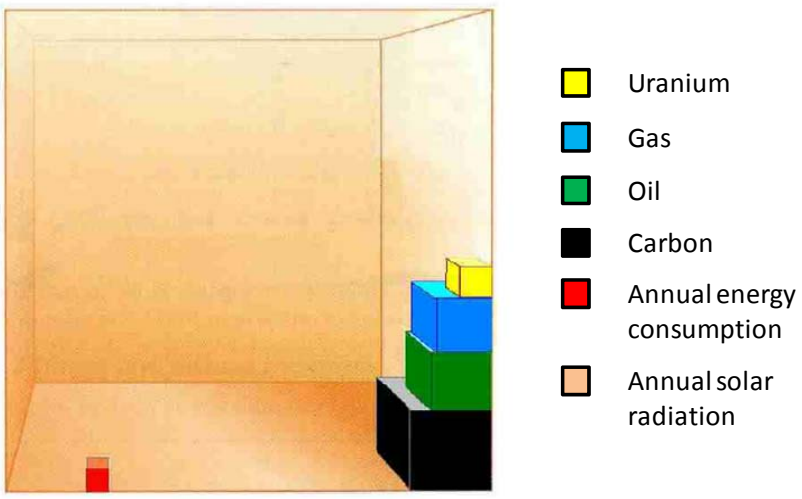

Figure 0-1: Comparision among conventional energy stocks, annual energy consumption and annual solar radiation

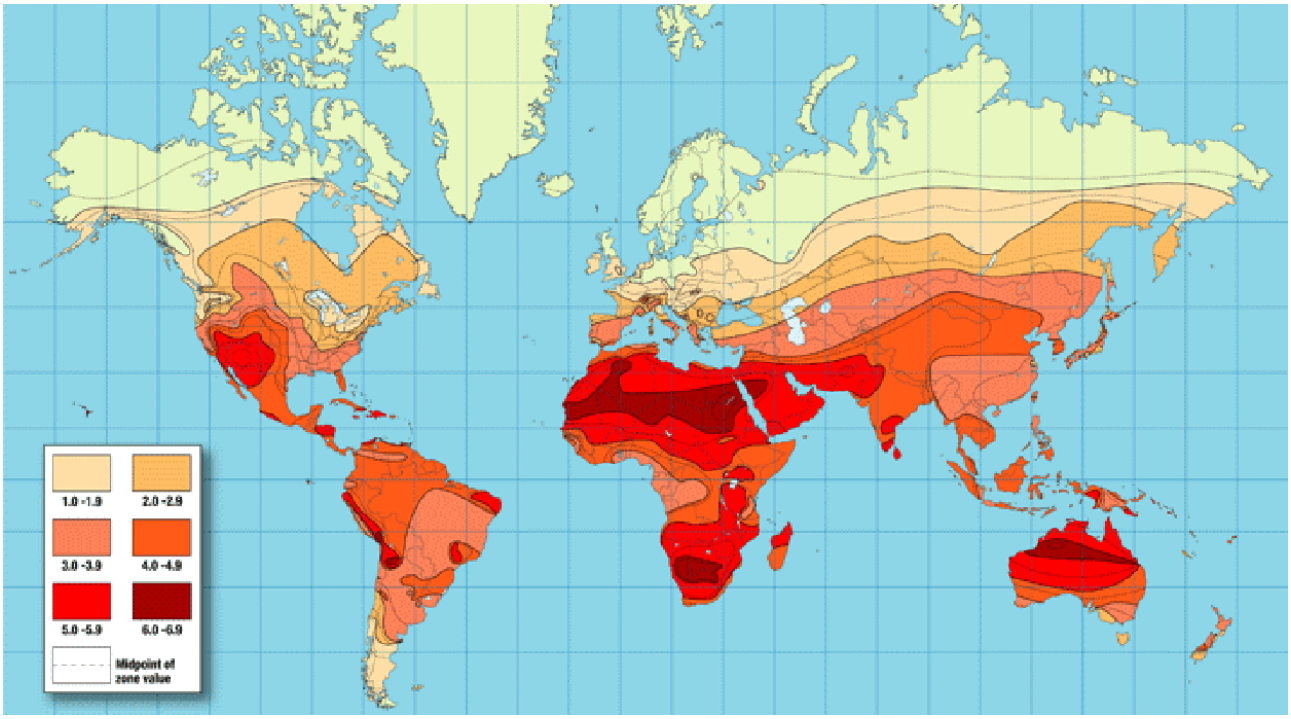

Figure 0-2: Map of world solar radiation (kWh/m^2 each day)

One of the most promising technologies with a great potential diffusion for these countries is Solar Cooling. This technology allows a reduction of electricity consumption for building air conditioning, as cooling demand matches quite well solar energy availability. Solar cooling systems are based on absorption chillers driven by low temperature heat provided by solar collectors. Many design parameters influence effectiveness of these systems and their economic performance, so many investigations have been carried out in the last years to optimize solar cooling systems. The aim is to get optimal configurations, giving high performance levels with viable costs, compared to conventional solutions.

A drawback of this technology, which still limits its deployment, is given by the need of large heat rejection devices like air coolers or cooling towers: single-stage machines with a *COP* of about 0.7 must reject about 2.5 kW_{th} for each kW of cooling output. To overcome this weakness one can re-use heat rejected by the absorption chiller to drive another system: for example a low temperature desalinator, creating a cogeneration of cooling energy and freshwater. This solution seems very attractive for applications in coastal areas of countries with high solar irradiation. Freshwater from desalination is an additional precious under-product of solar cooling. This application looks also promising for all the islands with scarcity of drinking water sources and need of refrigeration.

Among the possible desalination processes, the HD (Humidification/Dehumidification) process has been selected for this study, as it is the most suitable to use low grade heat. It is based on the fact that air can absorb a large amount of water that then is condensed in a heat exchanger, preheating inlet salt water.

The present Ph.D. Thesis shows the performance that can be obtained by this new cogeneration system producing cooling energy and freshwater, by using solar energy as a unique source. After the development of a simulation model of the whole system, including solar collectors, storage tank, absorption chiller and HD desalinator, the performances of the system have been analysed and an integrated design has been carried out.

Chapter 1: Desalination techniques - state of the art

Many countries in the world suffer from a shortage of natural fresh water. Increasing amounts of fresh water will be required in the future as a result of the rise in population rates and enhanced living standards, together with the expansion of industrial and agricultural activities. Available fresh-water resources from rivers and groundwater are presently limited and are being increasingly depleted at an alarming rate in many places. The oceans represent the earth's major water reservoir. About 97% of the earth's water is seawater while another 2% is locked in icecaps and glaciers. Available fresh water accounts for less than 0.5% of the earth's total water supply. Vast reserves of fresh water underlie the earth's surface, but much of it is too deep to access in an economically efficient manner. Additionally, seawater is unsuitable for human consumption and for industrial and agricultural uses. By removing salt from the virtually unlimited supply of seawater, desalination has emerged as an important source of fresh water.

The IDA Desalting Inventory 2004 Report [1] shows that at the end of 2002, installed and contracted brackish and seawater desalination plants worldwide were 17,348 units in 10,350 desalination plants with a total capacity of 37.75 million m^3/day of fresh water. The five world leading countries by desalination capacity are Saudi Arabia (17.4%), USA (16.2%), the United Arab Emirates (14.7%), Spain (6.4%), and Kuwait (5.8%).

The general layout of a desalination plant is presented in Figure 1-1: the plant separates saline seawater into two streams, a fresh water stream containing a low concentration of dissolved salts and a concentrated brine stream.

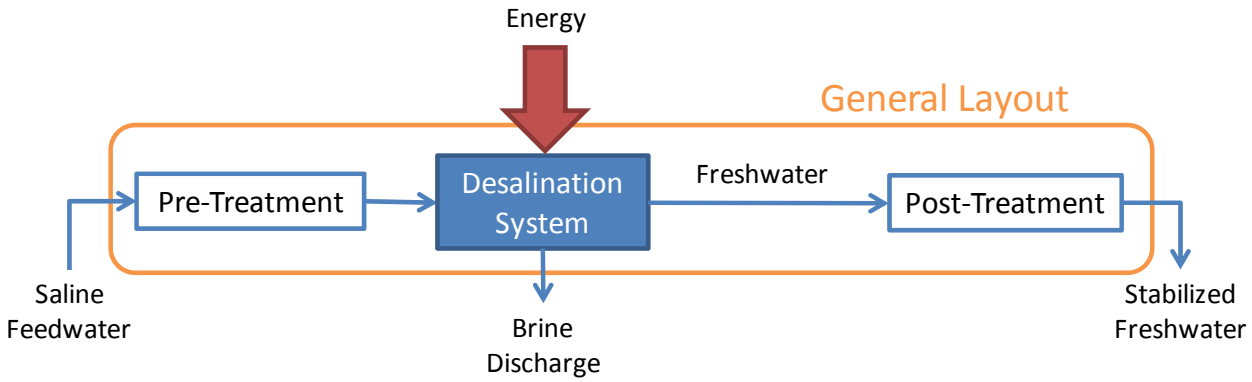

Figure 1-1: General layout of a desalination plant

This process requires some form of energy to desalinate, and utilizes several different technologies for separation. A variety of desalination technologies has been developed over the years on the basis of thermal distillation, membrane separation, freezing, electrodialysis, etc. [2–8]. Some of them are fully developed and applied on a large scale, while others are still used in small units for demonstration purposes or for research and development. Table 1-1 gives a selection of the most commonly applied technologies.

Separation	Energy Use	Process	Desalination Method
Water From Salts	Thermal	Evaporation	Multi-Stage Flash (MSF)
			Multiple-Effect Distillation (MED)
			Thermal Vapour Compression (TVC)
			Solar Distillation (SD)
			Humidification and dehumidification (HD)
			Natural Vacuum Desalination (NVD)
		FIltration / Evaporation	Membrane Distillation (MD)
		Crystallisation	Freezing (FR)
			Gas Hydrate Processes (GH)
	Mechanical	Evaporation	Mechanical Vapour Compression (MVC)
		Filtration	Reverse Osmosis (RO)
Salts From Water	Electrical	Selective Filtration	Electrodialysis (ED)
	Chemical	Exchange	Ion Exchange (IE)

Table 1-1: Overview of desalination methods

Commercially, the two most important technologies are based on the MSF and RO processes. At the end of 2002, MSF and RO accounted for 36.5% and 47.2%, respectively, of the installed brackish and seawater desalination capacity. For seawater desalination MSF accounted for 61.6% whereas RO accounted for 26.7%. The current world desalination plant capacity is 40 million m^3/day and the annual average growth rate for the last 5 years is 12% [9].

This chapter reviews the state-of-the-art of seawater desalination technologies. This review has been made with special emphasis on those process which make a good use of low grade thermal energy, like MED process, Solar Distillation, HD desalination, Natural Vacuum desalination and Membrane distillation.

1.1 Multi Stage Flash Distillation

MSF is a thermal distillation process that involves evaporation and condensation of water. The evaporation and condensation steps are coupled to each other in several stages so that the latent heat of evaporation is recovered for reuse by preheating incoming water (Figure 1-2).

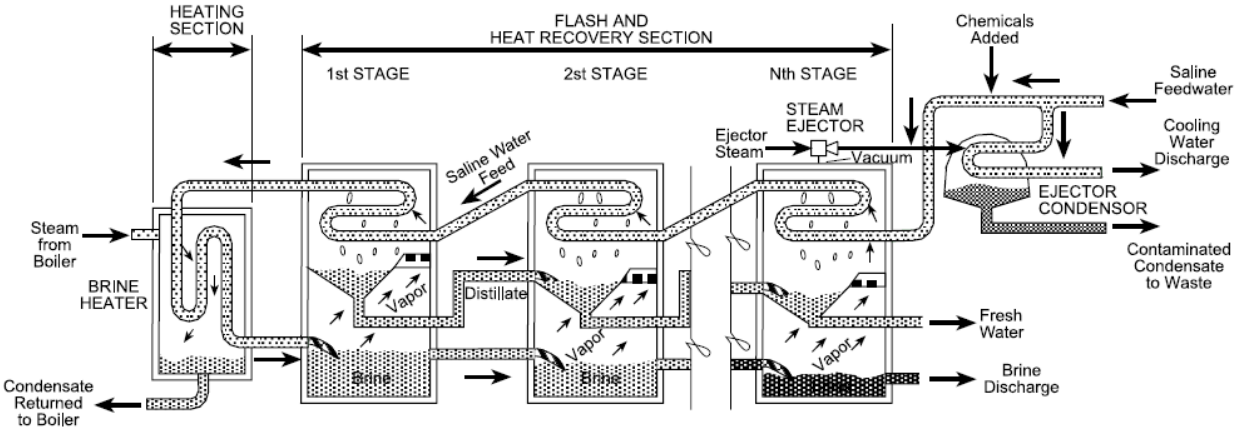

Figure 1-2: Layout of a MSF Distillation Unit

Seawater heating is accomplished in the brine heater by low pressure steam externally supplied by a cogeneration power plant such as a gas turbine with a heat recovery steam generator [10,11] or an extraction steam from a steam turbine power plant [11,12]. The hot seawater then flows into the first evaporation stage where the pressure is set lower. The sudden introduction of hot water into the chamber with lower pressure causes it to boil very quickly, almost exploding or "flashing" into steam. Only a small percentage of the water is converted to vapour, depending on the pressure maintained in this stage, since boiling will continue only until the water cools down to the equilibrium at the boiling point, furnishing the heat of vaporization.

The vapour generated by flashing is condensed on tubes of heat exchangers that run through the upper part of each stage. The tubes are cooled by the incoming feed water going to the brine heater, thus pre-heating that water and recovering part of the thermal energy used for evaporation in the first stage. This process is repeated in up to 40 stages, whereas mostly around 20 stages are employed [13–18].

To maximize water and energy recovery, each stage of an MSF unit operates at a successively lower pressure. The vacuum can be maintained by a steam ejector driven by high-pressure steam or by a mechanical vacuum pump. The MSF plants usually operate at top brine temperatures of 90–120°C, depending on the scale control method selected [19–31]. Operating the plant at higher temperature limits of 120°C tends to increase the efficiency, but it also increases the potential for scale formation [19,20] and accelerated corrosion of metal surfaces in contact with seawater.

MSF plants have been built since the 1950s [3]. In 1953 the US Navy constructed a 189 m^3/day MSF plant consisting of 5 stages. In 1957 four units of 2271 m^3/day capacity each were installed in Kuwait [4]. The Saline Water Conversion Corporation's Al-Jubail plant in Saudi Arabia is the world's largest plant with a capacity of 815,120 m^3/day [14]. The largest MSF unit with a capacity of 75,700 m^3/day is the Shuweiat plant, located in the United Arab Emirates [32].

1.2 Multiple Effect Distillation

The MED process takes place in a series of evaporators called effects, and uses the principle of reducing the ambient pressure in the various effects (Figure 1-3). This process permits the seawater feed to undergo multiple boiling without supplying additional heat after the first effect. The seawater enters the first effect and is raised to the boiling point after being preheated in tubes. The seawater is sprayed onto the surface of evaporator tubes to promote rapid evaporation. The tubes are heated by externally supplied steam from a normally dual purpose power plant. The steam is condensed on the opposite side of the tubes, and the steam condensate is recycled to the power plant for its boiler feedwater.

The MED plant's steam economy is proportional to the number of effects. The total number of effects is limited by the total temperature range available and the minimum allowable temperature difference between one effect and the next effect. Only a portion of the seawater applied to the tubes in the first effect is evaporated. The remaining feed water is fed to the second effect, where it is again applied to a tube bundle. These tubes are in turn heated by the vapors created in the first effect. This vapor is condensed to fresh water product, while giving up heat to evaporate a portion of the remaining seawater feed in the next effect. The process of evaporation and condensation is repeated from effect to effect each at a successively lower pressure and temperature.

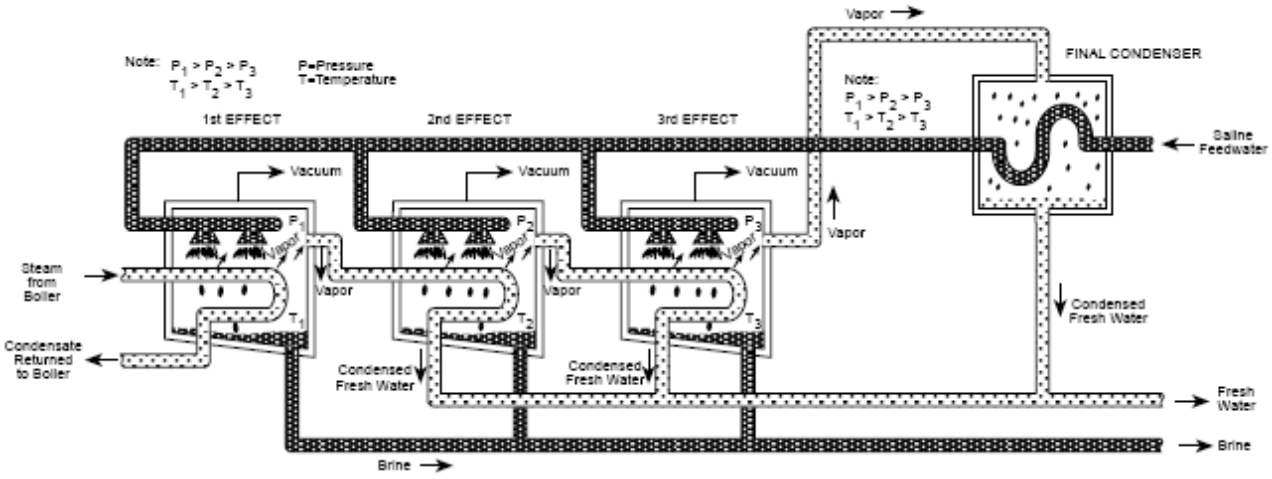

Figure 1-3: Layout of a MED Unit

This continues for several effects, with 4 to 21 effects and performance ratio from 10 to 18 being found in a typical large plant [33]. Some plants have been built to operate with a top brine temperature (TBT) in the first effect of about 70°C, which reduces the potential for scaling of seawater [34], but increases the need for additional heat transfer area in the form of tubes. The power consumption of an MED plant is significantly lower than that of an MSF plant, and the performance ratio of the MED plant is higher than that of the MSF plant. Therefore, MED is more efficient than MSF from a thermodynamic and heat transfer point of view [35].

Horizontal MED plants have been operating successfully for almost three decades [35]. MED plants can have horizontal, vertical, or submerged tubes. The size of low temperature MED units has increased gradually. Two MED units in Sharjah, UAE have a capacity of 22,700 m^3/day each [36]. A design and demonstration module for the MED process exists for a 45,400 m^3/day unit [36]. Most of the recent applications for the large MED plants have been in the Middle East. Although the number of MED plants is still relatively small compared to MSF plants, their numbers have been increasing.

1.3 Vapour Compression Desalination

In the VCD process [5,37], the heat for evaporating the seawater comes from the compression of vapor (Figure 1-4). The VCD plants take advantage of the principle of reducing the boiling point temperature by reducing the pressure. Two methods are used to condense water vapor to produce sufficient heat to evaporate incoming seawater: a mechanical compressor and a steam jet. The mechanical compressor is usually electrically driven. VCD units have been built in a variety of configurations to promote the exchange of heat to evaporate the seawater. The compressor creates a vacuum in the evaporator and then compresses the vapor taken from the evaporator and condenses it inside of a tube bundle. Seawater is sprayed on the outside of the heated tube bundle where it boils and partially evaporates, producing more vapor.

With the steam-jet type of VCD unit, called a thermocompressor, a venturi orifice at the steam jet creates and extracts water vapor from the evaporator, creating a lower ambient pressure. The extracted water vapor is compressed by the steam jet. This mixture is condensed on the tube walls to provide the thermal energy, heat of condensation, to evaporate the seawater being applied on the other side of the tube walls in the evaporator.

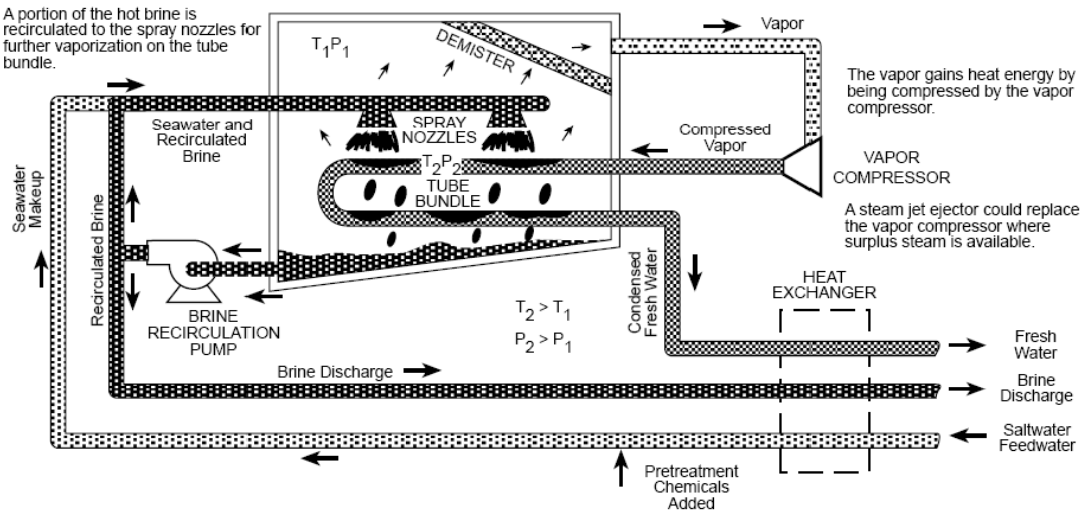

Figure 1-4: Layout of a VCD Unit

The low temperature VCD distillation is a quite simple, reliable, and efficient process requiring power only. Having a high capacity compressor allows operation at low temperatures below 70°C, which reduces the potential for scale formation and corrosion. The VCD process is generally used for small-scale desalination units. They are usually built up to the range of 3000 m^3/day. The larger unit's power consumption is about 8 kWh/m^3 of product water. VCD units are often used for resorts, industries, and drilling sites where fresh water is not readily available [37].

1.4 Humidification and Dehumidification

The HD process is based on the fact that air can be mixed with important quantities of vapor. The amount of vapor able to be carried by air increases with the temperature; in fact, 1 kg of dry air can carry 0.5 kg of vapor and about 670 kcal when its temperature increases from 30°C to 80°C [38]. When an airflow is in contact with salt water, air extracts a certain quantity of vapor at the expense of sensitive heat of salt water, provoking cooling. On the other hand, the distilled water is recovered by maintaining humid air at contact with the cooling surface, causing the condensation of a part of vapor mixed with air. Generally the condensation occurs in another exchanger in which salt water is preheated by latent heat recovery. An external heat contribution is thus necessary to compensate for the sensitive heat loss. Energy consumption is represented by this heat and by the mechanical energy required for the pumps and the blowers.

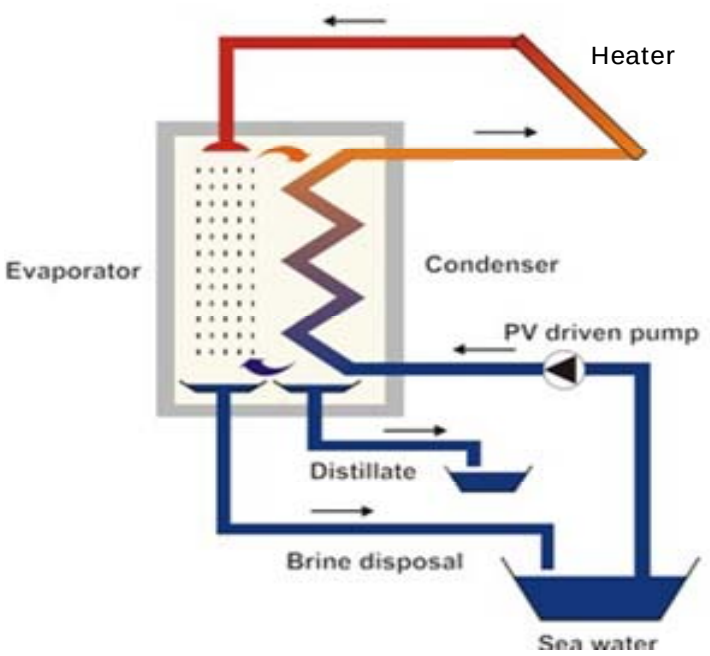

Figure 1-5: Sketch of the HD Unit

The basic cycle consists of a heat source, air humidifiers and dehumidifiers (Figure 1-5). The brine is passed through a heater where its temperature rises, then through packed towers where water vapor and heat are given up to the counter-current air stream, reducing the brine temperature.

One packed tower, or several in series, may be used as the humidifier depending on results to be achieved and design conditions. The fresh water stream, with its flow rate and temperature increased, leaves the humidifier and passes through a heat exchanger where it gives up its increase in enthalpy to the incoming brine stream. The dehumidifier consists of a series of packed towers, using fresh or salt water as the cooling phase. The air is cooled and dehumidified simultaneously since the humidity of saturated air decreases with temperature.

Water desalination by humidification and dehumidification has been the subject of many investigations. Different experimental data are available for using HD at the pilot or industrial scale. An inspection of these data allows establishing many perspectives for this process.

Most researchers [39-42] have performed the humidification–dehumidification desalination process in two separate columns, one for humidification and another for dehumidification, with the columns constructed in different structures with various materials. Al-Hallaj et al. [42] investigated a solar desalination unit functioning by humidification and dehumidification. In their unit the circulated air by natural or forced convection was heated and humidified by the hot water obtained either from a flat-plate solar collector or from an electrical heater. The latent heat of condensation was recovered in the condenser to preheat the saline feed water. Two units of different sizes were constructed from different materials. The productivity of these units was found to be much higher than those of the single-basin stills. Moreover, these units were able to product a large quantity of saline warm water for domestic uses other than drinking. The authors showed that no significant improvement in the performance of the desalination units was achieved using forced air circulation at high temperatures. While at lower temperatures, a larger effect was noticed. The authors related this behavior to the low mass transfer coefficients at low temperatures and to the non-linear increase in the water vapor pressure with temperature.

The authors highlighted a strong effect of water flow rate on unit production. In fact, the unit production first increases upon increasing the flow rate to an optimum value. Beyond that value the unit production decreases with increasing water flow rate. This is because increased water flow rate increases both heat and mass transfer coefficients as well as the solar collector efficiency. At the same time it lowers the operating water temperature in the unit and hence, lowers the evaporation and condensation efficiency. According to this investigation, it was shown that the mass of the unit is another factor that negatively affects the unit performance. A delay of 3 h was noticed between sunrise and the start of production of fresh water. It was noticed that most of the energy received in these early hours is used as sensible heat to warm up the large mass of the unit, which was about 300 kg. This lag time could be avoided by using a lighter material than galvanized steel for construction.

To reduce the capital cost of humidification installation, especially the solar collectors, other energy sources can be used. Bourouni et al. [43] developed a new HD process using geothermal energy. The unit consists of two horizontal-tube, falling-film exchangers (an evaporator and a condenser). Both exchangers are made of horizontal tube bundles made of polypropylene. In the evaporator the cooled hot water enters at a temperature of about 70°C and moves down in the tubes. The cooling air moves up in the space between the tubes. The salt liquid film is dripped

from a distributor in the top of the evaporator and falls from tube to tube. A fraction of water is evaporated and carried by the ascendant air flow, maintained by a blower. At the top of the exchanger the hot humid air is driven to the condenser where distilled water is recovered. Heat recovery in a low-temperature process requires an important exchange surface. For this reason, 2000 m of tubes are used in the evaporator and 3000 m in the condenser.

A new desalination process based on a combination of the principles of HD and mechanical vapor compression was developed by Vlachogiannis et al. [44]. This process combines the principles of intensive evaporation, vapor compression and heat pump. Air is injected in the evaporation chamber through a porous bottom wall and is dispersed as small diameter bubbles. The emerging saturated stream is compressed by a blower to a slightly higher pressure (Δp=0.05–0.25 bar) and is directed to the adjacent condensation chamber. Because of the increased pressure, water condensation occurs at a slightly higher temperature than evaporation, and the latent heat is transferred back to the evaporation chamber through the thermally conducting sidewall. The advantages of this process are low-cost construction, simple and flexible operation and suitability for modular design.

The principal variant consists in preheating air at the place of preheating salt water. Chafik [45] presented the development of a process using the solar energy to heat airflow up to a temperature between 50 and 80°C. The moderate solar heated air is humidified by injecting seawater into the air stream. Later on, the free of salt water is extracted from the humid air by cooling it. Using air as a heat carrier and keeping the maximum operating temperature in the process lower than 8O°C enables the use of cost effective polymers as construction material.

1.5 Natural Vacuum Distillation

Natural Vacuum Distillation is a thermal process that involves evaporation and condensation of water at a lower pressure than atmospheric one, by a 10,33m of water elevation which creates natural vacuum.

Midilli developed the first model with natural vacuum technique with free mass convection for wastewater distillation in 2001 [46, 47]. This model (Figure 1-6) has two columns which are the wastewater balance column (column A) and the distilled water balance column (column B).

Two different physical processes take place in the section between 3 and 5 of this model. These processes can be briefly expressed as evaporation between the points of 3 and 4, and condensation between the points of 4 and 5. By using the operation principle of this model of the NVD system with free mass convection, P-v and T-s diagrams were obtained as, respectively, shown in Figures 1-7(a) and 1-7(b).

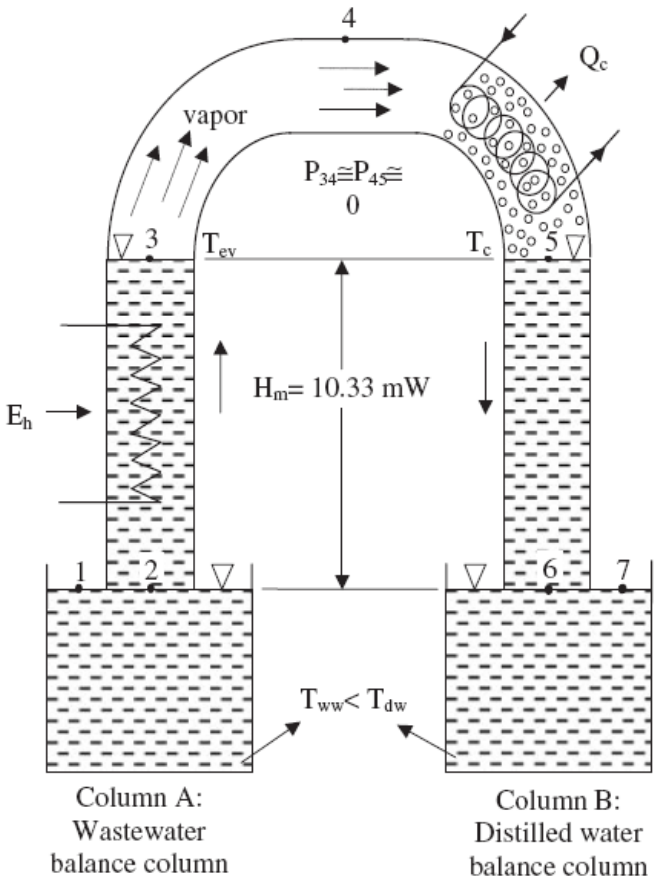

Figure 1-6: Theoretical model of NVD system with free mass convection

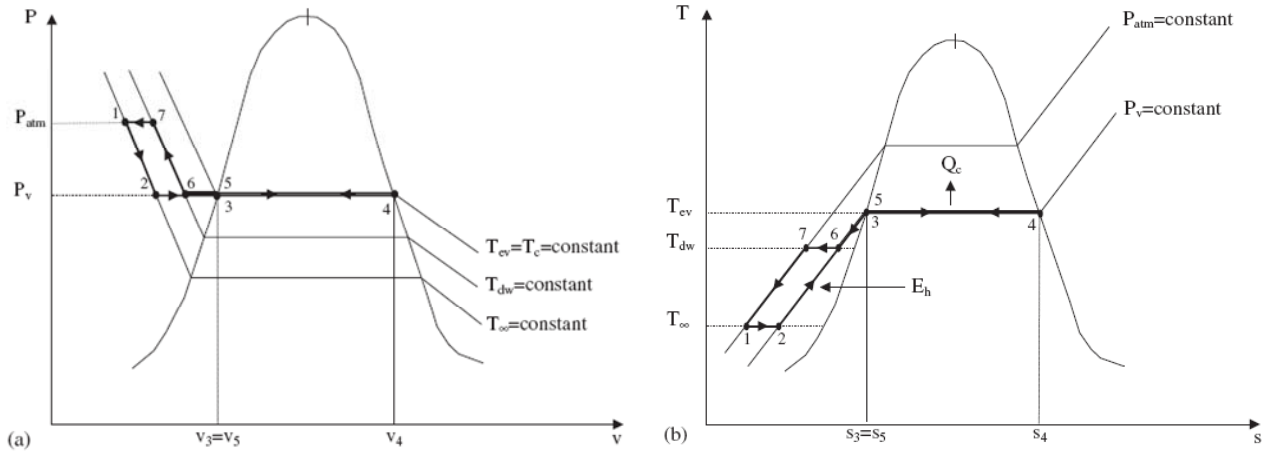

Figure 1-7: (a) P-v diagram of the NVD system with free mass convection. (b) T-s diagram of the NVD

The thermodynamic process flow including isothermal and isobaric processes of the NVD system with free mass convection can be explained as follows:

1-2: Pressure drop at constant temperature in column A.

2-3: Heating process at constant pressure in column A.

3-4: Evaporation at constant temperature and pressure in column A.

4-5: Condensation at constant temperature and pressure in column B.

5-6: Heat loss at constant pressure in column B.

6-7: Pressure increase at constant temperature in column B.

7-1: Heat loss at constant pressure in column B and return to the surrounding conditions.

Midilli modified his first model and developed a new model with natural vacuum technique with forced mass convection for wastewater distillation (Figure 1-8).

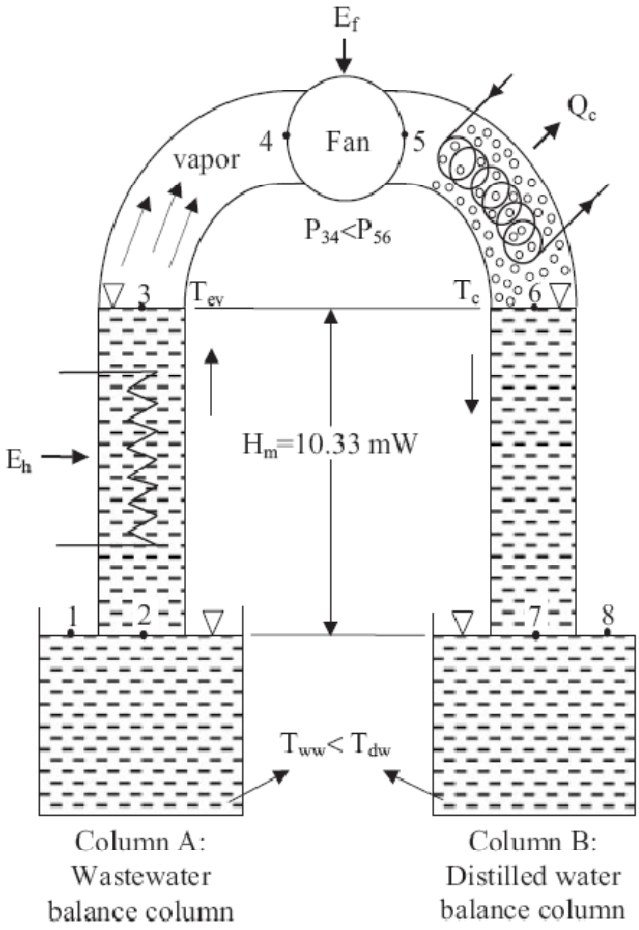

Figure 1-8: Theoretical model of the NVD system with forced mass convection

This model is similar to the first model from the point of construction. However, the operation principle of this model is different from the first one. Briefly, a radial circulation fan is placed between columns A and B to increase the amount of vapour transferred from columns A to B.

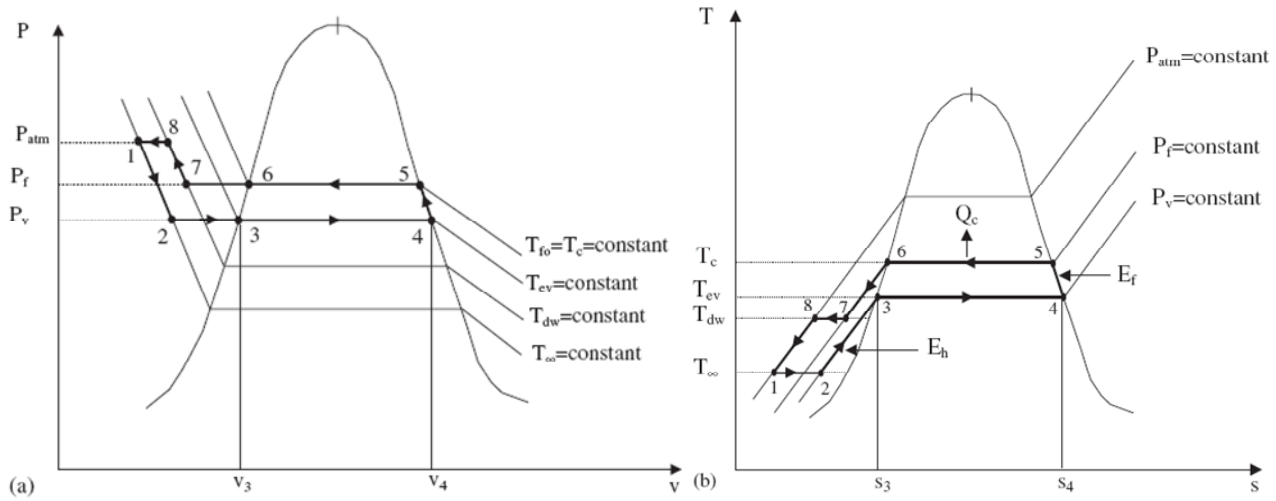

Figure 1-9: (a) P-v diagram of the NVD system with forced mass convection. (b) T-s diagram of the NVD

As shown in Figures 1-9(a) and 1-9(b), the thermodynamic process flow including isothermal and isobaric processes of the second model can be defined as:

1-2: Pressure drop at constant temperature in column A.

2-3: Heating at constant pressure in column A.

3-4: Evaporation at constant temperature and pressure in column A.

4-5: Compressing throughout the circulation fan.

5-6: Condensation at constant temperature and under pressure of the fan in column B.

6-7: Heat loss at constant pressure in column B.

7-8: Pressure increase at constant temperature in column B.

8-1: Heat loss at constant pressure in column B and return to surrounding conditions.

In literature we can find different application of this technique: a low-temperature desalination process developed at the New Mexico State University [48], and a feasibility study of a renewable energy powered seawater desalination technology using natural vacuum technique from University of Bahrain [49].

1.6 Solar Distillation

Owing to the diffuse nature of solar energy, the main problems with the use of solar thermal energy in large-scale desalination plants are the relatively low productivity rate, the low thermal efficiency and the considerable land area required. However, since solar desalination plants are characterized by free energy and insignificant operation cost, this technology is, on the other

hand, suitable for small-scale production, especially in remote arid areas and islands, where the supply of conventional energy is scarce.

Solar energy can directly or indirectly be harnessed for desalination. Collection systems that use solar energy to produce distillate directly in the solar collector are called direct collection systems whereas systems that combine solar energy collection systems with conventional desalination systems are called indirect systems. In indirect systems, solar energy is used either to generate the heat required for desalination and/or to generate electricity that is used to provide the required electric power for conventional desalination plants such as multi-effect (ME), multi-stage flash (MSF) , vapor compression (VC) or reverse osmosis (RO) systems. The method of direct solar desalination is mainly suited for small production systems, such as solar stills, in regions where the freshwater demand is less than 200 m^3/day [50]. This low production rate is explained by the low operating temperature and pressure of the steam.

1.6.1 Single-effect solar still

A solar still is a simple device which can be used to convert saline, brackish water into drinking water (Figure 1-10). Solar stills use exactly the same processes which in nature generate rainfall, namely evaporation and condensation. Its function is very simple; basically a transparent cover encloses a pan of saline water. The latter traps solar energy within the enclosure. This heats up the water causing evaporation and condensation on the inner face of the sloping transparent cover. This distilled water is generally potable; the quality of the distillate is very high because all the salts, inorganic and organic components and microbes are left behind in the bath. Under reasonable conditions of sunlight the temperature of the water will rise sufficiently to kill all pathogenic bacteria anyway. A film or layer of sludge is likely to develop in the bottom of the tank and this should be flushed out as often as necessary.

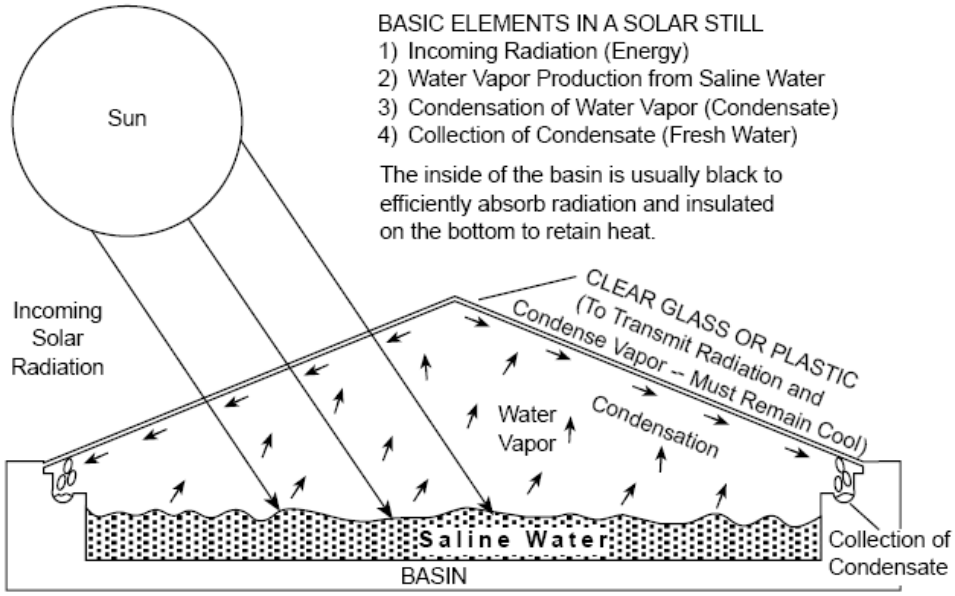

Figure 1-10: Layout of a simple solar still

In order to evaporate 1 kg of water at a temperature of 30°C about 2.4×10^6 J is required. Assuming an insolation of 250 W/m^2, averaged over 24 h, this energy could evaporate a maximum of 9 L/m^2/day. In practice heat losses will occur and the average daily yield which might be expected from a solar still is 4–5 L/m^2/day.

Today's state-of-the-art single-effect solar stills have an efficiency of about 30–40% [51]. Material selection for solar stills is very important. The cover can be either glass or plastic. Glass is considered to be best for most long-term applications, whereas a plastic (such as polyethylene) can be used for short-term use.

One of the main setbacks for this type of desalination plant is the low thermal efficiency and productivity. This could be improved by various passive and active methods. The solar still integrated with a heater or solar concentrator panel is generally referred to as an active solar distillation while others are referred to as passive stills. Passive solar distillation is an attractive process for saline water desalination in that the process can be self-operating, of simple construction and relatively maintenance free. These advantages of simple passive solar stills however, are offset by the low amounts of freshwater produced, approximately 2 L/m^2 for the simple basin type solar still [52] and for the need for regular flushing of accumulated salts [53]. Modifications using passive methods include basin stills, wick stills, diffusion stills, stills integrated with greenhouse, and other configurations.

1.6.2 Basin stills with passive improvements

The operating performance of a simple basin type passive still can be augmented by several techniques such as:

1) Single slope vs. double slope basin stills: Single slope still gave better performance than a double slope still under cold climatic conditions while the opposite is true under summer climatic conditions [53].

2) Still with cover cooling: Increasing the temperature difference between the basin (heat source) and the cover (heat sink) lead to increase the water evaporation rate [54]. In stills with cover cooling, cooling water or saline solution is fed in the gap of a double glass cover to maximize the temperature difference. The cost, as such, is increased.

3) Still with additional condenser: Fath [55] found that adding a passive condenser in the shaded region of a single slopped still increases the still efficiency by 45%.

4) Still with black dye: Injecting black dye in the seawater increases the distillate yield [55].

1.6.3 Wick stills

In a wick still, the feed water flows slowly through a porous, radiation-absorbing pad (the wick). Two advantages are claimed over basin stills. First, the wick can be tilted so that the feed water presents a better angle to the sun (reducing reflection and presenting a large effective area). Second, less feed water is in the still at any time and so the water is heated more quickly and to a higher temperature. Tanaka et al. [56] have proven the superiority of the tilted wick type solar still

and confirmed an increase in productivity by 20–50%. Simple wick stills are more efficient than basin stills and some designs are claimed to cost less than a basin still of the same output. A simple multiple wick solar still made of a frame of aluminum, a glass cover and a water reservoir made of galvanized iron was designed by Sodha et al. [57]. Foam insulation was supported beneath the aluminum bottom by a net of nylon ribbon. The authors claimed the present design to offer several advantages including lightweight and low cost of the still and a significant output.

1.6.4 Diffusion stills

Diffusion solar stills are comprised of two separate units. One is a hot storage tank, coupled to a solar collector, and the other is the distillation unit, which produces the distilled water. One of the most recent designs of this type of still is that described by Graeter et al. [58] and Rheinlander and Graeter [59] of a four-effect still.

1.6.5 Solar still greenhouse combination

The Seawater Greenhouse combines a solar desalination system with an environment for cultivating crops in which transpiration is minimized, at the same time producing sufficient water for its own use through a process of solar distillation.

A version of this system was constructed and analyzed by Chaibi [60], where the south slope of the greenhouse roof was built as a solar still. During the day, saline water was pumped from a reservoir to the rooftop of the greenhouse, from where it was distributed evenly to the evaporation surface in the still. The top cover of the still was a regular glass sheet, while the bottom of the solar still consisted of an only partly light transparent material, which absorbed a substantial amount of the solar irradiation, but transmitted the wavelengths that are favorable for the photosynthesis of vegetation (the photosynthetic active radiation, PAR, has the wavelength interval 380–710 nm).

Since most of the heat radiation was absorbed in the still, the temperature of the greenhouse air was lowered, which lead to better climate for the crops and less ventilation requirement. In the end, this lead to a decrease in the water consumption of the crops. The formed water vapor condensed on the top glazing, ran along the inner wall of the top cover, and was collected in the freshwater store. The residue of the feed water was collected in a separate storage. The returned feed water was partly returned to the feed water duct for another loop in the still, and some of the residue saline water was also mixed with the freshwater before the irrigation to bulk out the supply. The desalination roof was operated during both day and night, as excess heat was stored in the saline water storage.

1.6.6 Multiple-effect basin stills

Multiple-effect basin stills have two or more compartments. The condensing surface of the lower compartment is the floor of the upper compartment. The heat given off by the condensing vapor provides energy to vaporize the feed water above. Multiple-effect solar desalination systems are more productive than single effect systems due to the reuse of latent heat of condensation. The increase in efficiency, though, must be balanced against the increase in capital and operating

costs. Efficiency is therefore greater than for a single basin still typically being 35% or more but the cost and complexity are correspondingly higher.

1.6.7 Externally heated (active) solar stills

The temperature of saline water in the basin can be increased through additional (external heating). For this purpose the still is integrated with a:

1) solar heater

2) solar concentrator

3) waste heat recovery system.

Circulation through the heater or the concentrator could either be through natural circulation (Thermosyphon) or through forced circulation using a pump.

1.6.8 Solar humidification-dehumidification distillation

One of the problems that negatively influences the still performance is the direct contact between the collector and the saline water, this may cause corrosion and scaling in the still and thereby reduce the thermal efficiency. In HD desalination air is used as a working fluid, which eliminates this problem. Al-Hallaj et al., Bourouni et al. and Chafik [42,43,45] respectively reported on the operation of HD units in Tunisia, Jordan, and Egypt.

1.7 Freezing

During the process of freezing, dissolved salts are excluded during the formation of ice crystals. Under controlled conditions seawater can be desalinated by freezing it to form the ice crystals. Before the entire mass of water has been frozen, the mixture is usually washed and rinsed to remove the salts in the remaining water or adhering to the ice. The ice is then melted to produce fresh water. Therefore, the freezing process is made up of cooling of the seawater feed, partial crystallization of ice, separation of ice from seawater, melting of ice, refrigeration, and heat rejection.

The advantages of freezing include a lower theoretical energy requirement, minimal potential corrosion, and little scaling or precipitation. The disadvantage of freezing involves handling ice and water mixtures which are mechanically complicated to move and process. A small number of plants have been built over the past 40 years, but the freezing process has not been commercialized successfully to produce fresh water for municipal purposes. The most recent significant example of a freezing desalination plant was an experimental solar-powered unit constructed in Saudi Arabia in 1985 [61].

1.8 Membrane Distillation

Membrane distillation (MD) is an emerging technology for desalination [62]. Membrane distillation differs from other membrane technologies in that the driving force for desalination is the difference in vapor pressure of water across the membrane, rather than total pressure. The membranes for MD are hydrophobic, which allows water vapor (but not liquid water) to pass. The vapor pressure gradient is created by heating the source water, thereby elevating its vapor pressure.

The geometry of the model is schematically shown in Figure 1-11 [63]. The hot saline solution (h) flows in direct contact with hydrophobic microporous membranes (m), and the cold solution (c) flows on the cold side of the membrane. The temperature difference between the hot and cold faces of the membrane causes the vapor pressure of the concentrated solution to be higher than that of the cold fluid; as a result, water starts to evaporate at the hot side of the membrane, penetrates through the membrane pores, and then is convected to and condensed on the cold fluid (c) or condensed in a film (f) on a cooling plate (p).

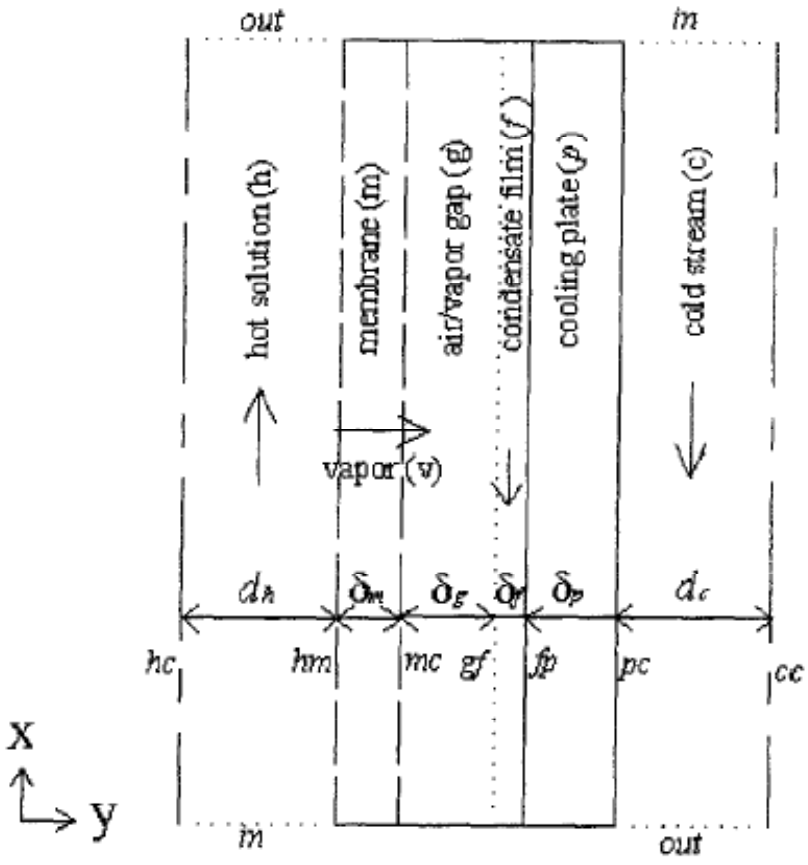

Figure 1-11: MD cell configurations; g, f and p included only in AGMD. h: hot solution, m: membrane, g: air gap, f: film condensate, p: cooling plate, c: cold solution for AGMD, cold pure water for DCMD, sweeping air for SGMD, and vacuum for VMD.13

MD systems can be classified into four configurations, according to the nature of the cold side of the membrane:

1) direct contact membrane distillation (DCMD), in which the membrane is in direct contact only with liquid phases, saline water on one side and fresh water on the other [64-66];

2) vacuum membrane distillation (VMD), in which the vapor phase is vacuumed from the liquid through the membrane, and condensed, if needed, in a separate device [67, 68];

3) air gap membrane distillation (AGMD), in which an air gap is interposed between the membrane and the condensation surface [69, 70];

4) sweeping gas membrane distillation (SGMD), in which a stripping gas is used as a carrier for the produced vapor, instead of vacuum as in VMD [71-75].

The advantages of membrane distillation are:

- It produces high-quality distillate.
- Water can be distilled at relatively low temperatures.
- Low-grade heat (solar, industrial waste heat, or desalination waste heat) may be used.
- The water does not require extensive pretreatment as in pressure-based membrane treatment.

1.9 Reverse Osmosis

In the reverse osmosis (RO) process, the osmotic pressure is overcome by applying external pressure higher than the osmotic pressure on the seawater. Thus, water flows in the reverse direction to the natural flow across the membrane, leaving the dissolved salts behind with an increase in salt concentration. No heating or phase separation change is necessary. The major energy required for desalting is for pressurizing the seawater feed. A typical large seawater RO plant [76-79] consists of four major components: feed water pre-treatment, high pressure pumping, membrane separation, and permeate post-treatment. Raw seawater flows into the intake structure through trash racks and traveling screens to remove debris in the seawater. The seawater is cleaned further in a multimedia gravity filter which removes suspended solids. Typical media are anthracite, silica and granite or only sand and anthracite. From the media it flows to the micron cartridge filter that removes particles larger than 10 microns.

Pretreatment is needed to eliminate the undesirable constituents in the seawater, which would otherwise cause membrane fouling [80-85]. A typical pretreatment includes chlorination, coagulation, acid addition, multi-media filtration, micron cartridge filtration, and dechlorination. The type of pretreatment to be used largely depends on the feed water characteristics, membrane type and configuration, recovery ratio, and product water quality.

High pressure stainless steel pumps raise the pretreated feedwater to a pressure appropriate to the RO membranes so that water can pass through them and the salts can be rejected. The membrane must be able to withstand the drop of the entire pressure across it. A relatively small amount of salts passes through the membrane and appear in the permeate. There are membranes available which are suitable for pump operation up to 84 kg/cm_2 discharge pressure. Centrifugal pumps are generally used for this application. This pressure ranges from 50 to 80 bar for seawater, depending on the salt content of the feed water. The post-treatment generally includes pH adjustment, addition of lime, removal of dissolved gases such as H_2S (if any) and CO_2, and disinfection.

In comparison to MSF, problems arising from corrosion of materials are significantly less due to the ambient temperature conditions. Therefore, the use of metal alloys is less and polymeric materials are utilized as much as possible. Various stainless steels are used quite extensively [86-88]. Two developments have helped to reduce the operating costs of RO plants during the past decade: the development of membranes that can operate efficiently with longer duration, and the use of energy recover devices [89-93]. The devices are connected to the concentrated stream as it leaves the pressure vessel. The concentrated brine loses only about 1–4 bar relative to the applied pressure from the high pressure pump. The devices are mechanical and generally consist of turbines or pumps of some type that can convert a pressure drop to rotating energy.

1.10 Electrodialysis

Electrodialysis (ED) is used to transport salt ions from one solution through ion-exchange membranes to another solution under the influence of an applied electric potential difference. This is done in a configuration called an electrodialysis cell. The cell consists of a feed compartment and a concentrate (brine) compartment formed by an anion exchange membrane and a cation exchange membrane placed between two electrodes. In almost all practical electrodialysis processes, multiple electrodialysis cells are arranged into a configuration called an electrodialysis stack, with alternating anion and cation exchange membranes forming the multiple electrodialysis cells. Electrodialysis processes are different compared to distillation techniques and other membrane based processes (such as reverse osmosis), because species are moved away from the feed stream rather than the reverse [94-98].

In an electrodialysis stack (Figure 1-12), the diluted (D) feed stream, brine or concentrate (C) stream, and electrode (E) stream are allowed to flow through the appropriate cell compartments formed by the ion exchange membranes. Under the influence of an electrical potential difference, the negatively charged ions in the diluted stream migrate toward the positively charged anode. These ions pass through the positively charged anion exchange membrane, but are prevented from further migration toward the anode by the negatively charged cation exchange membrane and therefore stay in the C stream, which becomes concentrated with the anions. The positively charged species in the D stream migrate toward the negatively charged cathode and pass through the negatively charged cation exchange membrane. These cations also stay in the C stream,

prevented from further migration toward the cathode by the positively charged anion exchange membrane. As a result of the anion and cation migration, electric current flows between the cathode and anode. Only an equal number of anion and cation charge equivalents are transferred from the D stream into the C stream and so the charge balance is maintained in each stream. The overall result of the electrodialysis process is an ion concentration increase in the concentrate stream with a depletion of ions in the diluate solution feed stream.

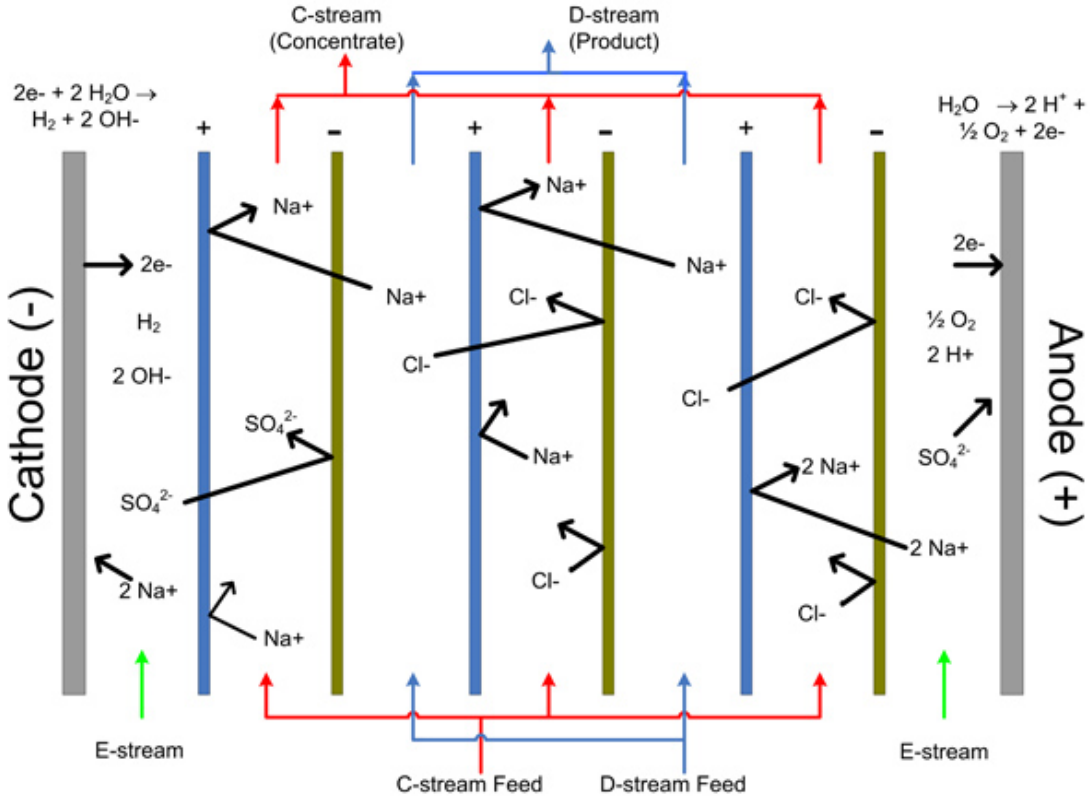

Figure 1-12: Electrodialysis stack

Electrodialysis has inherent limitations, working best at removing low molecular weight ionic components from a feed stream. Non-charged, higher molecular weight, and less mobile ionic species will not typically be significantly removed. Also, in contrast to RO, electrodialysis becomes less economical when extremely low salt concentrations in the product are required and with sparingly conductive feeds: current density becomes limited and current utilization efficiency typically decreases as the feed salt concentration becomes lower, and with fewer ions in solution to carry current, both ion transport and energy efficiency greatly declines. Consequently, comparatively large membrane areas are required to satisfy capacity requirements for low concentration (and sparingly conductive) feed solutions. As with RO, electrodialysis systems require feed pretreatment to remove species that precipitate onto, or otherwise "foul" the surface of the ion exchange membranes. This fouling decreases the efficiency of the electrodialysis system.

Chapter 2: HD desalinator - Design and performance evaluation

Among the different desalination technologies using a low grade thermal energy, the Humidification Dehumidification technique was chosen for these main reasons:

1) MED and NVD processes need a working pressure lower than atmospheric, while in HD distillation is possible to keep the atmospheric pressure, ensuring greater reliability and durability.

2) MD technique is really promising, but it's difficult to obtain membranes at reasonable prices with hydrophobic property, high porosity for the vapor phase, a high resistance to heat flow by conduction, a sufficient but not excessive thickness, and low moisture adsorptivity.

3) HD distillation produce desalinated water at higher rates than those usually obtained from solar stills under similar solar radiation [1].

4) HD distillation avoids the direct contact between the collector and the saline water, which may cause corrosion and scaling in the solar still.

The simulation of an HD unit has required the development of condenser and humidifier models, obtaining sufficient information on the process of heat and mass transfer in the unit. The process used in this study is a closed air cycle type, in which air is circulated in the unit by forced draft between the humidifier and condenser. A detailed description of the MATLAB code used to simulate the desalinator is given in [2].

2.1 Condenser

In order to use efficiently the latent heat of water condensation, the condenser area must be large, so a finned heat exchanger was chosen. The structure of the exchanger is shown in figure 2-1. A fin pitch of 5mm ($pitch_{fin}$), a fin thickness of 0,5mm ($thick_{fin}$), an external diameter of the tubes of 7mm (d_{ext}), an internal diameter of the tubes of 5mm (d_{int}), and a tubes pitch of 20mm ($pitch_z, pitch_y$) were chosen.

The flows inside the condenser are shown in figure 2-2. The condenser is crossed by sea water, with a temperature between 20 and 30°C, and by an hot humid air stream with a temperature between 35 and 45°C. The incoming feed water cools the hot humid air, while the hot air, releasing heat, loses the moisture that condenses on the surfaces of the exchanger.

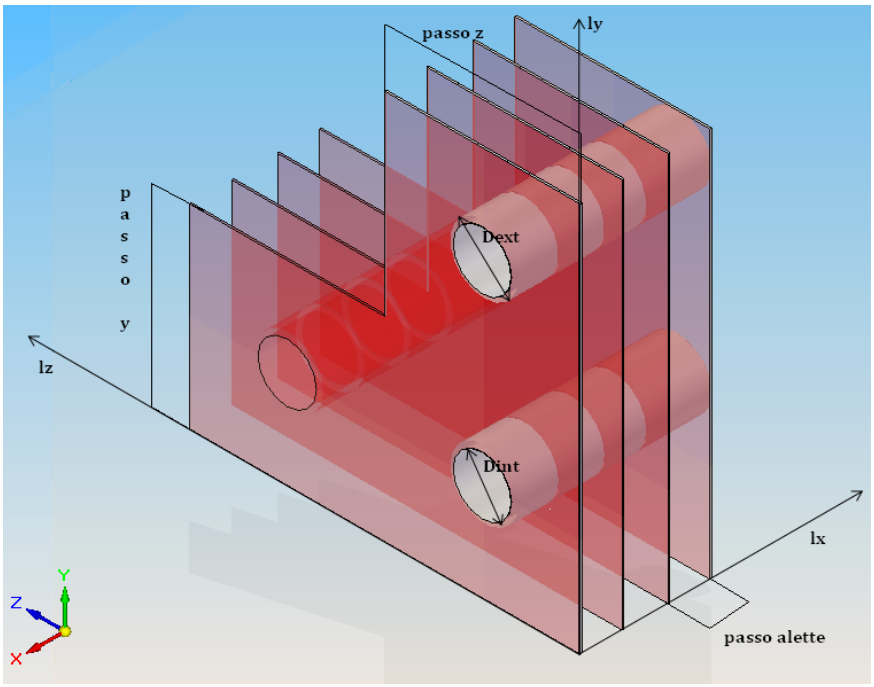

Figure 2-1: Scheme of the condenser portion

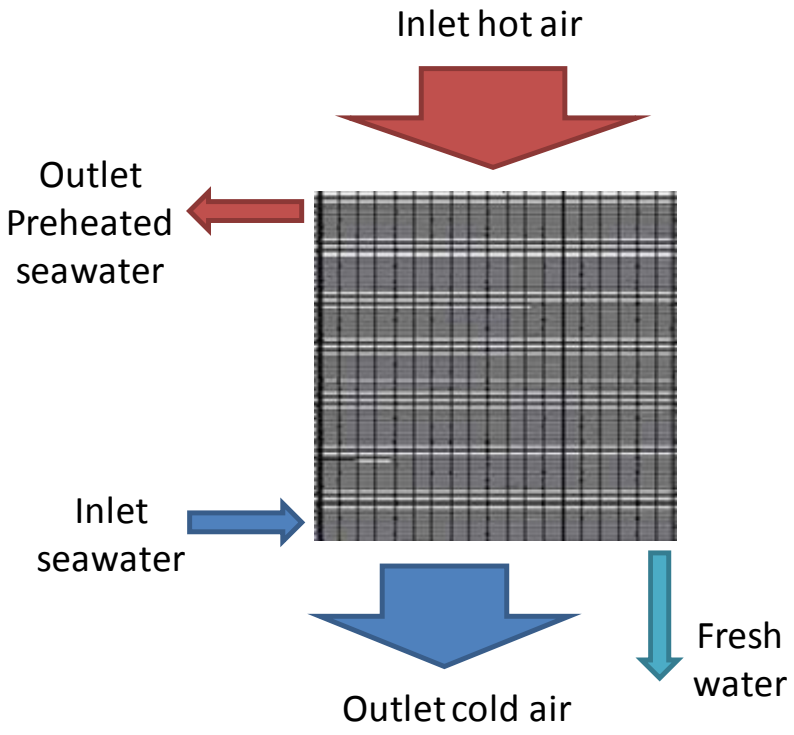

Figure 2-2: Flows inside the condenser

The heat and mass balances are represented by the following equations:

$$\begin{cases} \dot{Q}_{seawater} + \dot{Q}_{freshwater} + \dot{Q}_{loss} - \dot{Q}_{fan,cond} - \dot{Q}_{air} = 0 \\ \dot{Q}_{seawater} - \dot{Q}_{condensator} = 0 \end{cases} \quad (2.1)$$

Where:

$$\dot{Q}_{seawater} = L \cdot Cp_w \cdot (Tw_{out} - Tw_{in}) \quad [kW]$$

$$\dot{Q}_{freshwater} = D \cdot Cp_w \cdot (Ta_{in} - Ta_{out}) \quad [kW]$$

$$\dot{Q}_{loss} = 0.5 \cdot U_{loss} \cdot A_{unit} \cdot \left(\frac{Ta_{in} + Ta_{out}}{2} - T_{amb}\right) \quad [kW]$$

$$\dot{Q}_{fan,cond} = 0{,}5 \cdot \dot{Q}_{fan} \quad [kW]$$

$$\dot{Q}_{air} = G \cdot (Ha_{in} - Ha_{out}) \quad [kW]$$

$$\dot{Q}_{condensator} = U_{cond} \cdot A_{cond} \cdot \left(\frac{(Ta_{in} - Tw_{out}) - (Ta_{out} - Tw_{in})}{ln \frac{(Ta_{in} - Tw_{out})}{(Ta_{out} - Tw_{in})}} \right) \quad [kW]$$

The overall heat transfer coefficient *Ucond* is expected to be small due to:

1) the low velocity of the air circulated in the unit, even in forced circulation, which was necessary to avoid excessive pressure drop.
2) the large reduction in the condensation heat transfer coefficient due to the mass transfer resistance occurring in the process of condensation of water vapor with non-condensable air.
3) the low water side heat transfer coefficient due to the low water flow rate per unit of condenser area.

The following expression was used to define it:

$$U_{cond} = \frac{1}{\frac{1}{h_{int}} \cdot \frac{A_{ext}}{A_{int}} + \frac{A_{ext}}{2 \cdot k_{alu} \cdot \pi \cdot lx} \cdot log\left(\frac{d_{ext}}{d_{int}}\right) + \frac{1}{ng \cdot h_{ext}}} \quad \left[\frac{kW}{m^2 \cdot K}\right]$$

The term *ng* represents the fin efficiency, and can be calculated by this correlation:

$$ng = 1 - \frac{Afin_{square}}{A_{ext} \cdot (1 - nf)}$$

Where:

$$Afin_{square} = 2 \cdot (n_{fin} - 1) \cdot pitch_z \cdot pitch_y - 2 \cdot \left(\frac{d_{ext}}{2}\right)^2 \cdot \pi \cdot (n_{fin} - 1) \quad [m^2]$$

$$A_{ext} = Afin_{square} + \left(lx - n_{fin} \cdot thick_{fin}\right) \cdot d_{ext} \cdot \pi \qquad [m^2]$$

$$A_{int} = d_{int} \cdot \pi \cdot lx \qquad [m^2]$$

The definition of nf is the following [3]:

$$nf = \frac{tanh\left(\frac{m \cdot pitch_y}{2}\right)}{\frac{m \cdot pitch_y}{2}}$$

With:

$$m = \sqrt{\frac{2 \cdot h_{ext}}{k_{alu} \cdot thick_{fin}}}$$

The water side heat transfer coefficient h_{int} is defined by this expression:

$$h_{int} = \frac{Nu_w \cdot k_w}{d_{int}} \qquad \left[\frac{W}{m^2K}\right]$$

Nu_w represents the Nusselt number, calculated by the Chilton-Colburn relation. This relation is applicable for tubes with circular section and only in the complete evolution flow region:

$$Nu_w = 0.023 \cdot Re_w^{\frac{4}{5}} \cdot {Pr_w}^{\frac{1}{3}}$$

The water flow Reynolds Number Re_w inside the tube correlates the inertia and viscous effects:

$$Re_w = \frac{4 \cdot L}{nz \cdot 3.14 \cdot d_{int} \cdot \mu_w}$$

The water side Prandtl number represents the ratio between thermal diffusivity and viscous effects:

$$Pr_w = \frac{Cpw \cdot \mu_w}{k_w}$$

The C. Bougriou correlation [4] was used to define the air side heat transfer coefficient h_{ext} :

$$h_{ext} = 0{,}29 \cdot \left(\frac{k_a}{d_{ext}}\right) \cdot {Re_a}^{0{,}633} \cdot Pr_a^{\frac{1}{3}} \cdot F^{-0{,}17} \qquad \left[\frac{W}{m^2K}\right]$$

The air density ρ_a, air thermal conductivity k_a, Prandtl Number Pr_a and kinematics viscosity μ_a are functions of temperature (expressed in Kelvin):

$$\rho_a = 319{,}57 \cdot T^{-0{,}984} \qquad \left[\frac{kg}{m^3}\right]$$

$$k_a = -3 \cdot 10^{-8} \cdot T^2 + 10^{-4} \cdot T - 4 \cdot 10^{-5} \qquad \left[\frac{W}{mK}\right]$$

$$\begin{cases} Pr_a = 1{,}26889 \cdot T^{(-0{,}10257)} & 200°K < T < 300°K \\ Pr_a = 1{,}432439 \cdot T^{(-0{,}0840914)} & 300°K \leq T < 400°K \end{cases}$$

$$\begin{cases} \mu_a = 1.7355085638 \cdot 10^{-7} \cdot T^{(0{,}818440068)} & 200°K < T < 300°K \\ \mu_a = 2.336115 \cdot 10^{-7} \cdot T^{(0{,}7662279)} & 300°K \leq T < 400°K \end{cases}$$

The air side Reynolds Number Re_a is calculated by this expression:

$$Re_a = \frac{(4 \cdot \rho_a \cdot speed_a \cdot a_{cond})}{\mu_a}$$

Where:

$$speed_a = \frac{G}{nz \cdot \rho_a \cdot (pitch_z - d_{ext}) \cdot lx} \qquad \left[\frac{m}{s}\right]$$

$$a_{cond} = \frac{V_{cond}}{A_{cond}} \qquad \left[\frac{m^3}{m^2}\right]$$

The coefficient *F* represents the ratio between the external surface of the finned tube for length unit and the corresponding external surface of the same tube without fins:

$$F = \frac{S_{fin}}{S_{smooth}} \qquad 4 < F < 34$$

$$S_{fin} = \frac{A_{ext}}{lx} \qquad [m]$$

$$S_{smooth} = \frac{d_{ext} \cdot \pi \cdot lx}{lx} \qquad [m]$$

The pressure drop in this kind of finned heat exchanger can be calculated using Yudin and Tokhtarova correlation [5]:

$$\Delta p_{\text{cond}} = \frac{Eu \cdot \rho_a \cdot {speed_a}^2 \cdot ny}{2} \qquad [Pa]$$

Where Eulero Number is a dimensionless quantity:

$$Eu = 0.52 \cdot \left(\frac{d_{eq}}{d_{hydr}}\right)^{0.3} \cdot \left(\frac{b-1}{c-1}\right)^{0.68} \cdot {Re_{eq}}^{-0.08} \cdot Cz$$

$$d_{eq} = \frac{S_{smooth} \cdot D_{ext}}{S_{fin}} + \frac{S_{square}}{S_{fin}} \cdot \sqrt{\frac{Afin_{total}}{2 \cdot \frac{n_{fin}}{lx}}} \qquad [m]$$

$$S_{square} = \frac{pitch_z \cdot pitch_y - \left(\frac{d_{ext}}{2}\right)^2 \cdot \pi}{pitch_{fin}} \qquad [m]$$

$$Afin_{total} = 2 \cdot (n_{fin} - 1) \cdot ly \cdot lz - 2 \cdot \left(\frac{d_{ext}}{2}\right)^2 \cdot \pi \cdot (n_{fin} - 1) \cdot ny \cdot nz \quad [m^2]$$

$$d_{hydr} = \frac{4 \cdot ((pitch_z - d_{ext}) \cdot lx \cdot nz)}{(lx + lz) \cdot 2} \quad [m]$$

$$Re_{eq} = \frac{speed_a \cdot d_{eq}}{\mu_a}$$

$$b = \frac{pitch_y}{d_{ext}}$$

$$c = \frac{pitch_z}{d_{ext}}$$

$$Cz = 0.738 + \frac{1.509}{ny - 0.250}$$

2.2 Humidifier

The humidifier is a typical cooling tower with wooden slats packing: a wooden sheet thickness of 2mm ($thick_{sheet}$), and a sheet pitch of 50mm ($pitch_x, pitch_z$) were chosen. The structure of the humidifier and the flows inside it are shown in figure 2-3.

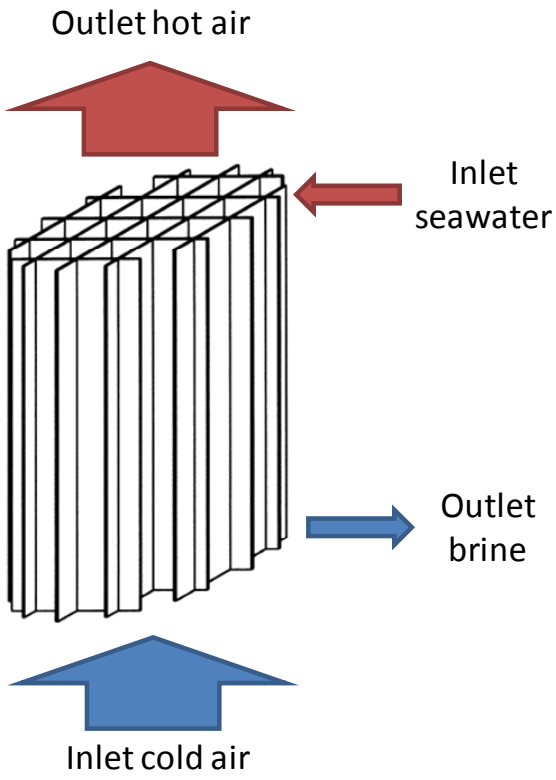

Figure 2-3: Flows inside the humidifier

In the humidifier energy and mass exchanges take place at the same time: air gains heat and humidity from hot seawater, while the outlet seawater increases his salt concentration. The wooden sheet are wetted by sea water, with a temperature between 30 and 60°C. A counterflow cold air stream is blown inside the fill, allowing the air to rise in temperature and evaporate water from wooden packing.

The heat and mass balances are represented by the following equations:

$$\begin{cases} \dot{Q}_{water} - \dot{Q}_{loss} + \dot{Q}_{fan,humid} - \dot{Q}_{air} = 0 \\ \dot{Q}_{air} - \dot{Q}_{humidifier} = 0 \\ D - G \cdot (Xa_{out} - Xa_{in}) = 0 \end{cases} \tag{2.2}$$

Where:

$$\dot{Q}_{water} = L \cdot Cp_w \cdot Tw_{in} - (L - D) \cdot Cp_w \cdot Tw_{out}$$

$$= L \cdot Cp_w (Tw_{in} - Tw_{out}) + D \cdot Cp_w \cdot Tw_{out} \quad [kW]$$

$$\dot{Q}_{loss} = \left(\frac{0{,}5}{n_{comp} - 1}\right) \cdot U_{loss} \cdot A_{unit} \cdot \left[\frac{Ta_{in} + Ta_{out}}{2} - T_{amb}\right] \quad [kW]$$

$$\dot{Q}_{fan,humid} = \left(\frac{0{,}5}{n_{comp} - 1}\right) \cdot \dot{Q}_{fan} \quad [kW]$$

$$\dot{Q}_{air} = G \cdot (Ha_{out} - Ha_{in}) \quad [kW]$$

$$\dot{Q}_{humidifier} = K_{humid} \cdot a_{humid} \cdot V \cdot \left[\frac{(Hw_{in} - Ha_{out}) - (Hw_{out} - Ha_{in})}{ln\frac{(Hw_{in} - Ha_{out})}{(Hw_{out} - Ha_{in})}}\right] \quad [kW]$$

The second equation of the system (2) derives from Merkel Theory [6,7]. The critical simplifying assumptions of the Merkel Theory are:

• The Lewis factor relating heat and mass transfer is equal to 1. This assumption has a small influence but affects results at low ambient temperatures.

• The air exiting the tower is saturated with water vapor and it is characterized only by its enthalpy. This assumption regarding saturation has a negligible influence above an ambient temperature of 20°C but is of importance at lower temperatures.

• The reduction of water flow rate by evaporation is neglected in the energy balance. This energy balance simplification has a greater influence at elevated ambient temperatures.

According to this theory, equation (2.3) and (2.4) are obtained from mass and energy balances of the control volumes shown in figure 2-4, where air is in counterflow with a downwards flowing water stream.

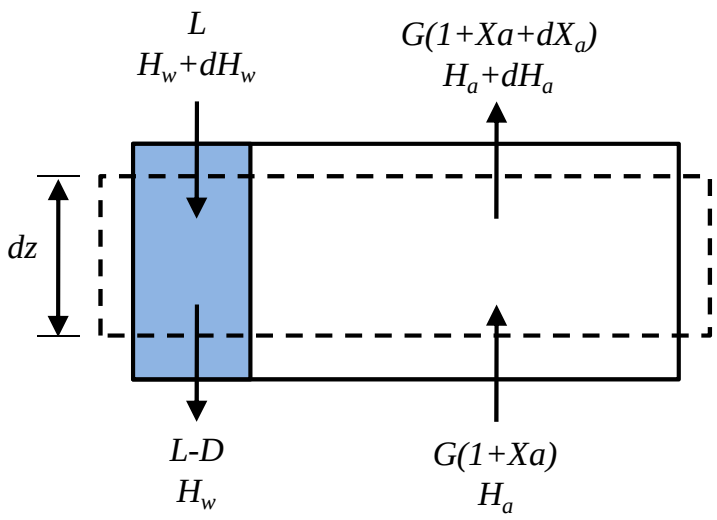

Figure 2-4: Control volume of counterflow fill

$$\frac{dHa}{dz} = \frac{K_{humid} \cdot a_{humid} \cdot A_{fr} \cdot (Hw - Ha)}{G} \tag{2.3}$$

$$\frac{dTw}{dz} = \frac{G}{L} \cdot \frac{1}{Cp_w} \cdot \frac{dHa}{dz} \tag{2.4}$$

Equation (2.3) and (2.4) describe, respectively, the change in the enthalpy of the air-water vapor mixture and the change in water temperature as the air travel distance changes. This equations can be combined to yield upon the Merkel equation (2.5):

$$\frac{dTw}{dz} = \frac{G}{L} \cdot \frac{1}{Cp_w} \cdot \frac{K_{humid} \cdot a_{humid} \cdot A_{fr} \cdot (Hw - Ha)}{G} \Rightarrow \frac{Cp_w \cdot dTw}{(Hw - Ha)} = \frac{K_{humid} \cdot a_{humid} \cdot A_{fr} \cdot dz}{L}$$

$$\Rightarrow \frac{K_{humid} \cdot a_{humid} \cdot V}{L} = \int_{Tw_{out}}^{Tw_{in}} \frac{Cp_w \cdot dTw}{(Hw - Ha)} = Me_M \tag{2.5}$$

where Me_M is the Merkel Number according to the Merkel approach, a is the surface area of the fill per unit volume of the fill, and K is the mass transfer coefficient (kg evaporated water/m^2 s).

Bourillot [8] stated that the Merkel method is simple to use and can correctly predict cold water temperature when an appropriate value of the coefficient of evaporation is used. In contrast, it is insufficient for the estimation of the characteristics of the warm air leaving the fill and for the calculation of changes in the water flow rate due to evaporation. These quantities are important to estimate water consumption and to predict the behavior of plumes exiting the cooling tower.

The estimation of the mass transfer coefficient should need the application of Poppe method, as explained by Kroger [6] and Besana [7]. The Poppe method governing equations can be solved by a fourth order Runge–Kutta method, with a significant increase in the computation time of simulation program.

Hence, it was decided to adopt the same geometry of humidifier studied and realized by Nawayseh in Malaysia [1] (shown in figure 2-3). Figure 2-5 shows a sketch of the desalination unit realized by Nawayseh. The hot water leaving the flat plate solar collector was sprayed on the packing using a simple distributor. The concentrated brine was rejected from the bottom of the humidifier section, while the fresh water was withdrawn from the bottom of the condenser section. The air was circulated in the unit either by natural draft or forced draft, using an electrical fan fixed at the upper section. The unit was operated in a steady state mode using an electrical heater and in an unsteady state mode using solar energy for heating the water. However, only the steady state, well controlled measurements, were used in the study of the heat and mass transfer of the units.

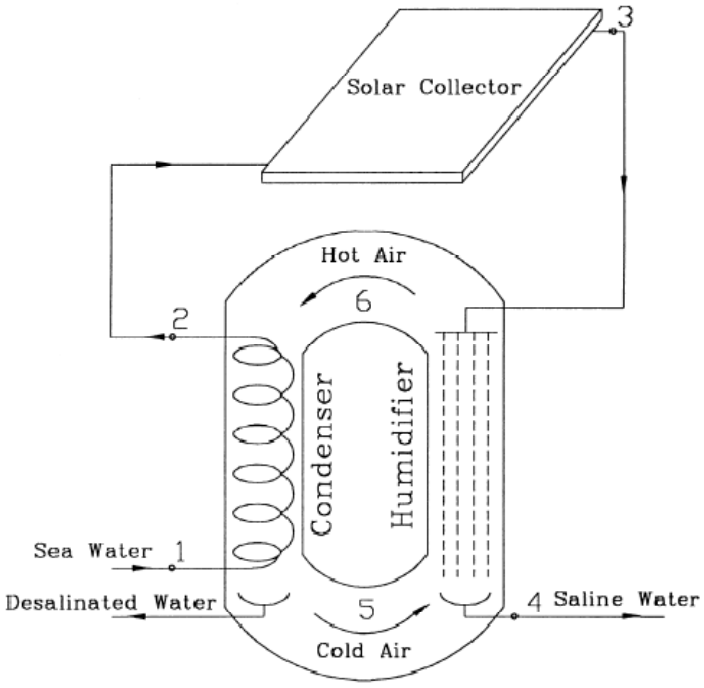

Figure 2-5: Sketch of Nawayseh unit

In each run, the electrical heating power and water flow rate were set to the desired values. In the forced air circulation mode, different air velocities were obtained by applying a variable AC power supply to the fan. Then, the desalination unit was left running for a few hours to reach steady state. The humidity of the air at the top and bottom of the unit were measured and found saturated. The inlet and outlet temperatures of the condenser, humidifier and solar collector were measured. The air temperature at the top and bottom of the unit, as well as the ambient temperature, were measured. The temperature measurements were made using thermocouples and multi-channel programmable recorder/data acquisition units. The water inlet flow rate was measured using a rotameter, while the brine and desalinated water flow rates were measured by graduated cylinder.

The experimental results showed that the humidification effect is greatly dependent on both the gas and liquid flow rates. The figure 2-6 shows the effect of *L/G* ratio on the mass transfer characteristic *KaV/L* for forced draft operation: It can be noticed that a decrease of the sea water mass flow rate or an increase of the air flow rate induces an increase of the mass transfer coefficient K_{humid}.

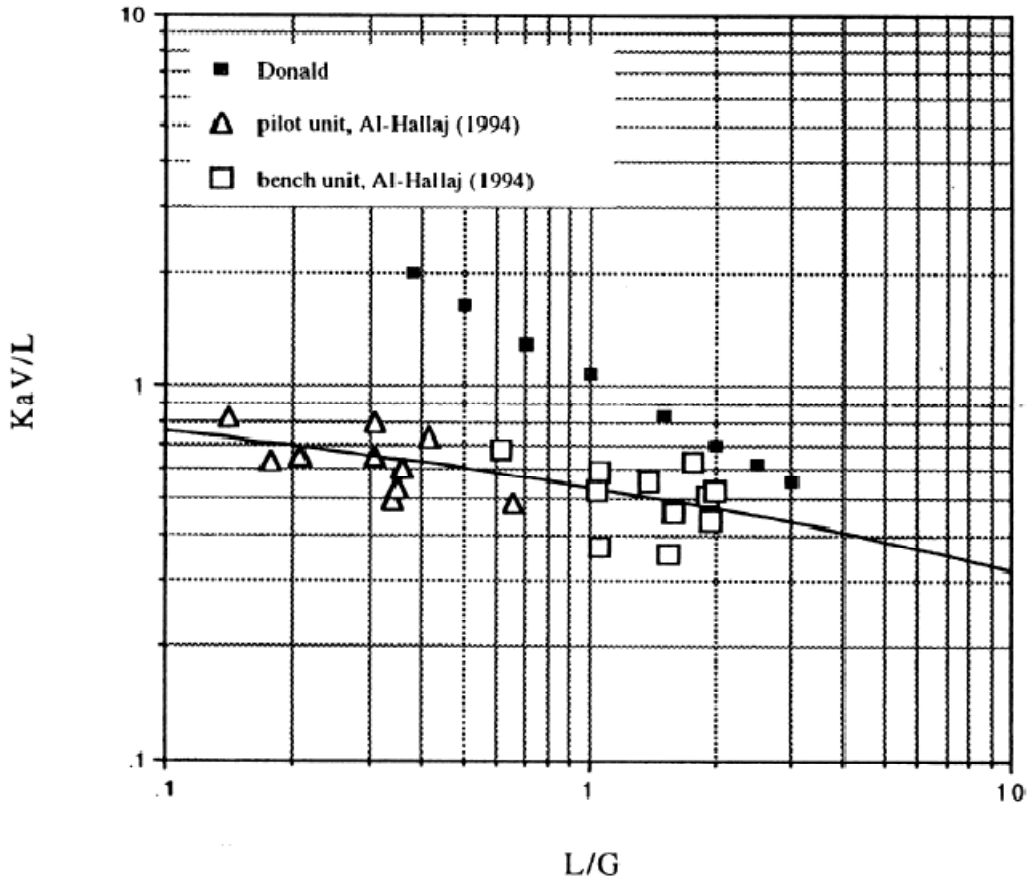

Figure 2-6: The effect of *L/G* ratio on the mass transfer characteristic *KaV/L* for forced draft operation [1].

The correlation (2.6) was found from the best fit to the data of figure 2-6:

$$\frac{K_{humid} \cdot a_{humid} \cdot V}{L} = 0{,}52 \cdot \left(\frac{L}{G}\right)^{-0{,}16} \; with \; 0{,}1 < \frac{L}{G} < 2 \qquad (2.6)$$

The adoption of humidifier geometry shown in figure 2-3 allowed the use of the correlation (2.6) to determine the value of K_{humid}.

The total pressure drop of this kind of humidifier can be calculated with the following expression [5]:

$$\Delta p_{humid} = C_{tot} \cdot \frac{\rho}{2} \cdot speed_a^2 \qquad [Pa]$$

Where C_{tot} is the global coefficient of pressure drop:

$$C_{tot} = C_{in} + C_{pack} + C_{out}$$

C_{in} is the inlet pressure drop:

$$C_{in} = 10 \cdot \left(\frac{A_r}{A_c}\right)^2$$

A_r is the effective air flow area:

$$A_r = lx \cdot lz - (nx_{umid} + 1) \cdot (nz_{umid} + 1) \cdot thick_{sheet} \cdot lx \qquad [m^2]$$

A_c is the external area of humidifier:

$$A_c = (lx + lz) \cdot 2 \cdot ly \qquad [m^2]$$

C_{pack} is the crossing pressure drop:

$$C_{pack} = \frac{25}{Fg^2}$$

$$Fg = \frac{A_{humid}}{lx \cdot lz}$$

At last C_{out} is the outlet pressure drop:

$$C_{out} = 1{,}05 \cdot \left(\frac{4 \cdot lz \cdot lx}{\pi \cdot d_{eq}^2}\right)^2$$

$$d_{eq} = 1{,}3 \cdot \left(\frac{(lx \cdot lz)^5}{(lx + lz)^2}\right)^{\frac{1}{8}}$$

2.3 Estimation of air enthalpy

Both in condenser and in humidifier, the value of humid air enthalpy is obtained from the following expression:

$$Ha = Cp_a \cdot Ta + X_a \cdot \left(Cp_w \cdot Ta + H_{vap}\right) \qquad \left[\frac{kJ}{kg}\right]$$

Where the water vaporization enthalpy H_{vap} is equal to 2500kJ/kg. Specific humidity X_a is evaluated considering air always saturated: the reason is the closed air cycle loop between the humidifier and condenser.

Atmospheric and partial saturation vapor pressure are used to calculate the specific humidity:

$$X_a = 0{,}622 \cdot \frac{p_g}{(p_a - p_g)}$$

The atmospheric pressure p_a is estimated with this expression:

$$p_a = \frac{1{,}01325 \cdot 10^5}{e^{\frac{altitude}{\xi}}}$$

Where *altitude* is the altitude above sea level, while $\xi = 8472{,}5 - 0{,}114 \cdot altitude$.

The partial saturation vapor pressure is calculated from the humid air temperature:

$$p_g = 100 \cdot \sum_{n=0}^{n=5} b_n \cdot Ta^n \qquad 0°C < Ta < 70°C$$

The polynomial coefficients are shown in table 2-1:

n	b_n
0	6,10145
1	$4{,}47854 \cdot 10^{-1}$
2	$1{,}37213 \cdot 10^{-2}$
3	$2{,}94769 \cdot 10^{-4}$
4	$2{,}25894 \cdot 10^{-6}$
5	$3{,}06754 \cdot 10^{-8}$

Table 2-1: Polynomial coefficients for partial saturation vapor pressure

2.4 HD unit configurations

After the definition of condenser and humidifier models, 4 different configurations of HD desalinator were chosen for the next analysis:

(1) HD desalinator with 1 humidifier (figure 2-7);
(2) HD desalinator with 1 humidifier and 1 humidifier recuperator (figure 2-8);
(3) HD desalinator with 2 humidifiers and 2 humidifier recuperators (figure 2-9);
(4) HD desalinator with 1 humidifier and 1 condenser recuperator (figure 2-10);

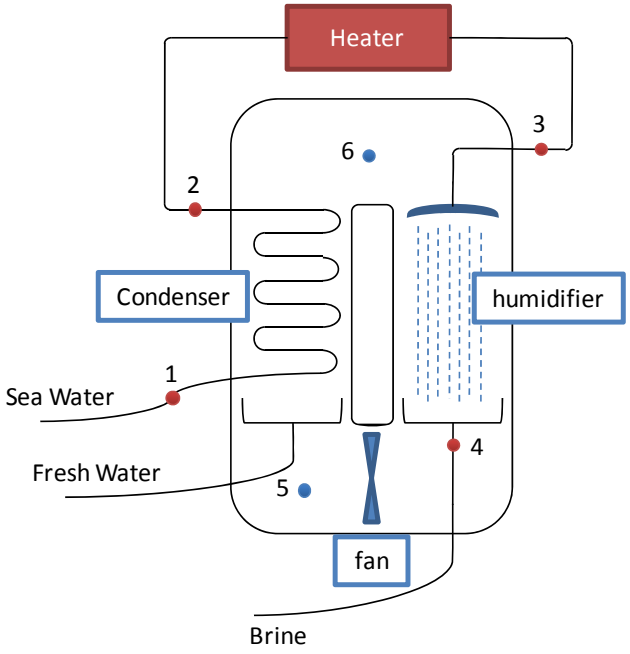

Figure 2-7: HD desalinator in configuration (1)

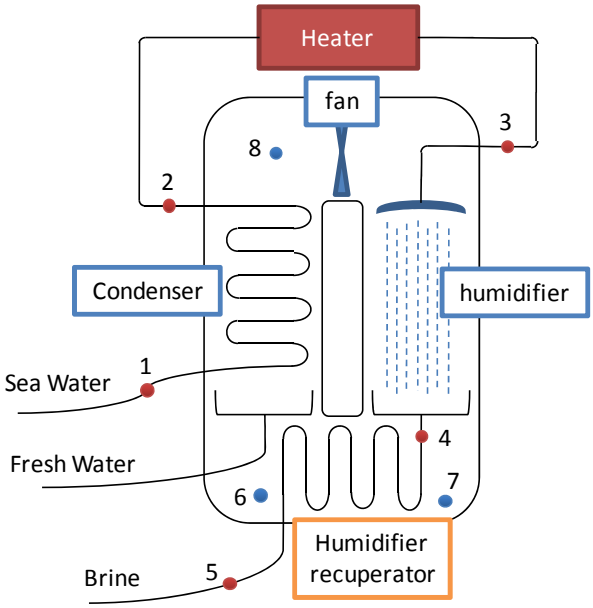

Figure 2-8: HD desalinator in configuration (2)

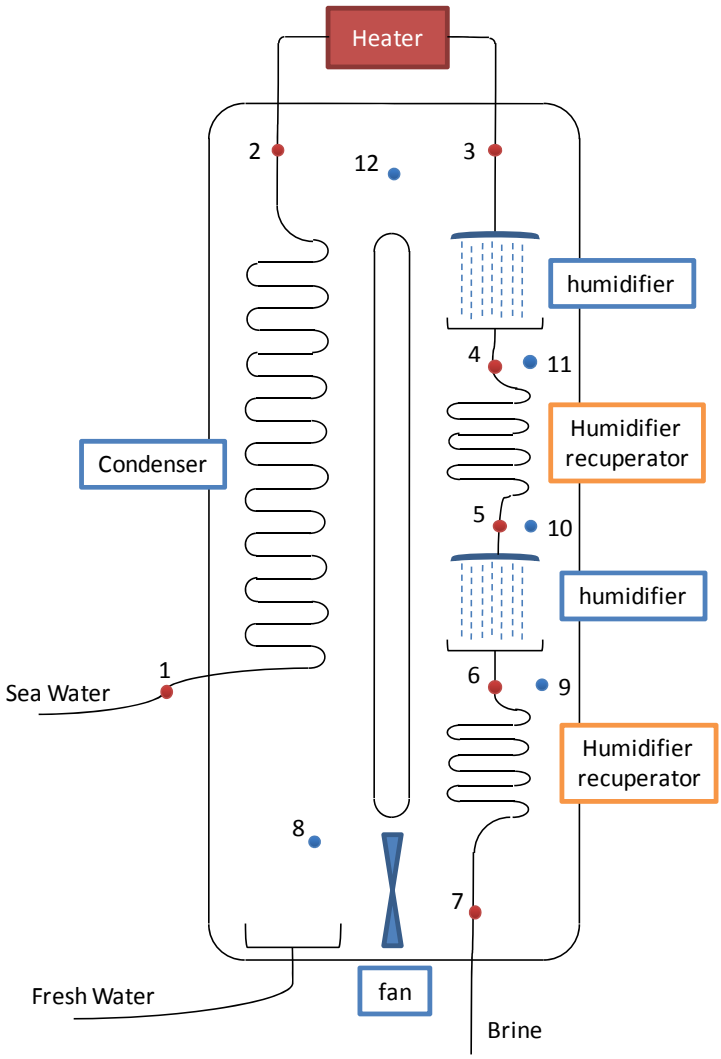

Figure 2-9: HD desalinator in configuration (3)

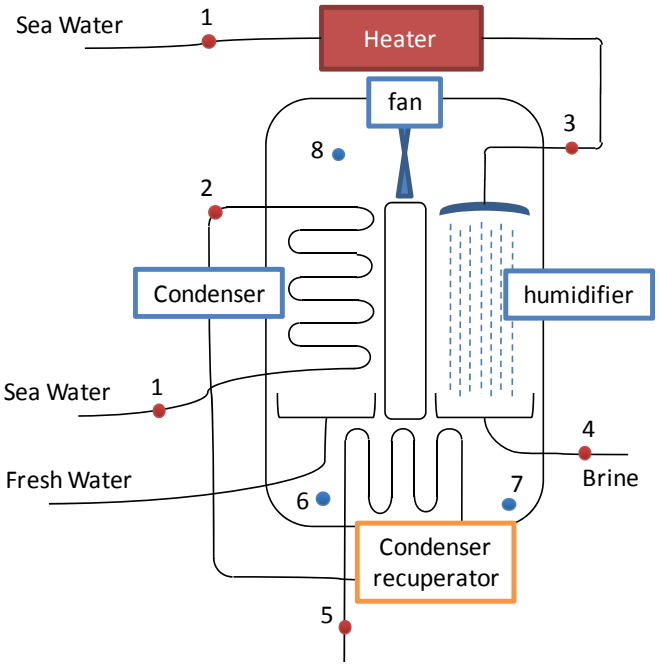

Figure 2-10: HD desalinator in configuration (4)

All these configurations use a closed air cycle loop with a fan for the forced draft. In addition to the fan, the figures show new components not yet defined: the heater and the recuperator.

The definition of the heater in this chapter is represented by an heat exchanger which provide a constant power of 120kW ($\dot{Q}_{heater}$), heating the seawater leaving the condenser and entering the humidifier. Hence, the calculation of seawater temperature *T(3)* (as shown in figures 2-7,8,9,10) is very simple:

$$T(3) = T(2) + \frac{\dot{Q}_{heater}}{L \cdot Cp_w} \qquad [°C]$$

In the next chapter the seawater leaving the condenser will be used to cool the absorption chiller for the cogeneration system, and the temperature T(3) will depend on the chiller operation.

The structure of the recuperator is identical to the condenser, the only difference lies in his function: the recuperator must heat the air entering the humidifier, while the condenser cools down the air to obtain fresh water. So the equations (2.1) are modified in this way:

$$\begin{cases} \dot{Q}_{seawater} - \dot{Q}_{loss} + \dot{Q}_{fan,rec} - \dot{Q}_{air} = 0 \\ \dot{Q}_{seawater} - \dot{Q}_{recuperator} = 0 \end{cases} \qquad (2.7)$$

Where:

$$\dot{Q}_{seawater} = L \cdot Cp_w \cdot (Tw_{in} - Tw_{out}) \qquad [kW]$$

$$\dot{Q}_{loss} = \left(\frac{0{,}5}{n_{comp} - 1}\right) \cdot U_{loss} \cdot A_{unit} \cdot \left(\frac{Ta_{in} + Ta_{out}}{2} - T_{amb}\right) \qquad [kW]$$

$$\dot{Q}_{fan,rec} = \left(\frac{0{,}5}{n_{comp} - 1}\right) \cdot \dot{Q}_{fan} \qquad [kW]$$

$$\dot{Q}_{air} = G \cdot (Ha_{out} - Ha_{in}) \qquad [kW]$$

$$\dot{Q}_{recuperator} = U_{rec} \cdot A_{rec} \cdot \left(\frac{(Tw_{in} - Ta_{out}) - (Tw_{out} - Ta_{in})}{ln\frac{(Tw_{in} - Ta_{out})}{(Tw_{out} - Ta_{in})}}\right) \qquad [kW]$$

The fan power $\dot{Q}_{fan}$ is obtained from this expression:

$$\dot{Q}_{fan} = \frac{G \cdot \Delta p_{tot}}{\rho_a \cdot \eta_{el} \cdot 1000} \qquad [kW]$$

The total pressure drop Δp_{tot} is obtained by the sum of the pressure drops in each component of the desalination unit (condenser, humidifiers, recuperators) and in each pipe between components.

Hence, every component is represented by equations which contain the energy and mass balances:

- Condenser includes equations (2.1) to calculate 2 variables: Tw_{out} and Ta_{out}. The estimation of fresh water flow rate is obtained from the subtraction of specific humidity of inlet and outlet air flow rate.
- Humidifier includes equations (2.2) to calculate 3 variables: Tw_{out}, Ta_{out} and D. The value of vapor flow rate D permits to calculate the outlet brine flow rate.
- Recuperator includes equations (2.7) to calculate 2 variables: Tw_{out} and Ta_{out}.

The Gauss-Newton algorithm is used to solve these equations systems, while the components of the desalination unit are connected inside the iterative algorithms shown in figure 2-11 and 2-12.

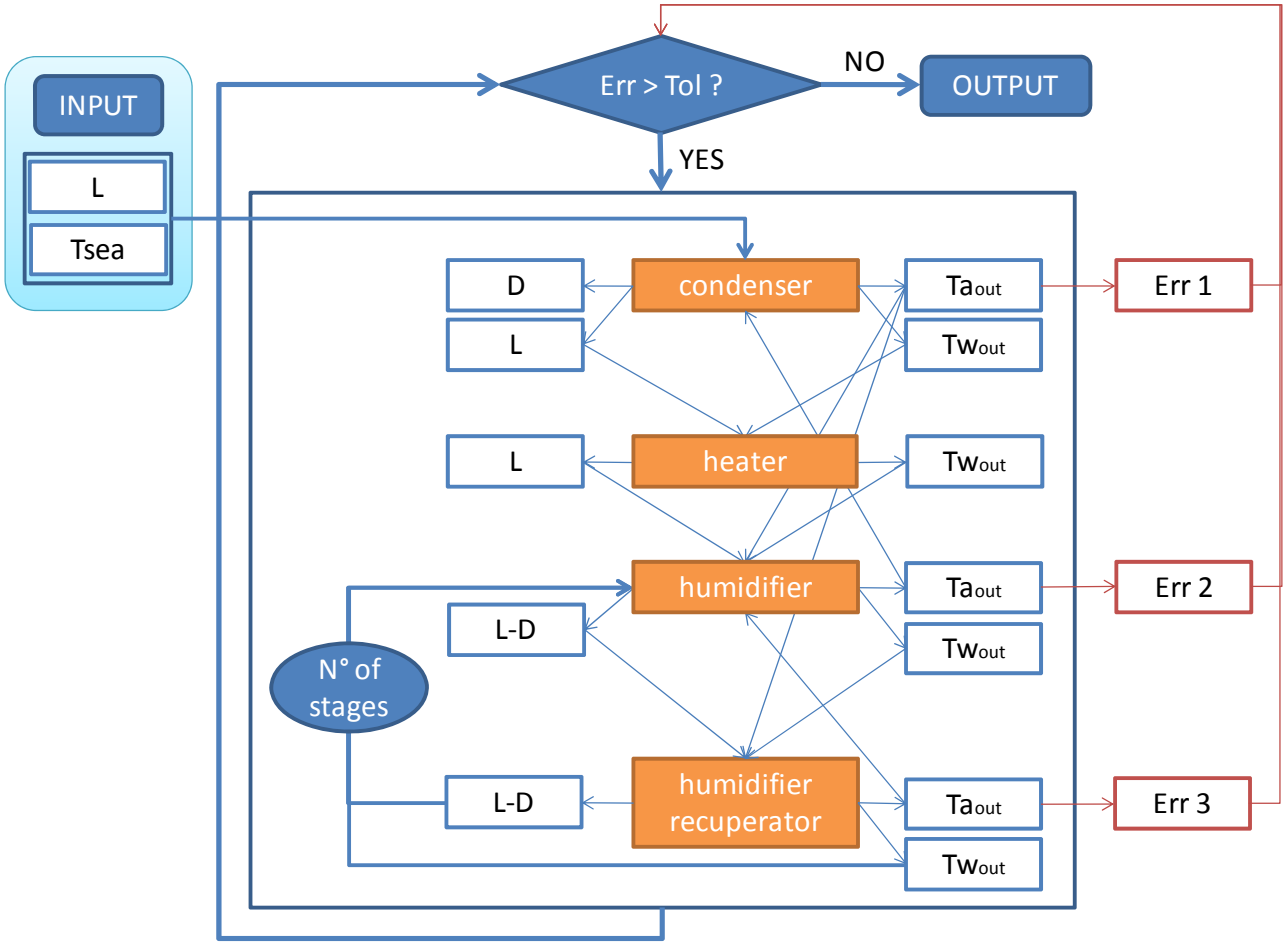

Figure 2-11: Iterative algorithm to simulate HD desalinator in configuration (1), (2) and (3)

The first algorithm (figure 2-11) simulate the HD desalinator in configuration (1), (2), and (3):

1) The condenser function receives the feeding seawater flow rate *L* and the seawater temperature *T(1)* as inputs. The function outputs are fresh water (*D*) and seawater (*L*) flow rates, the temperature of outlet seawater (*T(2)*) and air flow rates.

2) The outlet seawater from the condenser became the input for the heater function. The heater outputs are the seawater temperature *T(3)*, and the seawater flow rate *L*.
3) The heater outputs became the input for the humidifier function. The humidifier outputs are the brine seawater flow rate, the brine temperature and the outlet air temperature. The outlet air is considered always saturated.
4) The iterative algorithm contemplates the presence of a humidifier recuperator: the recuperator function calculate the outlet air temperature (in input to the corresponding humidifier) and the outlet brine temperature after the thermal exchange between air and brine.
5) The iterative algorithm can set an arbitrary number of humidification (and recovery) stage.
6) The variables evaluation continues until *Err<Tol* , where *Err* is calculated from the difference of the outlet air temperature values (for each component) of the current and previous cycles.

The iterative algorithm shown in figure 2-12 has been developed for the HD desalinator in configuration (4). In this case 2 different seawater flow rate have been considered: one for heater-humidifier block, called *L* as usual, and one for the condenser-recuperator block, called L_{cond}.

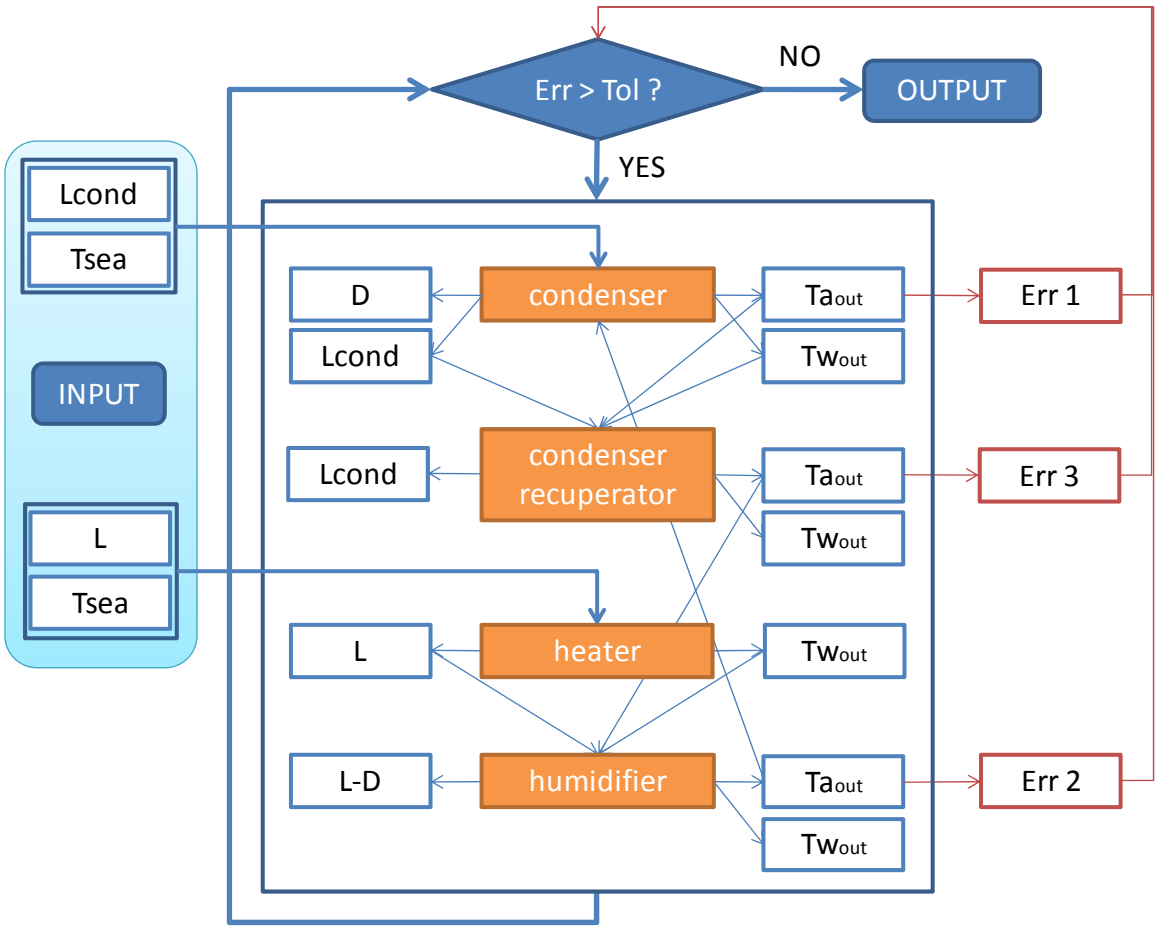

Figure 2-12: Iterative algorithm to simulate HD desalinator in configuration (4)

The steps solved by this algorithm are similar to the previous case:

1) The condenser function receives the seawater flow rate L_{cond} and the seawater temperature *T(1)* as inputs. The function outputs are fresh water (*D*) and seawater (L_{cond}) flow rates, the temperature of outlet seawater (*T(2)*) and air flow rates.
2) The outlet seawater and air flow rate from the condenser became the inputs for the condenser recuperator. This recuperator heats the outlet air from condenser by the same outlet seawater from the condenser. Hence, it's possible to provide not satured air to the humidifier, and air is able to absorb more humidity from the seawater.
3) The heater input are the feeding seawater flow rate *L* and the temperature of seawater *T(1)*. The heater outputs are the seawater flow rate *L*, and the seawater temperature *T(3)*.
4) As before, the heater outputs became the input for the humidifier function. The humidifier outputs are the brine seawater flow rate, the brine temperature and the outlet air temperature. The outlet air is considered always saturated. The algorithm does not consider the presence of a humidifier recuperator, because it would be irrelevant with respect to the condenser recuperator. For this reason, only one humidification stage has been provided.
5) The variables evaluation continues until *Err<Tol* , where *Err* is calculated from the difference of the outlet air temperature values (for each component) of the current and previous cycles.

2.5 Sensitivity analysis in steady state

A sensitivity analysis in steady state is carried out to seek the design point of the HD unit in different configurations. The only known parameters are:

- Seawater temperature: $\mathrm{T_{sea}} = 20°\mathrm{C}$
- Ambient temperature: $\mathrm{T_{amb}} = 30°\mathrm{C}$
- Heater Power: $\dot{Q}_{heater} = 120kW$

The design variables modified during the sensitivity analysis are:

- Condenser surface area: A_{cond}
- Humidifier surface area: A_{humid}
- Recuperator surface area: A_{rec}
- Seawater mass flow rate: L
- Seawater on air mass flow ratio: L/G
- Seawater mass flow rate for condenser in configuration (4): L_{cond}

The monitored parameters to evaluate the desalination unit efficiency are:

- Specific energy: $\dot{Q}_{heater}/D \ \ [kJ/kg]$
- Fresh water production: $D \ \ [kg/s]$
- Percentage of fresh water on seawater: $D \cdot 100/L \ \ [\%]$
- Air side total pressure drop inside the HD unit: $\Delta p_{tot} \ [Pa]$

2.5.1 Analysis on condenser surface area

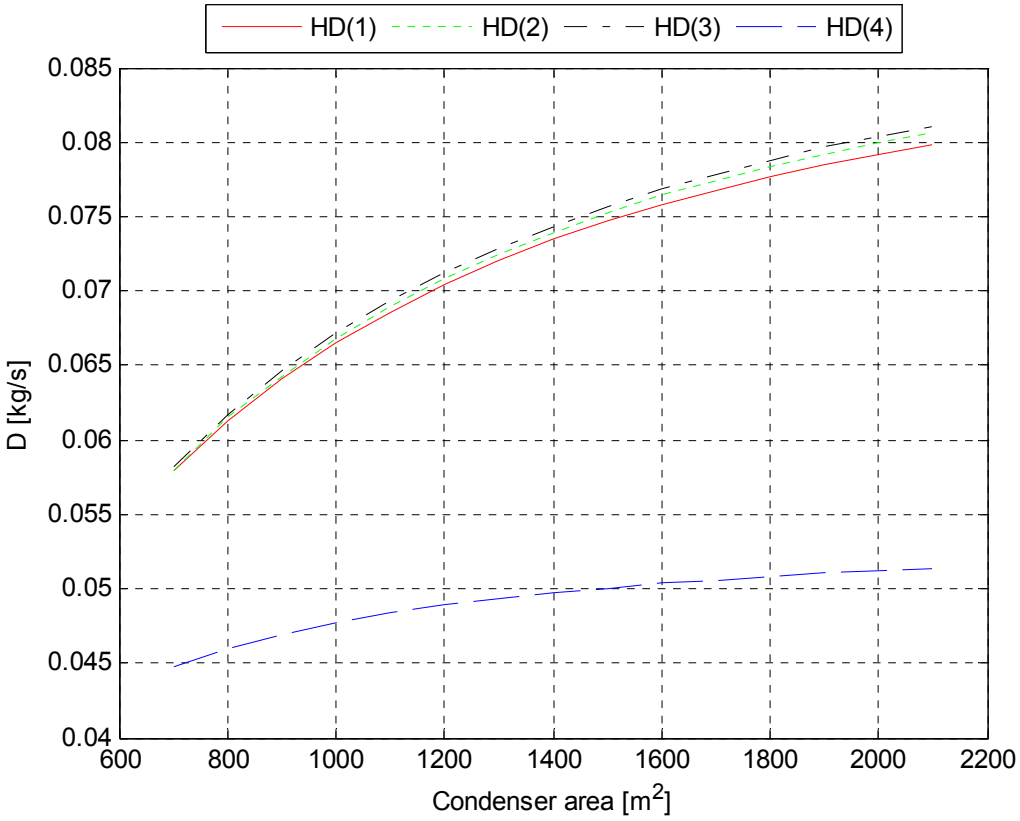

Figure 2-13: Fresh water flow rate as function of condenser area

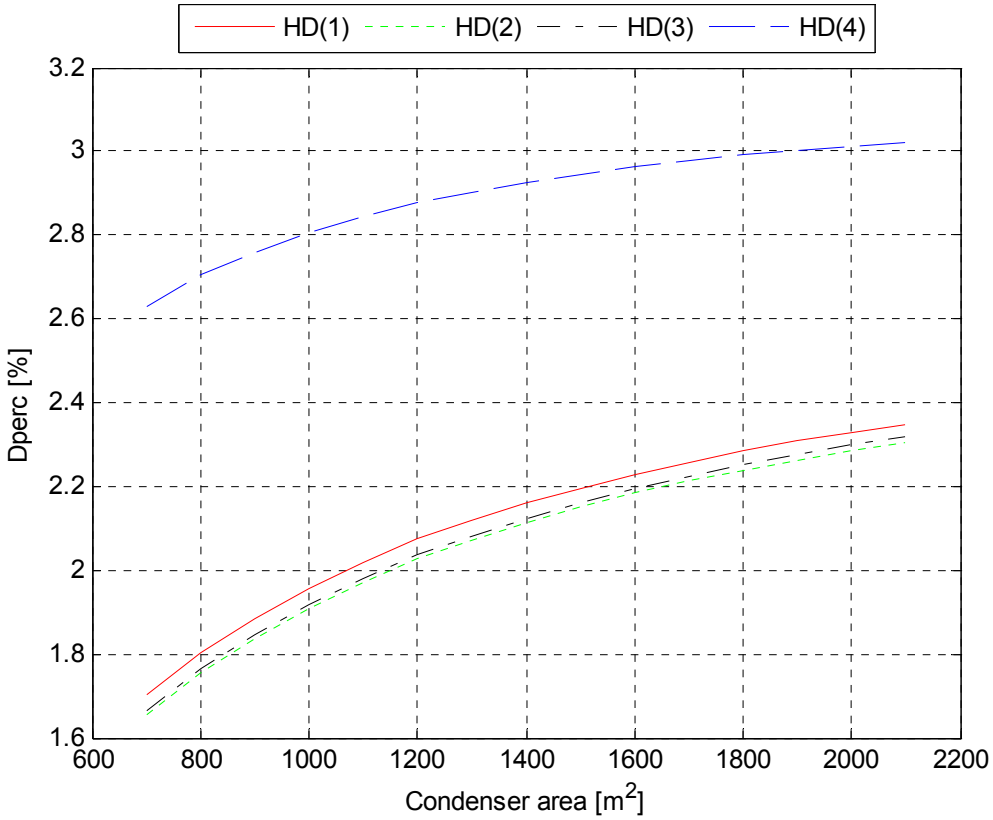

Figure 2-14: Percentage of fresh water on sea water flow rate as function of condenser area

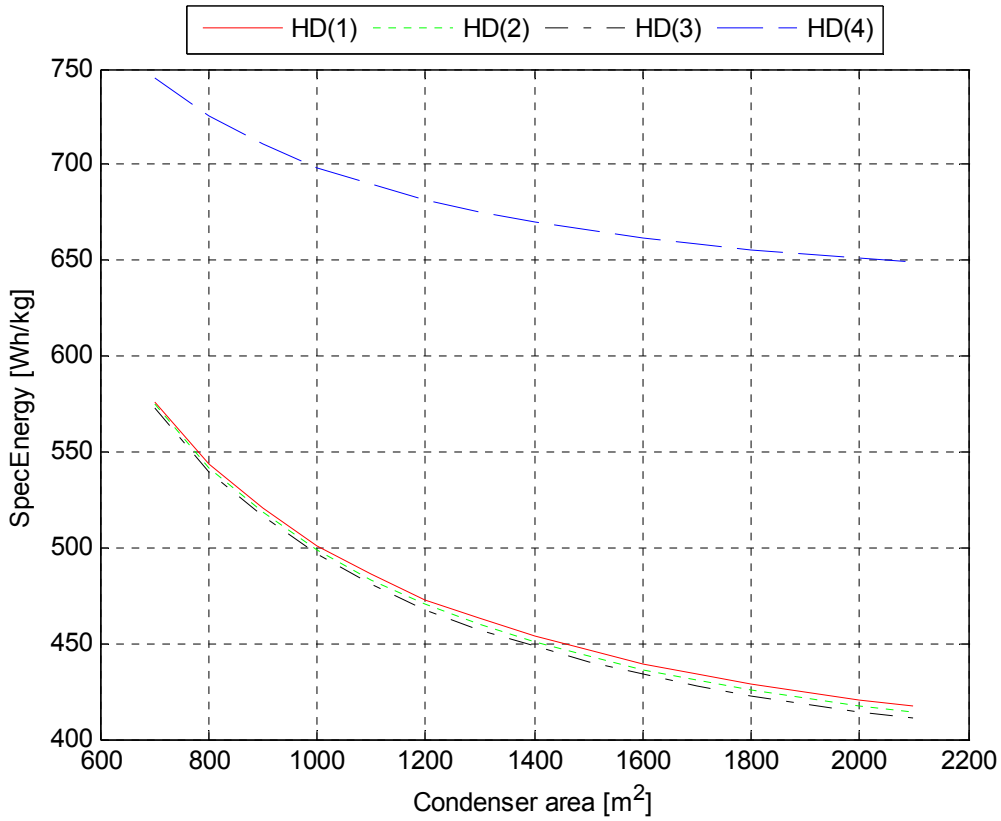

Figure 2-15: Specific energy as function of condenser area

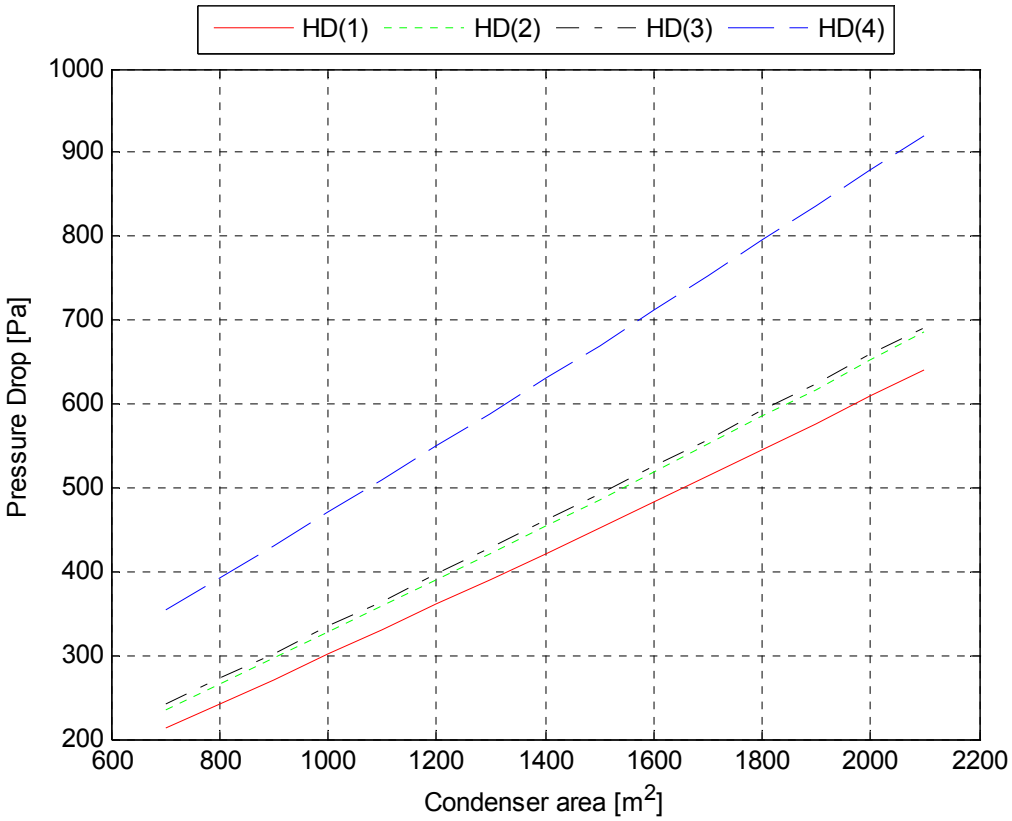

Figure 2-16: Total pressure drop as function of condenser area

2.5.2 Analysis on humidifier surface area

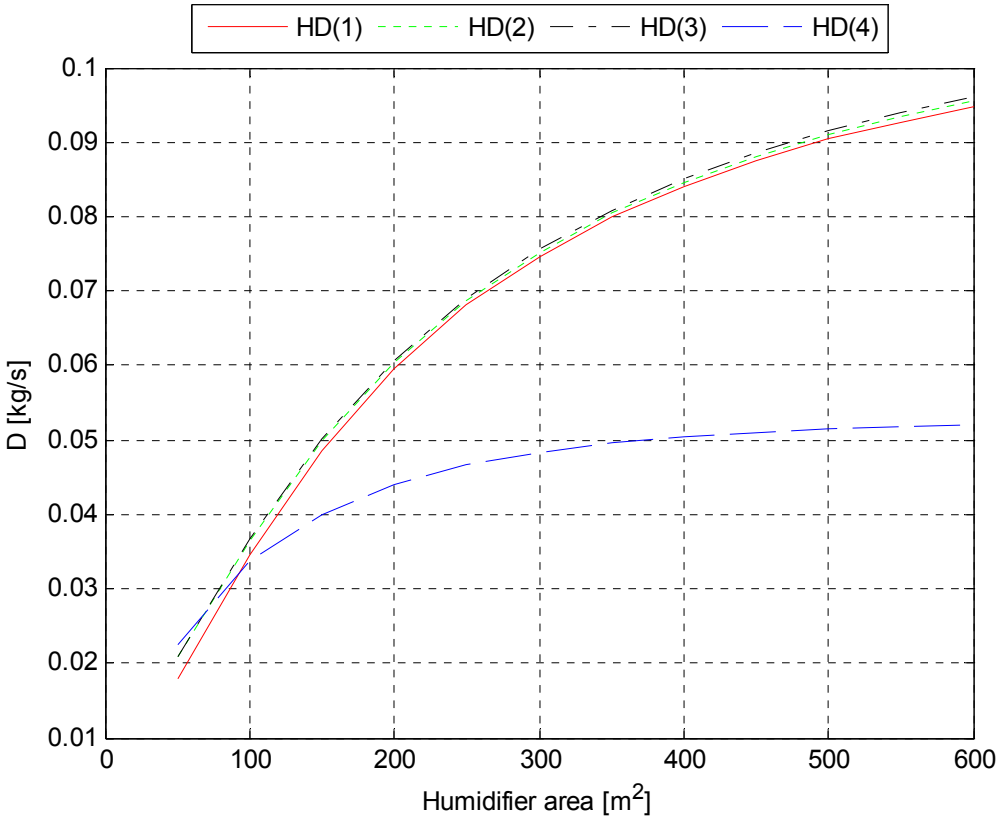

Figure 2-17: Fresh water flow rate as function of humidifier area

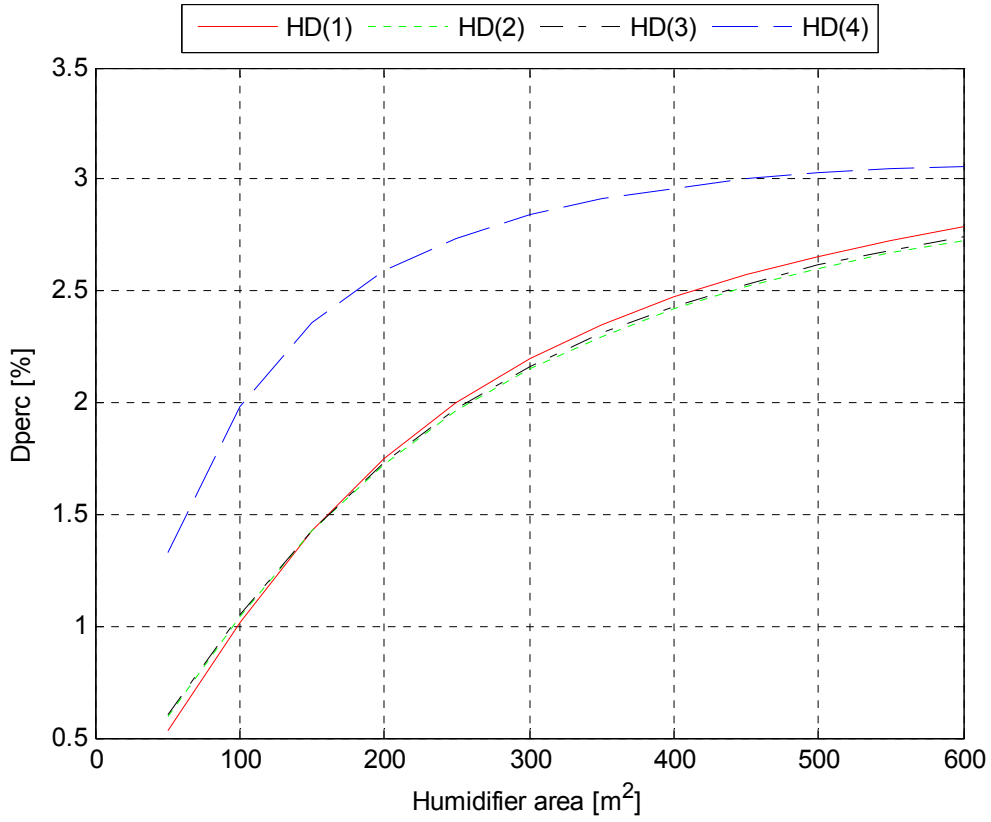

Figure 2-18: Percentage of fresh water on sea water flow rate as function of humidifier area

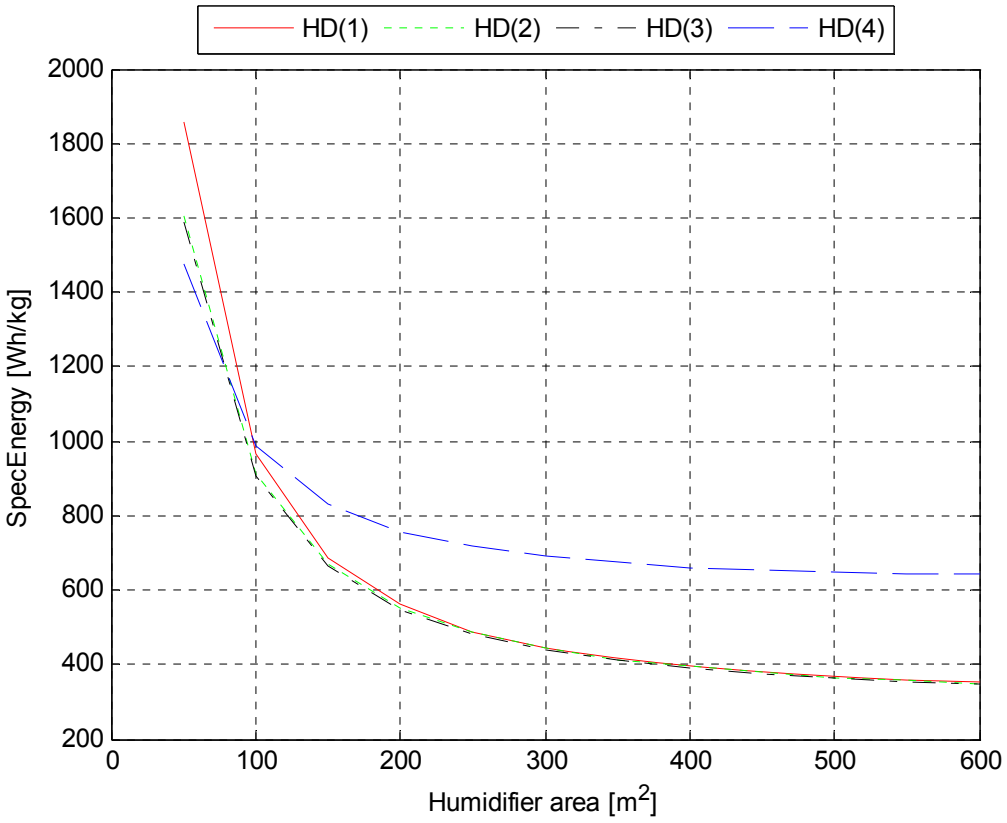

Figure 2-19: Specific energy as function of humidifier area

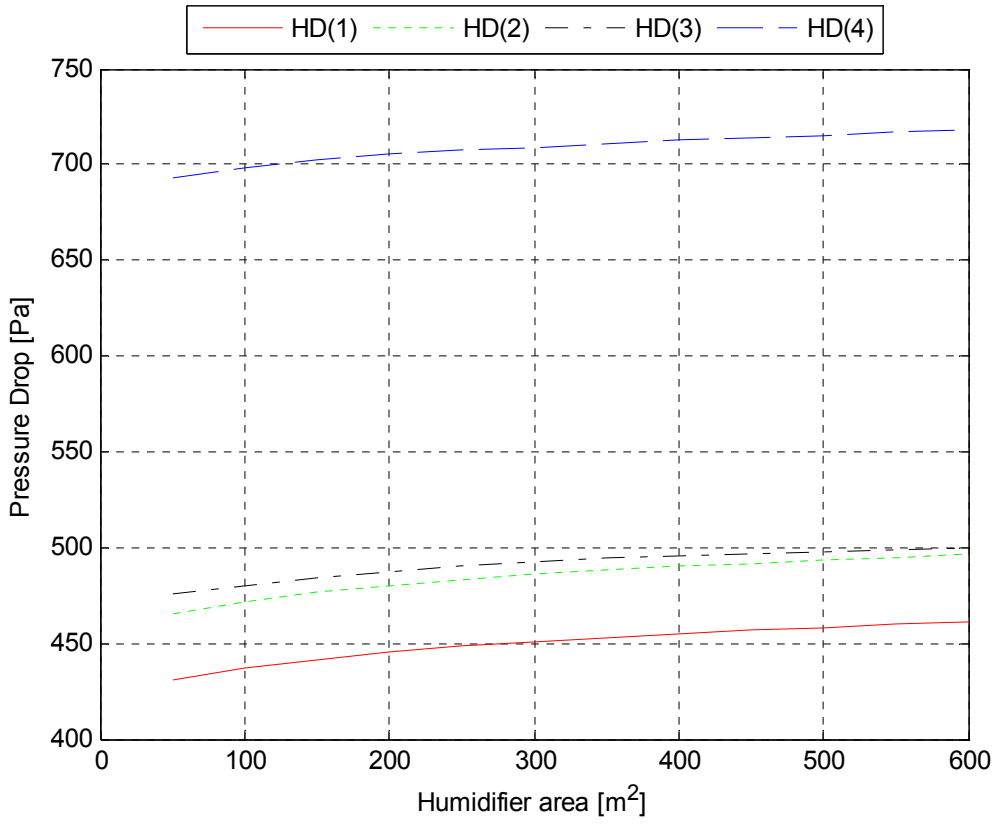

Figure 2-20: Total pressure drop as function of humidifier area

2.5.3 Analysis on recuperator surface area

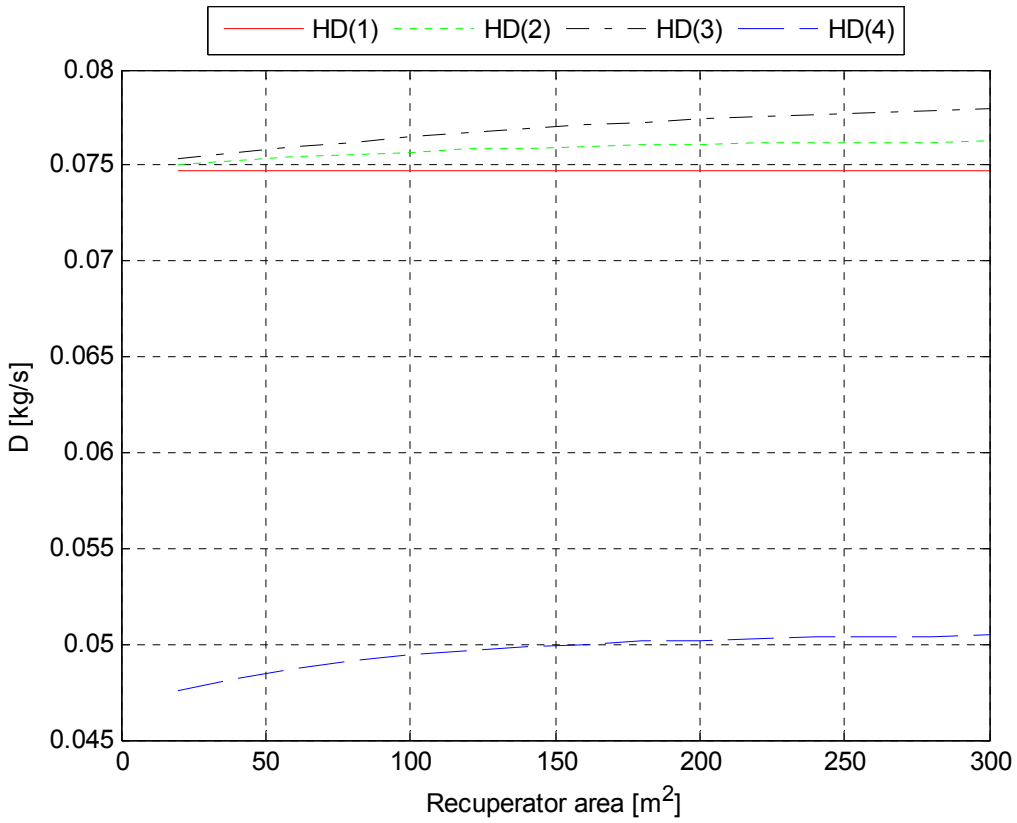

Figure 2-21: Fresh water flow rate as function of recuperator area

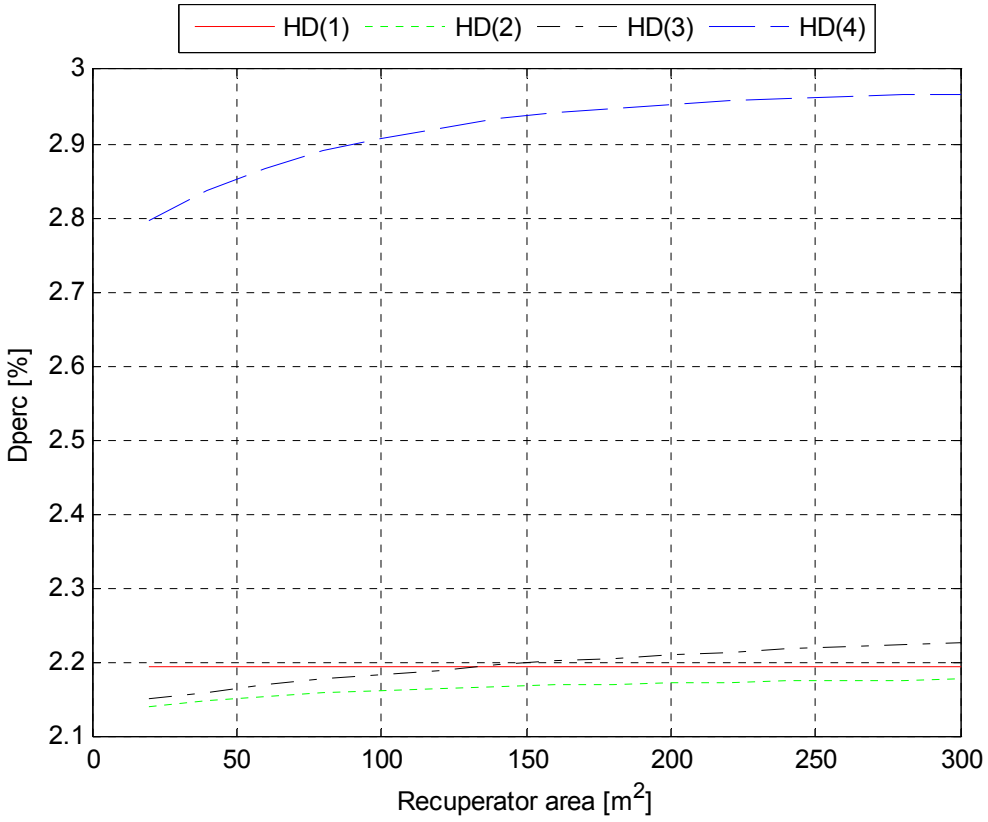

Figure 2-22: Percentage of fresh water on sea water flow rate as function of recuperator area

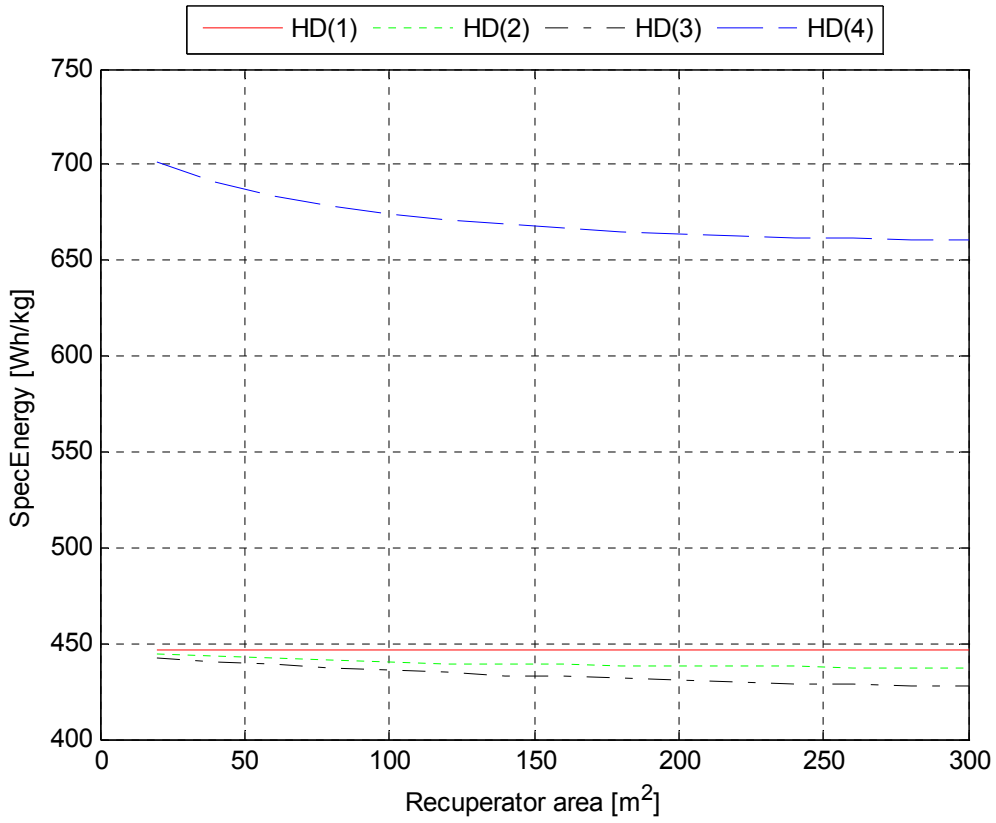

Figure 2-23: Specific energy as function of recuperator area

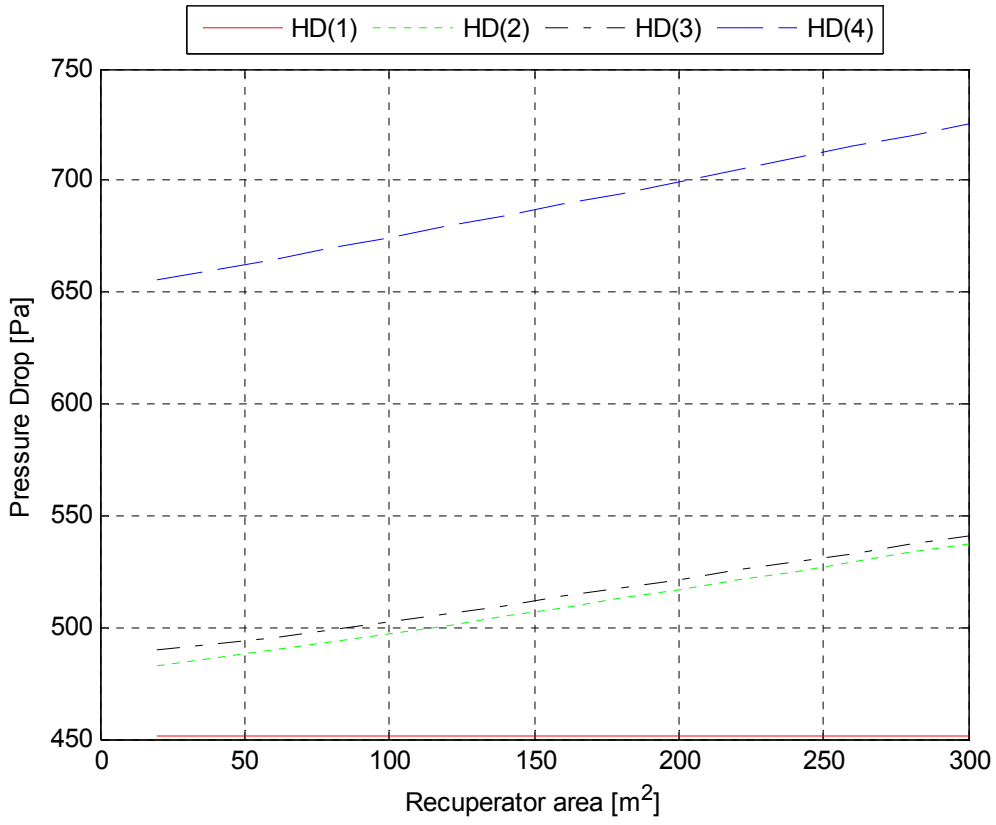

Figure 2-24: Total pressure drop as function of recuperator area

2.5.4 Analysis on sea water flow rate

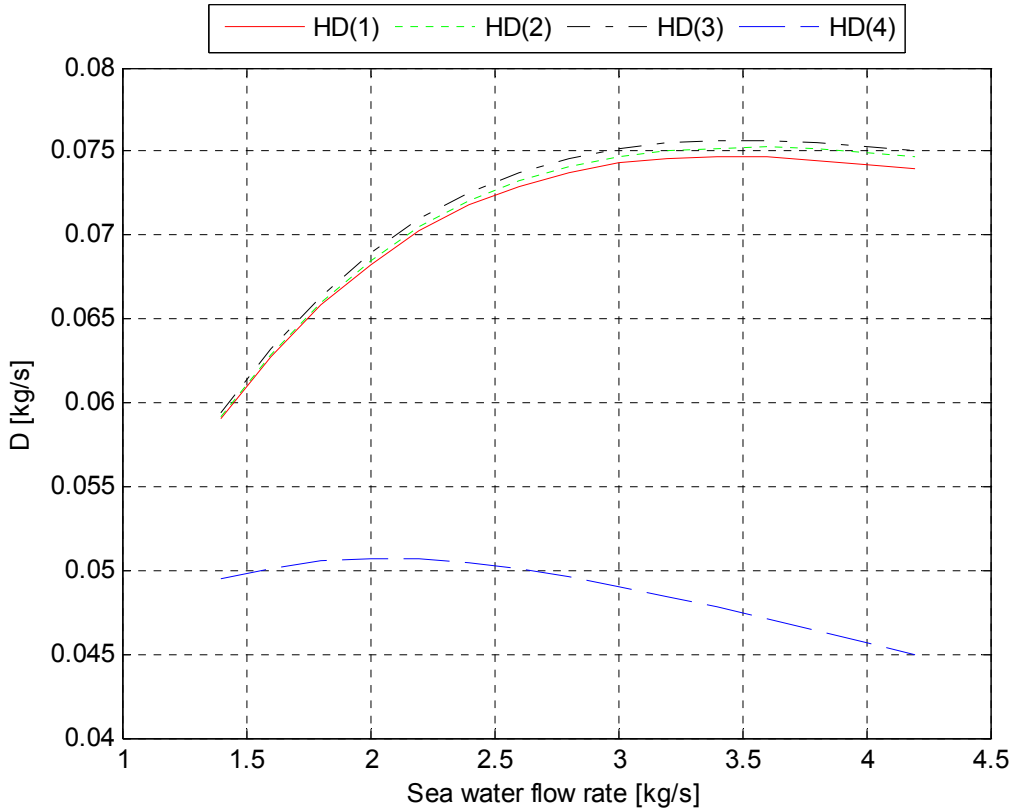

Figure 2-25: Fresh water flow rate as function of sea water flow rate

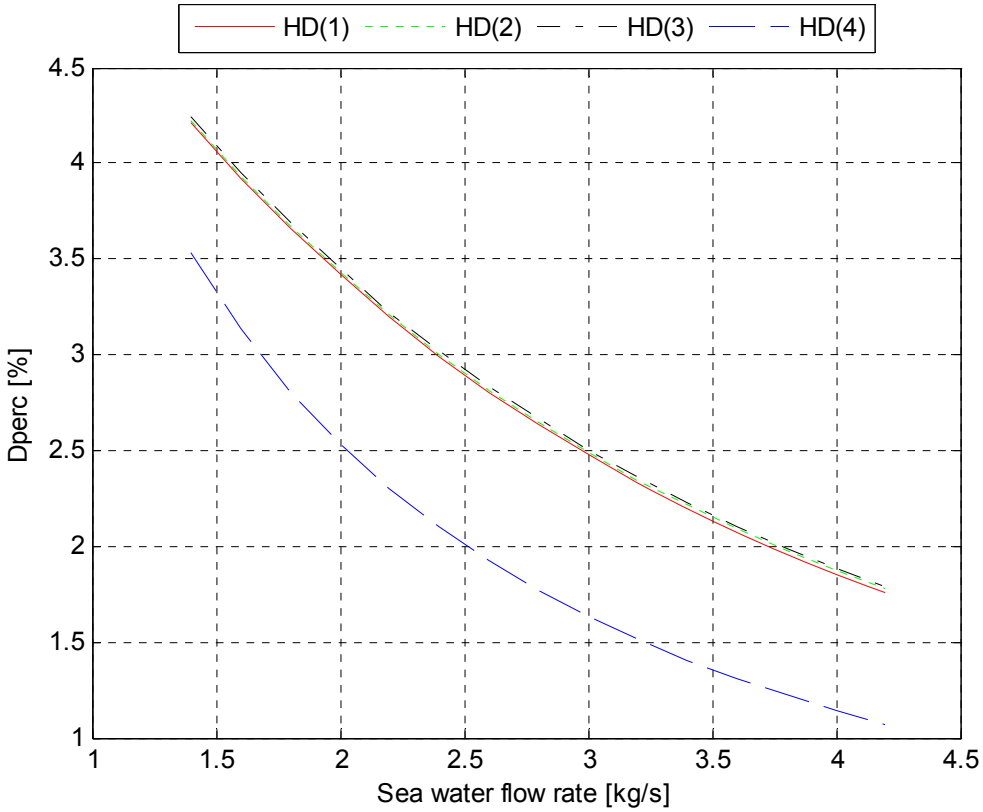

Figure 2-26: Percentage of fresh water on sea water flow rate as function of sea water flow rate

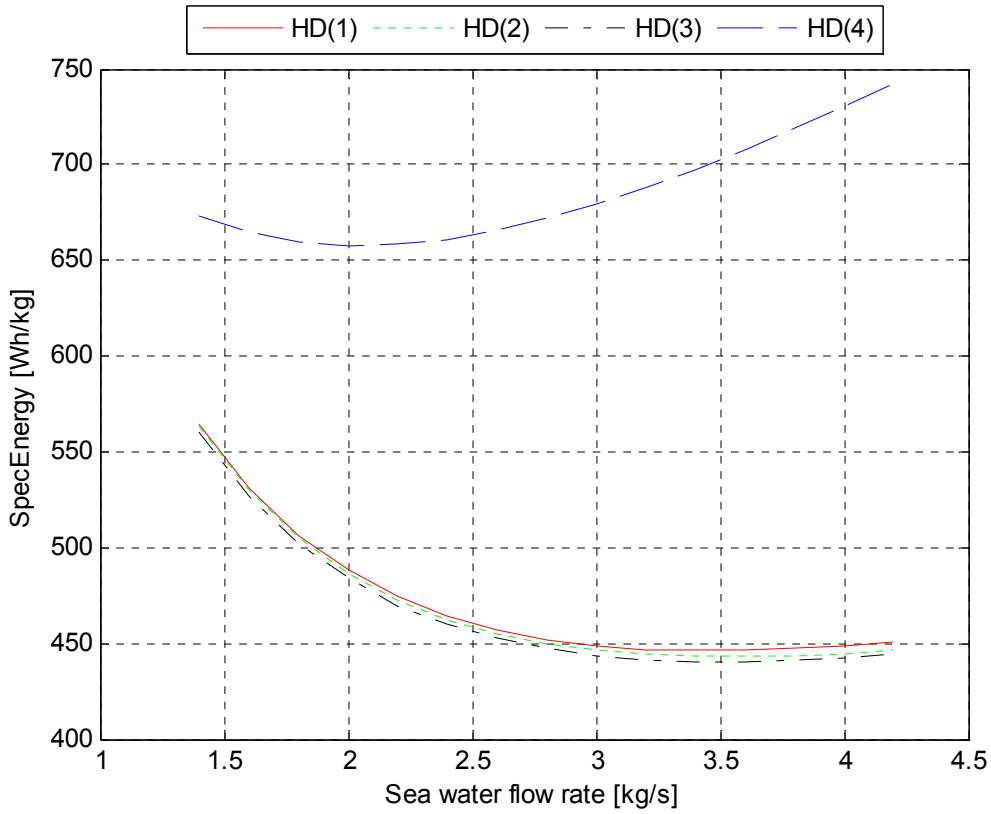

Figure 2-27: Specific energy as function of sea water flow rate

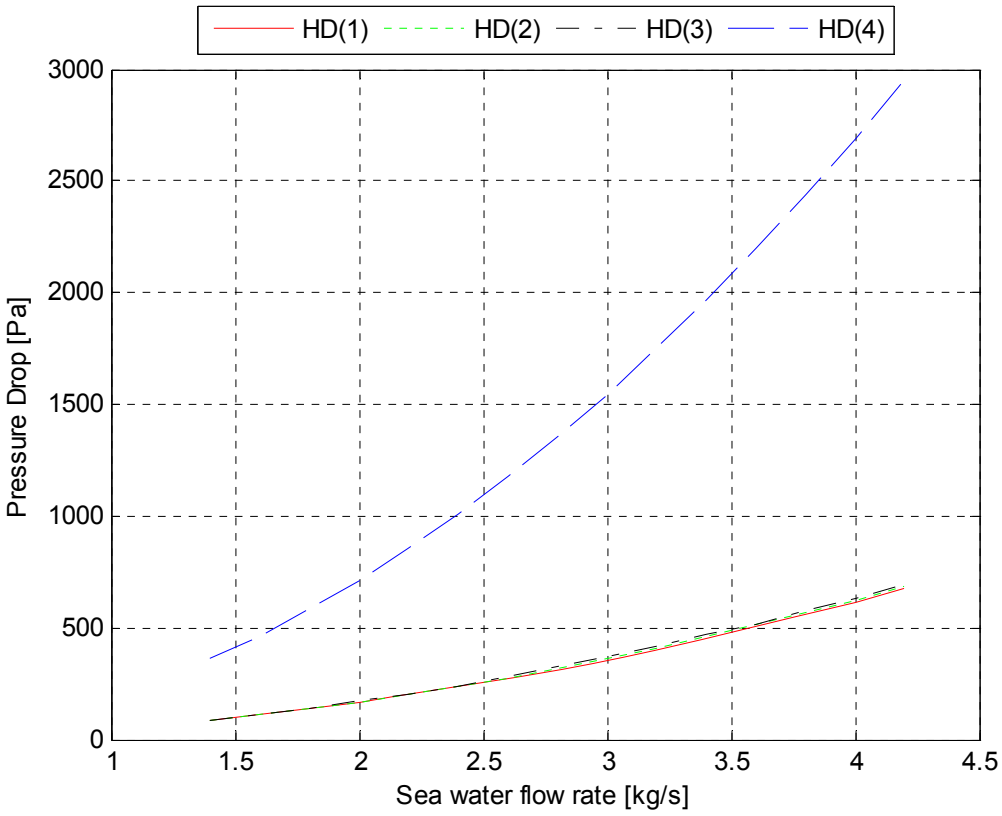

Figure 2-28: Total pressure drop as function of sea water flow rate

2.5.5 Analysis on sea water on air flow rate ratio

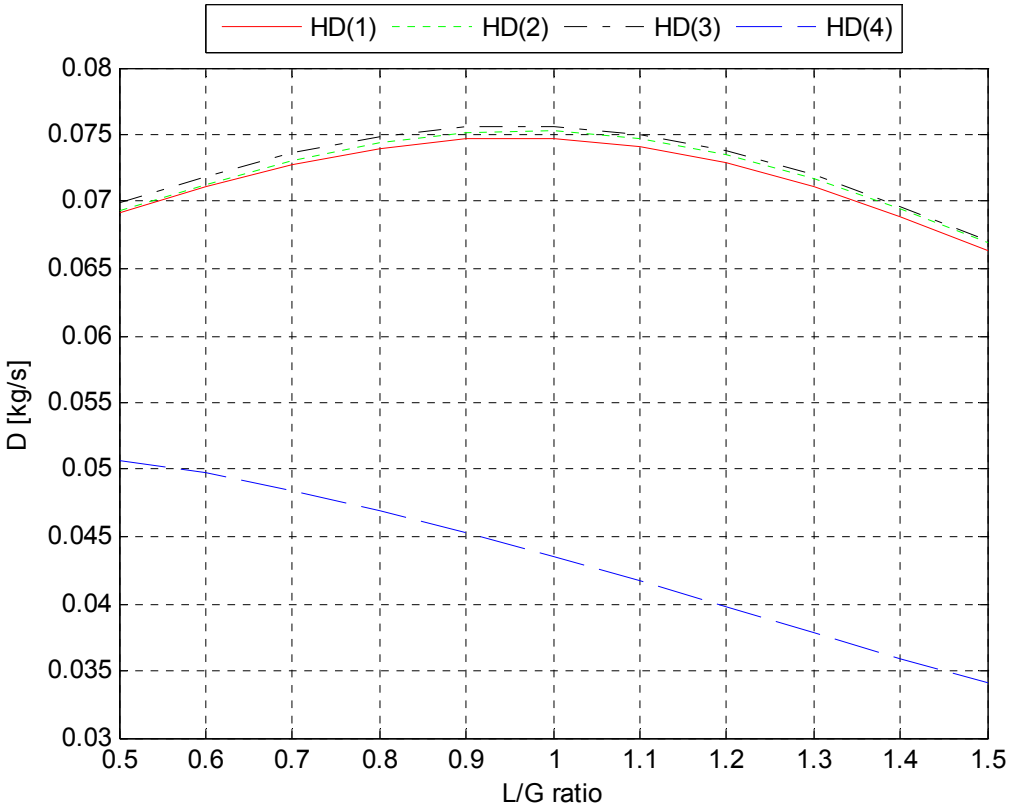

Figure 2-29: Fresh water flow rate as function of L/G ratio

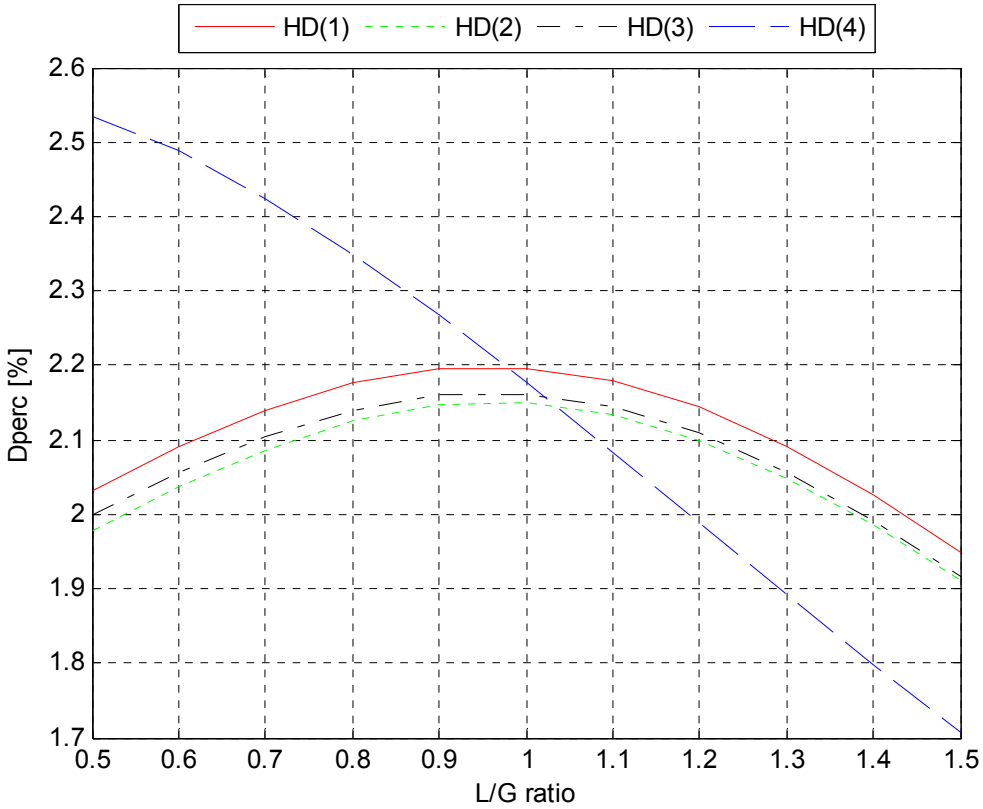

Figure 2-30: Percentage of fresh water on sea water flow rate as function of L/G ratio

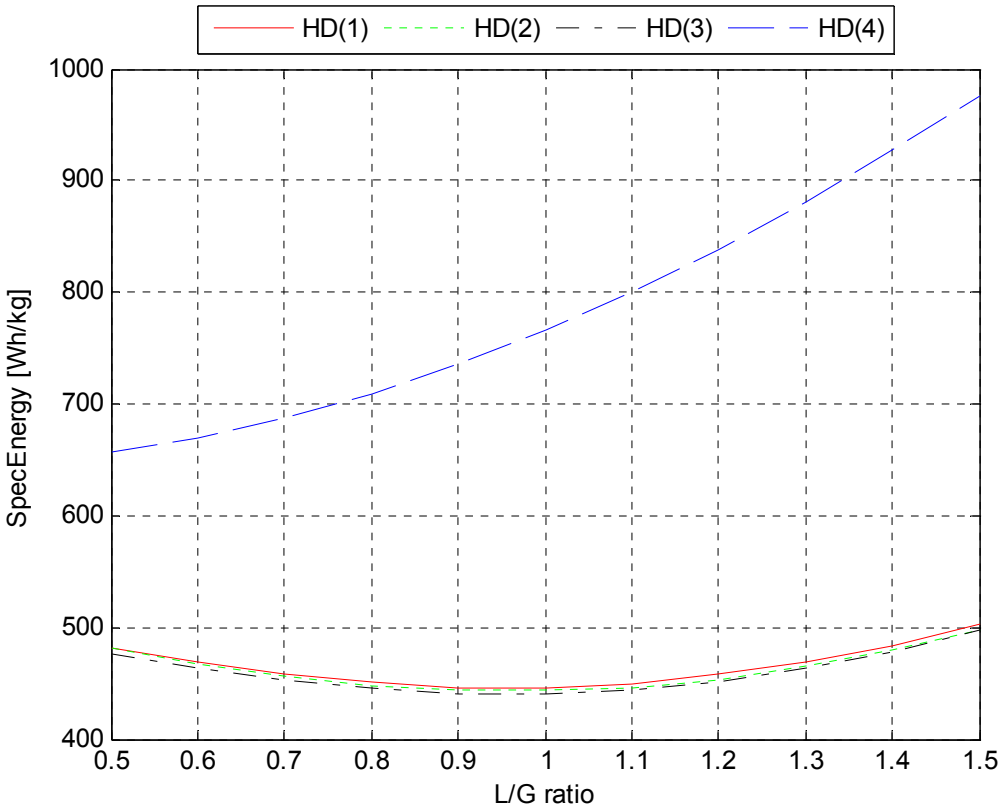

Figure 2-31: Specific energy as function of L/G ratio

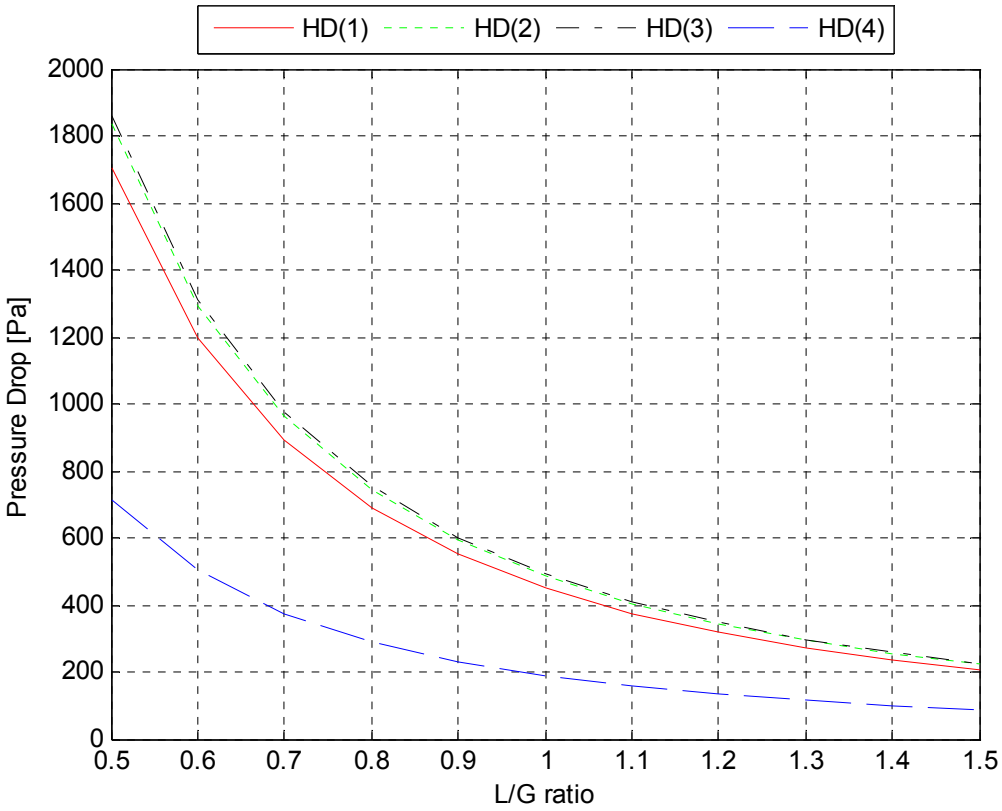

Figure 2-32: Total pressure drop as function of L/G ratio

2.5.6 Analysis on sea water flow rate for condenser in configuration (4)

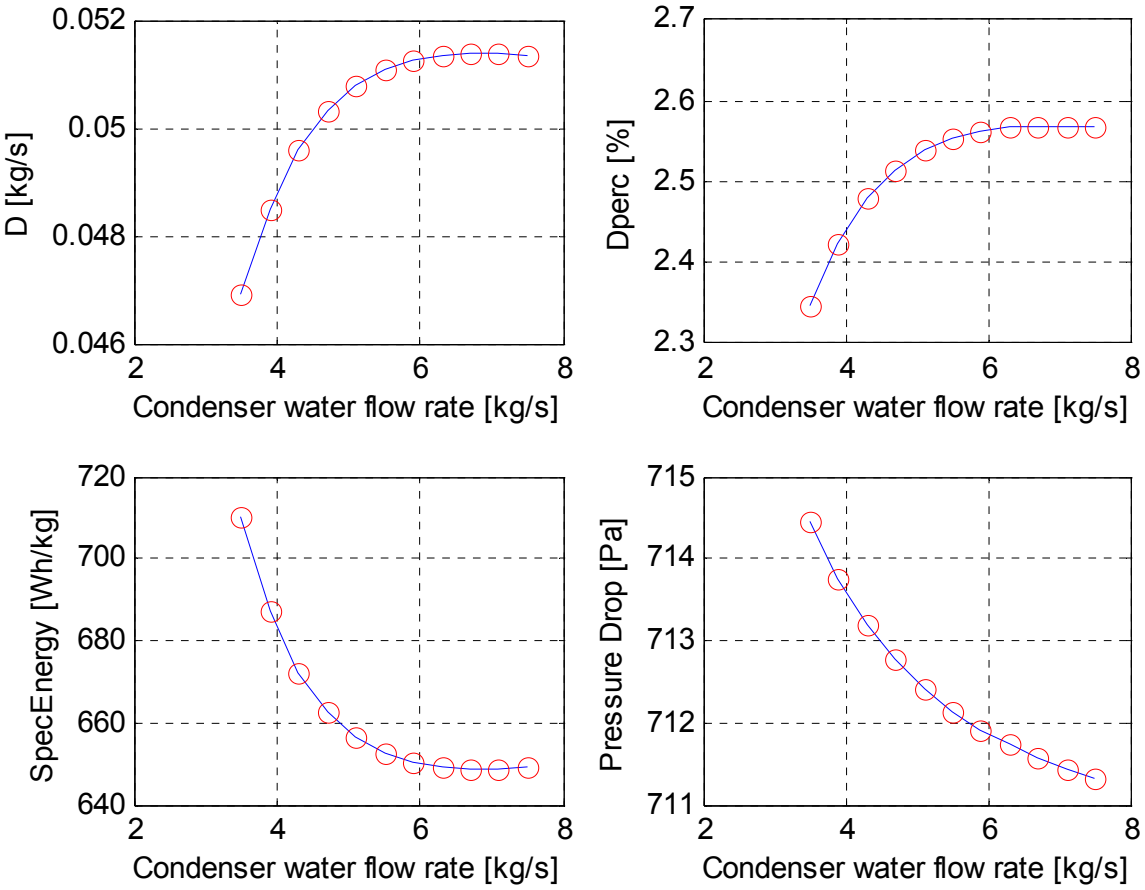

Figure 2-33: Monitored parameters as function of condenser water flow rate (Configuration 4)

2.6 Results

From the previous charts it can be noted the similar performances of the desalinators in configurations (1), (2), and (3). The surface areas of condensers, humidifiers and recuperators were deliberately chosen identical to allow a direct comparison among these three configurations:

- Condenser surface area: 1500m^2;
- Humidifier surface area: 300m^2; two humidifiers of 150m^2 for the HD unit in conf. (3);
- Recuperator surface area: one humidifier of 40m^2 for the HD unit in conf. (2), two humidifiers of 20m^2 for the HD unit in conf. (3).

Figure 2-21 represents the fresh water productivity as function of the recuperator surface area: the recuperator improves slightly the performance desalinator. For this reason a small surface area was chosen for the component. It's interesting to note how two humidifier of 20m^2 work better than one humidifier of 40m^2. Figure 2-23 confirm this behavior.

The analysis on condenser surface area (Figure 2-13,14,15) shows that a surface larger than 2000m^2 could be chosen, but it was preferred to limit this area to 1500m^2. The same is true for the humidifier surface area (Figure 2-17,18,19): a surface larger than 500m^2 could be chosen, but this area was limited to 300m^2. The reasons for these area limitations were the augmentation of HD unit height and the increase of the total pressure drops at surfaces increasing (Figure 2-16,20).

The fresh water production of HD unit in configuration (4) is 30% lower than HD units in previous configurations, while the specific energy needed to the process in conf. (4) is almost 45% bigger than previous cases. HD unit in conf. (4) allows to provide cooler sea water to the heat source, but it is necessary to double the consume of sea water to obtain this advantage. The results of the sensitivity analysis are shown in table 2-2.

	HD unit configurations			
Design parameters	**(1)**	**(2)**	**(3)**	**(4)**
Height of HD unit (m)	6,120	6,200	6,200	8,005
Condenser Area (m^2)	1500	1500	1500	1600
Humidifier Area (m^2)	300	300	150 x 2	400
Humidifier recuperator Area (m^2)	/	40	20 x 2	/
Condenser recuperator Area (m^2)	/	/	/	250
Sea water flow rate L (kg/s)	3,4	3,5	3,5	2,0
Condenser water flow rate Lcond (kg/s)	/	/	/	5,0
L/G ratio	1,0	1,0	1,0	0,5
Performance parameters	**(1)**	**(2)**	**(3)**	**(4)**
Heater power (kW)	120	120	120	120
Fan power (kW)	1,9	2,1	2,1	3,4
Fresh water production (kg/hr)	269,3	271,3	272,7	182,94
Specific Energy (Wh/kg)	445,6	442,3	440,0	655,9
Fresh water on seawater percentage (%)	2,20	2,15	2,16	2,54
Total pressure drop (Pa)	451,0	485,9	492,4	712,5

Table 2-2: Results of sensitivity analysis

The following tables (2-3,4,5,6) show the fluid properties achieved by HD units in steady state.

Fluids Properties					
Water			Air		
Point	Properties		Point	Properties	
1	T (°C)	20,00	5	T (°C)	26,49
	H (kJ/kg)	83,72		H (kJ/kg)	82,63
2	T (°C)	36,24		Spec. Humid (kg/kg dry air)	0,0220
	H (kJ/kg)	151,69		Rel. Humid	100%
3	T (°C)	44,67	6	T (°C)	38,19
	H (kJ/kg)	186,98		H (kJ/kg)	151,43
4	T (°C)	28,93		Spec. Humid (kg/kg dry air)	0,0440
	H (kJ/kg)	121,11		Rel. Humid	100%
Fresh Water	T (°C)	26,49			
	H (kJ/kg)	110,89			

Table 2-3: Fluid properties for HD unit in configuration (1)

Fluids Properties					
Water			Air		
Point	Properties		Point	Properties	
1	T (°C)	20,00	6	T (°C)	26,32
	H (kJ/kg)	83,72		H (kJ/kg)	81,86
2	T (°C)	35,93		Spec. Humid (kg/kg dry air)	0,0218
	H (kJ/kg)	150,40		Rel. Humid	100%
3	T (°C)	44,12	7	T (°C)	27,37
	H (kJ/kg)	184,69		H (kJ/kg)	82,96
4	T (°C)	28,93		Spec. Humid (kg/kg dry air)	0,0218
	H (kJ/kg)	121,09		Rel. Humid	94%
5	T (°C)	28,70	8	T (°C)	37,91
	H (kJ/kg)	120,13		H (kJ/kg)	149,31
Fresh Water	T (°C)	26,32		Spec. Humid (kg/kg dry air)	0,0433
	H (kJ/kg)	110,16		Rel. Humid	100%

Table 2-4: Fluid properties for HD unit in configuration (2)

Fluids Properties					
Water			Air		
Point	Properties		Point	Properties	
1	T (°C)	20,00	8	T (°C)	26,37
	H (kJ/kg)	83,72		H (kJ/kg)	82,10
2	T (°C)	36,01		Spec. Humid (kg/kg dry air)	0,0218
	H (kJ/kg)	150,72		Rel. Humid	100%
3	T (°C)	44,20	9	T (°C)	26,94
	H (kJ/kg)	185,01		H (kJ/kg)	82,69
4	T (°C)	36,85		Spec. Humid (kg/kg dry air)	0,0218
	H (kJ/kg)	154,27		Rel. Humid	96%
5	T (°C)	36,66	10	T (°C)	33,03
	H (kJ/kg)	153,45		H (kJ/kg)	116,51
6	T (°C)	28,82		Spec. Humid (kg/kg dry air)	0,0325
	H (kJ/kg)	120,64		Rel. Humid	100%
7	T (°C)	28,70	11	T (°C)	33,85
	H (kJ/kg)	120,12		H (kJ/kg)	117,39
Fresh Water	T (°C)	26,37		Spec. Humid (kg/kg dry air)	0,0325
	H (kJ/kg)	110,39		Rel. Humid	95%
			12	T (°C)	37,98
				H (kJ/kg)	149,88
				Spec. Humid (kg/kg dry air)	0,0435
				Rel. Humid	100%

Table 2-5: Fluid properties for HD unit in configuration (3)

Fluids Properties					
Water			Air		
Point	Properties		Point	Properties	
1	T (°C)	20,00	6	T (°C)	21,49
	H (kJ/kg)	83,72		H (kJ/kg)	60,94
2	T (°C)	28,08		Spec. Humid (kg/kg dry air)	0,0161
	H (kJ/kg)	117,53		Rel. Humid	100%
3	T (°C)	34,33	7	T (°C)	27,67
	H (kJ/kg)	143,72		H (kJ/kg)	67,75
4	T (°C)	25,73		Spec. Humid (kg/kg dry air)	0,0157
	H (kJ/kg)	107,71		Rel. Humid	67%
5	T (°C)	26,90	8	T (°C)	30,99
	H (kJ/kg)	112,61		H (kJ/kg)	110,10
Fresh Water	T (°C)	21,49		Spec. Humid (kg/kg dry air)	0,0288
	H (kJ/kg)	89,96		Rel. Humid	100%

Table 2-6: Fluid properties for HD unit in configuration (4)

Chapter 3: Cogeneration system

The insertion of the desalinator model in a cogeneration system able to produce both fresh water and chiller energy was the following step. The system was simulated by MATLAB and TRNSYS, while GenOpt was used to optimize the project parameters.

3.1 Heat pumps as a source of heat energy for seawater desalination

The use of heat pump to drive the desalination process is not a new concept: in open literature is possible to find many works dealing with this option.

Gunzbourg and Larger [1] presented an economic assessment of a dual purpose plant in which an AHP is coupled to an MED unit with a capacity of 9600 m^3/d. Not only an MED process has been proposed for coupling to an AHP, but also multistage flash (MSF) distillation [2-5].

With regard to small capacity and low performance ratio desalination systems, several authors proposed the use of a single-effect absorption cycle of LiBr-H_2O for a single effect MED process; different designs are reported in the literature: Al-Juwayhel et al. [6], Elshamarka [7], Nguyen et al. [8], Huicochea et al. [9], Mandani et al. [10], Siquieros and Holland [11]. Such systems could be technically and economically feasible for remote areas even though they have low fresh water on seawater ratio. Al-Juwayhel et al. [6] and Mandani et al. [10] presented a detailed thermodynamic model for the proposed systems. Additionally, the system proposed by Nguyen et al. [8] is driven by a hybrid gas/solar system. Moreover, Siquieros and Holland [11] reported the implementation of a small pilot plant with production of $4{,}5 \cdot 10^{-3}$ m^3/h.

Among the possible applications in the world, two case studies deserve to be mentioned: the experimental desalination plant in Almeria (Spain), and a simulation study in New Mexico (USA).

3.1.1 Almeria

In 2002 a double effect absorption heat pump (DEAHP) has been implemented and connected to a MED unit at the Plataforma Solar de Almería (CIEMAT), Spain [12,13].

The seawater system designed under the AQUASOL Project consists of:

- A multi-effect distillation plant with 14 effects
- A stationary CPC (compound parabolic concentrator) solar collector field
- A thermal storage system based on water
- A double effect (LiBr-H_2O) absorption heat pump
- A smoke-tube gas boiler
- An advanced solar dryer for final treatment of the brine

These subsystems are interconnected as shown in Figure 3-1. The system operates with water as heat transfer fluid, which is heated as it circulates through the solar collectors.

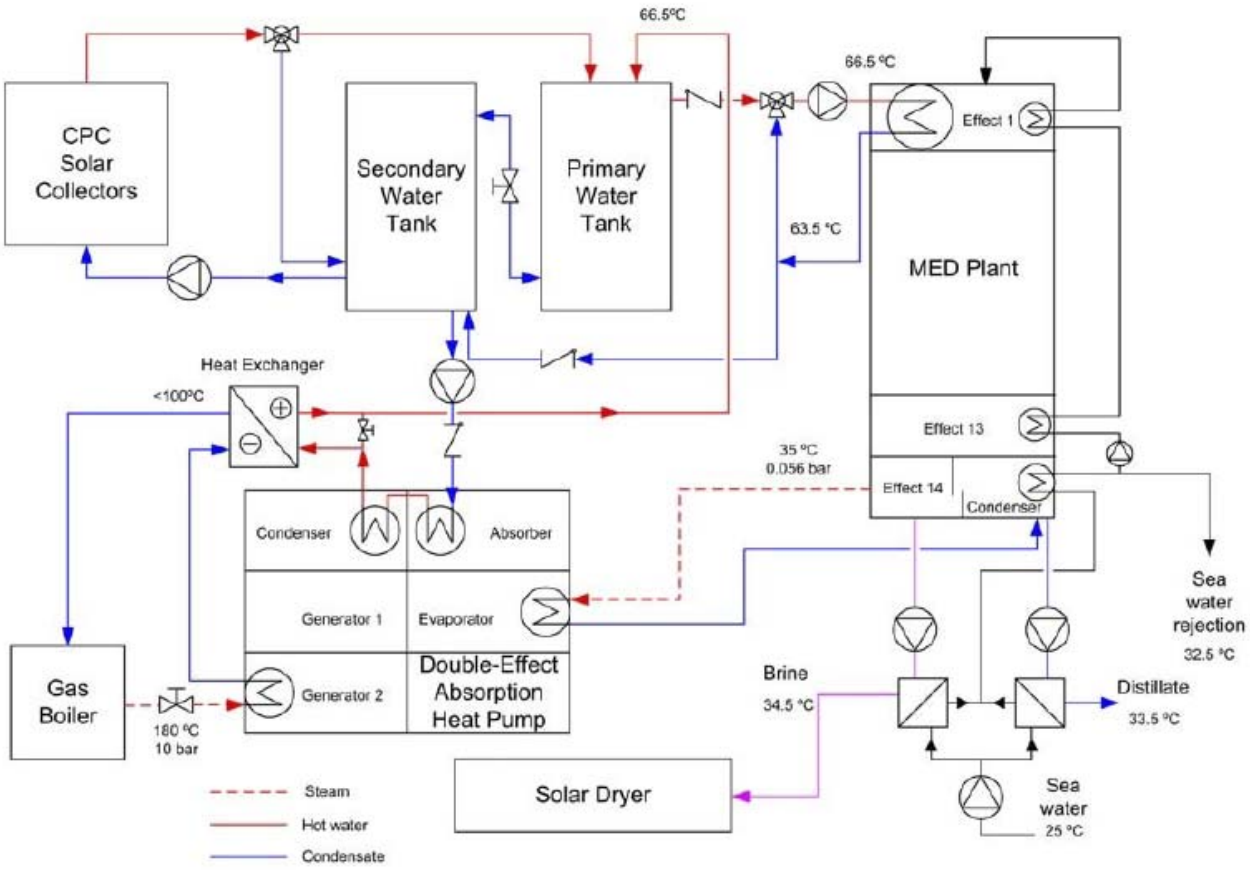

Figure 3-1: Conceptual layout and main subsystems of AQUASOL plant.

The solar energy is thus converted into thermal energy in the form of the sensible heat of the water, and is then stored in the primary water tank. Hot water from the storage system provides the MED plant with the required thermal energy. In absence of solar radiation, the gas boiler feeds the absorption heat pump, which is also feed with low temperature steam from the last MED plant effect , in order to heat the water coming from first effect from 63,3°C up to 66,5°C.

The storage system is composed of two interconnected 12 m^3 capacity water tanks required in order to store the surplus energy provided by the solar field, match the inlet and outlet flows of the different subsystems and permit the partial load operation of the DEAHP.

The gas (propane) to be burnt is stored in a 2450 l tank installed next to the distillation plant building. This tank volume provides an estimated autonomy of 143 h at full load. Return condensate flow must be cooled in order to avoid flashing, and a heat exchanger was installed for this reason, transferring the energy to the stream that connects the absorption heat pump with the thermal storage tank.

Figure 3-2 shows a diagram of the energy balance of MED plant coupled to the DEAHP. The heat pump supplies the 200 kW of thermal energy at 65°C required by the first effect of the MED plant. From this quantity 110 kW are recovered by the evaporator of the heat pump in the form of steam at low temperature (35°C). In order to drive this process, the heat pump needs 90 kW of thermal

energy at 180°C. The thermal consumption of the combined system corresponds to 30kWh/m^3 of fresh water.

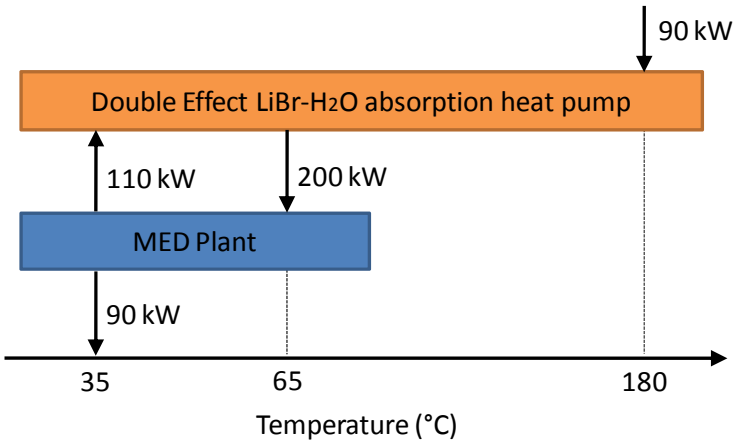

Figure 3-2: Energy balance of MED plant coupled to a DEAHP

Furthermore, the DEAHP is able to operate at partial load, which results very useful for desalination process. Table 3-1 shows the thermal design parameters of the DEAHP prototype working at different load values. As it can be seen, the coefficient of performance (COP), defined as the ratio of the energy delivered by the heat pump to the primary energy received by it at 180°C, drops as the steam load decreases.

		DEAHP load (%)			
		100	75	50	30
Low pressure steam	Power, kW	100	75	50	30
	Pressure inlet, bar	0.056	0.056	0.056	0.056
	Temp. inlet, °C	35	35	35	35
	Flow rate, kg/s	0.041	0.031	0.021	0.012
Cooling water	Power, kW	182	138	92	56
	Temp. inlet, bar	64	64	64	64
	Temp. outlet, °C	67.62	66.74	65.84	65.12
	Flow rate, kg/s	12	12	12	12
High pressure steam	Power, kW	82	63	42	26
	Pressure inlet, bar	10	10	10	10
	Temp. inlet, °C	180	180	180	180
	Flow rate, kg/s	0.041	0.031	0.021	0.014
COP		2.22	2.20	2.18	2.14

Table 3-1: Thermal design of the DEAHP installed in AQUASOL Project

3.1.2 New Mexico

Gude and Nirmalakhandan [14] proposed the system shown in figure 3-3. Main components of the system are a desalination unit, a sensible heat thermal energy storage (TES) unit, and an absorption refrigeration system (ARS). The desalination unit includes an evaporation chamber

(EC), a condenser (CON), two heat exchangers (HE1 and HE2), and three 10-m tall columns. These three columns serve as the saline water column; the brine withdrawal column; and the desalinated water column, each with its own holding tank, SWT, BT, and DWT, respectively. The heat input to EC is provided by the TES, which, in turn, is maintained at 50°C by the ARS.

The EC is installed at the top of the three columns at a height of about 10 m above the free surfaces in the three holding tanks, creating a Torricelli's vacuum in the head space of the EC. The temperature of the head space of the feed water column is maintained slightly higher than that of the desalinated water column. Since the head spaces are at near-vacuum level pressures, temperature differential as small as 10°C is adequate to evaporate water from the saline water side and condense in the fresh water side. In this manner, saline water can be desalinated at about 40–50°C, which is in contrast to the 60–100°C range employed in traditional solar stills and other distillation processes. A continuous stream of brine is withdrawn from the EC through HE1 preheating the saline water feed entering the EC and maintaining the desired salt level in the EC.

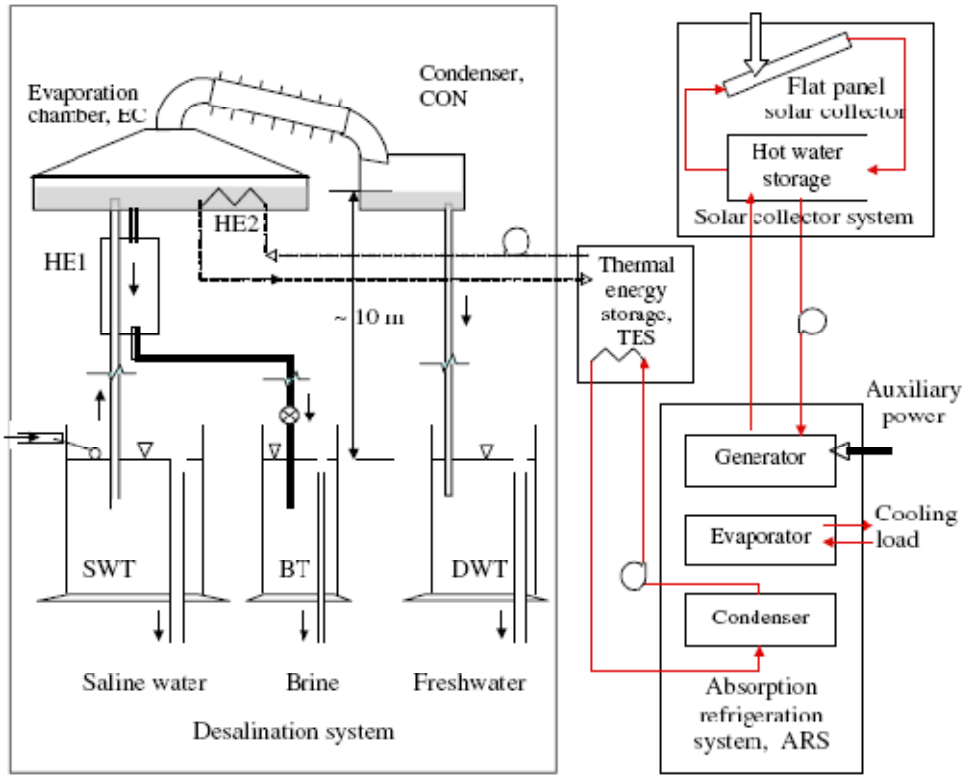

Figure 3-3: Layout of the desalination system proposed by Gude and Nirmalakhandan

This configuration drives the desalination process without any mechanical pumping. Thermal energy to maintain the EC at the desired temperature is provided by the thermal energy storage (TES) system, whose temperature is set at 50°C. The thermal energy required to maintain the TES at this temperature is provided by the heat rejected by an absorption refrigeration system (ARS). The ARS evaluated in this study operates with LiBr–H_2O as refrigerant under a pressure range of 1–

16 kPa. Energy required to heat the generator of ARS is supplied by a solar collector during sunlight hours and by an auxiliary electric heater during non-sunlight hours. In this manner, the thermal energy to drive the desalination process is available round the clock. The generator of the ARS is maintained at 100°C. Since the evaporator of the ARS feeds the cooling load, the proposed system performs two functions of continuous desalination and cooling with reduced amount of external non-renewable energy input.

Apart from the solar energy, the proposed system requires additional mechanical energy to drive the pumps and additional heat energy for the generator to drive the ARS during non-sunlight hours. Simulation results show that the additional mechanical energy requirement is 16 kJ/kg of product plus auxiliary heat energy of 192 kJ/kg of product, totaling to a specific energy requirement of 208 kJ/kg. In comparison, a typical multi-stage flash distillation process requires mechanical energy of 45 kJ/kg of product plus heat energy of 310 kJ/kg of product, totaling to a specific energy requirement of 355 kJ/kg [15].

3.2 Development of a new cogeneration system

In this study the heat pump is used not only to drive the desalination process, but also to produce chiller energy, like in the New Mexico case study [14]: this kind of coupling between a low temperature desalination unit and a refrigeration unit powered by solar energy appears new and essentially unexplored.

The layout of the solar driven fresh water/cooling integrated system is shown in figure 3-4. A field of evacuated tube solar collectors feeds a single stage LiBr–H_2O absorption chiller. An hot storage is interposed to smooth hot water temperature variations, related to solar radiation changes. The heat rejected from the chiller is recovered as heat source for the desalinator. The system produces cooling power by the absorption chiller and then fresh water from the desalination unit. Sea water is used as cooling medium of the absorption machine. The main difference with the Gude and Nirmalakhandan system [14] is the direct coupling of the chiller with the desalinator, while in their case the coupling was indirect.

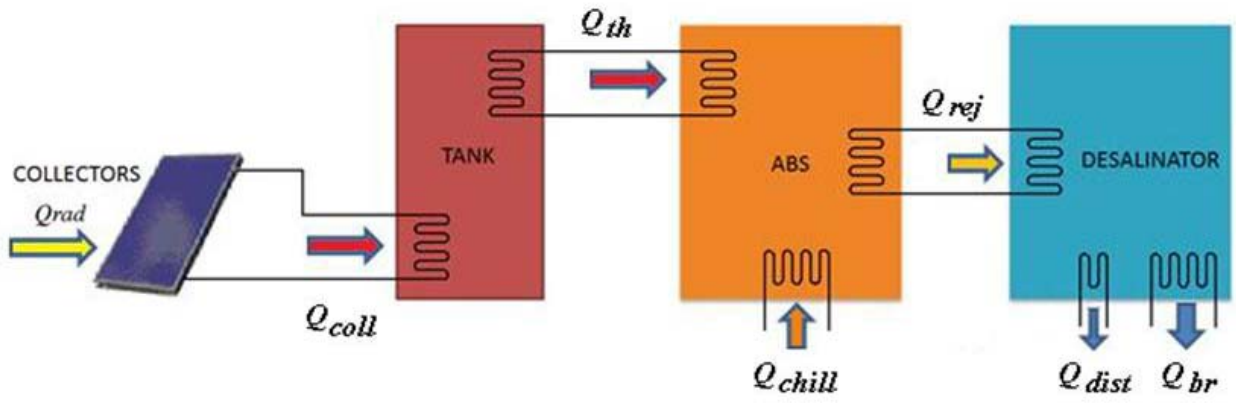

Figure 3-4: Layout of the freshwater/cooling cogeneration system

For this study a Thermax absorption chiller from the LT series was selected, with a nominal cooling capacity of 50 kW. In Figure 3-5 a schematic of the chiller shows the internal heat exchanger and the external circuits. Absorber and condenser are cooled in series. Nominal operating conditions of this unit when employed for a standard solar cooling plant are reported in Table 3-2.

Concerning absorption chiller performance, it is well known that it is strongly influenced by temperature levels of heat transfer in the internal heat exchangers (evaporator, condenser, absorber and generator). Higher temperatures both of inlet hot water and outlet chilled water lead to a higher efficiency (*COP*) and cooling capacity. On the opposite higher temperature levels of heat rejection cause a significant performance decrease. An appropriate choice of these temperatures can significantly improve overall performance of the cogeneration system. In order to predict the chiller behavior all over the wide range of possible operating conditions occurring in this study, a simulation code, capable to solve the thermodynamic cycle of LiBr absorption machine, has been used [16, 17]. Once heat exchanger surface data have been set and main input data (inlet temperature levels of hot water, chilled water and cooling water) have been given, the code calculates all working fluid conditions all over the cycle, i.e. pressure, temperature, concentration of LiBr-water mixture and flow rate. The main assumptions of the model are the steady state conditions and fixed mass flow rates of external flows.

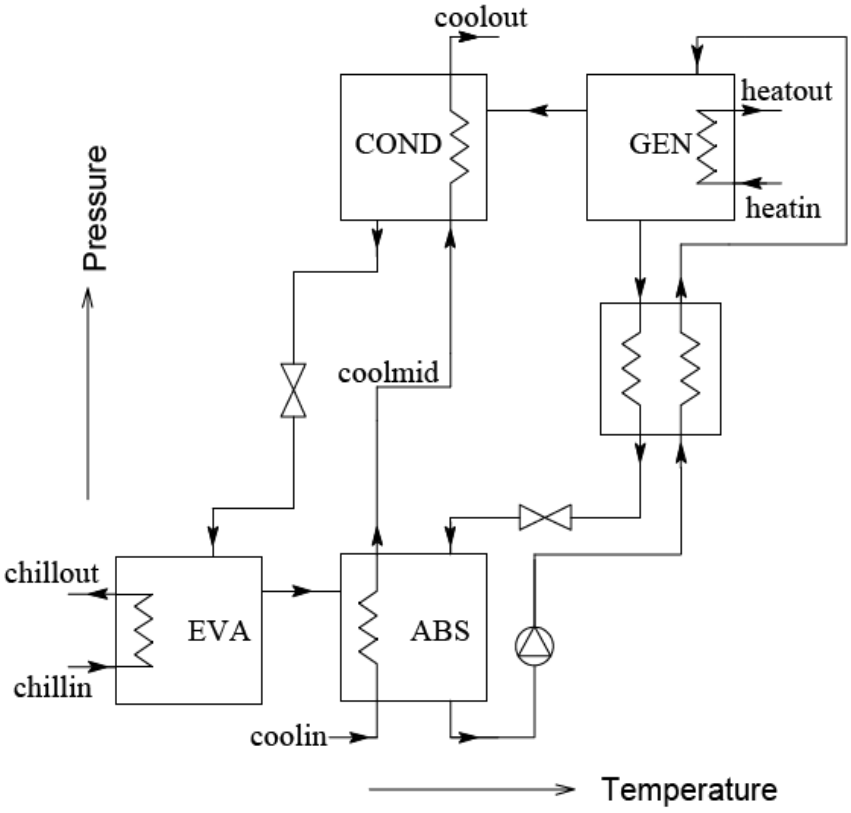

Figure 3-5: Schematic of a single stage LiBr Chiller

Capacity	50 kW	$T_{heat,in}$	90°C
COP	0.697	$T_{heat,out}$	80°C
Heat source	71.7 kW	$T_{chill,in}$	12°C
Rejected heat	121.7 kW	$T_{chill,out}$	7°C
m_{heat}	1.71 kg/s	$T_{cool,in}$	29°C
m_{chill}	2.39 kg/s	$T_{cool,out}$	33.6°C
m_{cool}	6.32 kg/s	Evaporator pressure	715 Pa
		Condenser pressure	5346 Pa

Table 3-2: Nominal performance and operation conditions of the chiller

Figure 3-6 shows a typical trend of non-dimensional capacity (a) and *COP* (b) vs. inlet temperature of the cooling water, for 100%, 50% and 25% design flow rate. Plotted data have been obtained for an inlet hot water temperature of 90°C and an inlet chilled water temperature of 12°C.

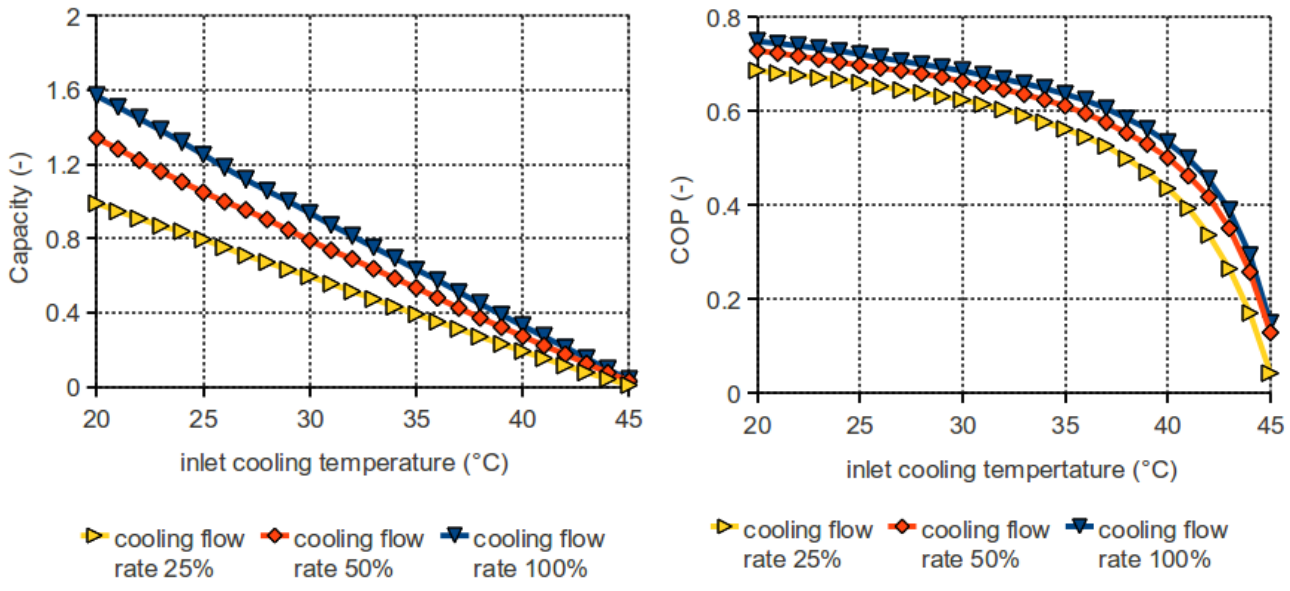

(a) **(b)**

Figure 3-6: Chiller performance vs. inlet cooling temperature

When inlet cooling water temperature is increased, both cooling capacity and chiller efficiency undergo a strong decrease. This effect is amplified if a reduction of the mass flow rate takes place: this stands specifically for the capacity. With regard to desalination process, a temperature increase of the cooling flow is expected to produce beneficial effects. So it is clear that the key point in the design of cooling-fresh water cogeneration system is the selection of the temperature level at which heat is rejected form the chiller. By changing this temperature level the cogeneration can be alternatively oriented towards cooling or distilled water production.

The desalination units considered for the design simulations are the HD desalinators in configuration (1) and (4):

- Configuration (1): Sea water is first preheated inside the desalinator condensing section, then it is used to cool the absorption chiller; here it flows first through the absorber and then through the condenser. At the exit, heated salt water is sprayed into humidifier to saturate circulating air. Hot saturated humid air then flows through the condenser/dehumidifier section, where condensation of air water vapor takes place, producing fresh water. The global layout of this configuration is shown in Figure 3-7.

- Configuration (4): there are two different sea water flows, one for the condenser and his recuperator (Lcond), and another one for the absorption chiller and the humidifier (L). The chiller is cooled with not preheated seawater, so we expect an increased production of cooling energy and a lower production of fresh water than the previous case. The global layout of this configuration is shown in Figure 3-8.

A fresh water to cooling power index I_d has been defined in order to evaluate the ratio between the two outputs of the system. This index is non-dimensional thanks to a reference specific energy for unit of fresh water produced: $E_{sp,ref}$. This value has been assumed equal to the specific thermal energy consumption of a large scale standard MSF (Multi Stage Flash desalination) or MED (Multi Effect Distillation) desalinating system (86 Wh/kg or 310kJ/kg) [15]:

$$I_d = D \cdot E_{sp,ref} / \dot{Q}_{chill} \tag{3.1}$$

An overall efficiency of the cogeneration system with respect to the inlet heat was also defined:

$$\eta_{ov} = \left(\dot{Q}_{chill} + D \cdot E_{sp,ref}\right) / \dot{Q}_{th} \tag{3.2}$$

Other significant parameters to describe the performance of this system are:

- distilled to sea water flow rate ratio (productivity): D/L (3.3)
- distilled water specific thermal energy : $E_{sp} = \dot{Q}_{rej}/D$ (3.4)

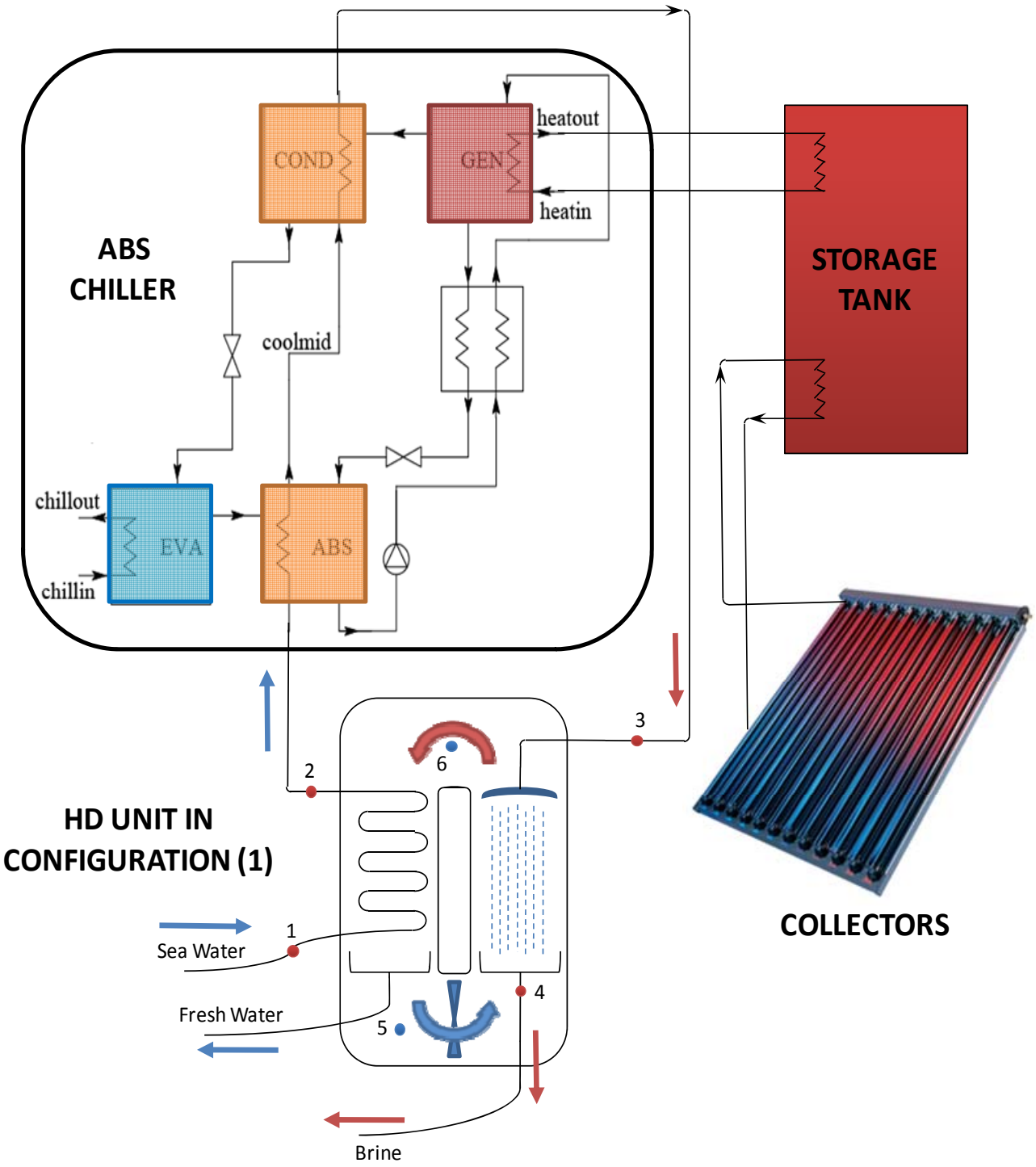

Figure 3-7: Global layout of the cogeneration system with HD unit in configuration (1)

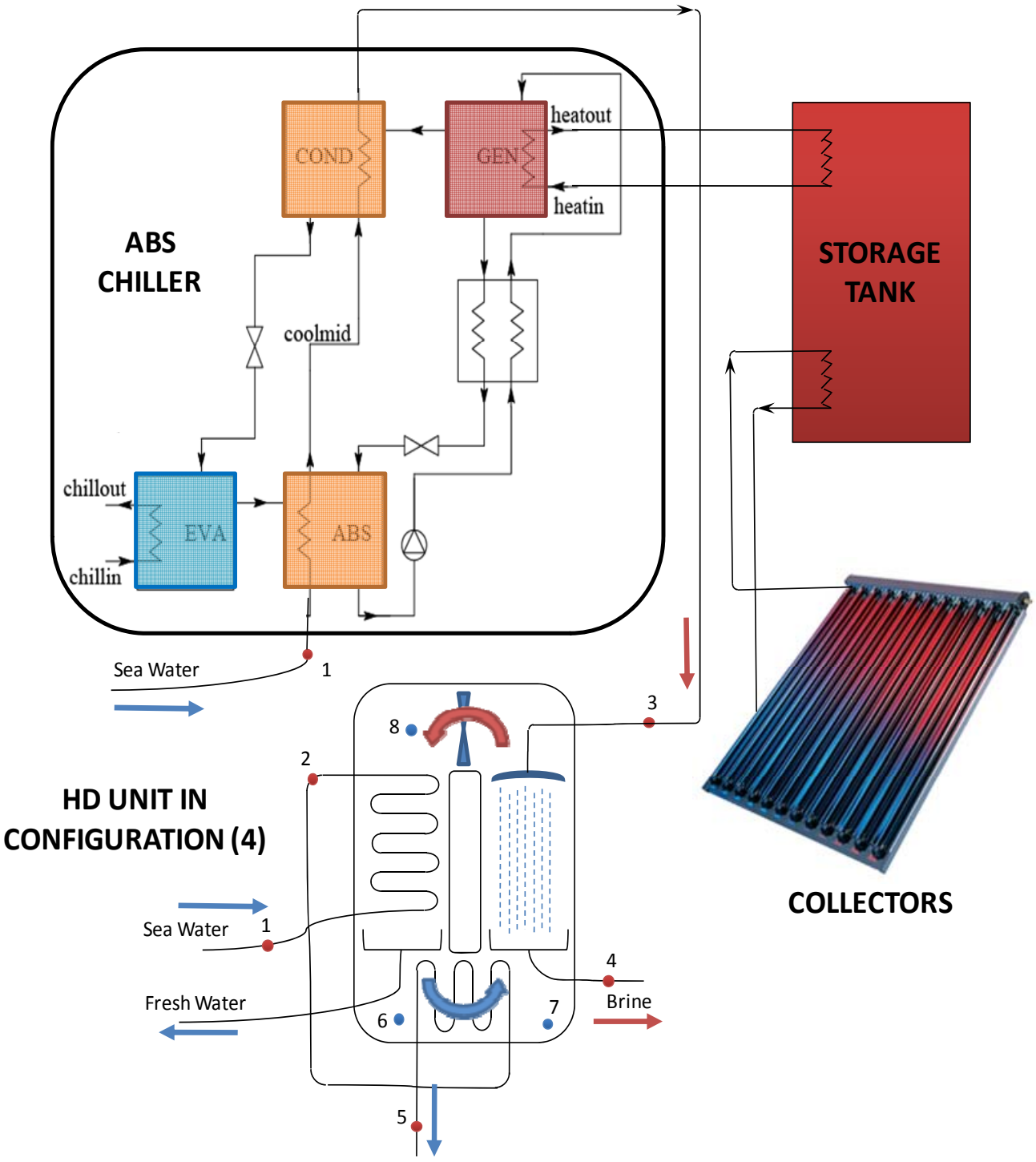

Figure 3-8: Global layout of the cogeneration system with HD unit in configuration (4)

3.3 Design simulation

The design simulation of the cogeneration system was performed in MATLAB, using the code developed for the HD desalinator. The addition of the absorption chiller was implemented by a mapping of all the Capacity and COP values, corresponding to T_{coolin}, T_{heatin} and mass sea water flow rate (L) changes. An interpolation on the actual values of T_{coolin}, T_{heatin} and L allows to calculate the heat power provided by the chiller to the desalination process. The chiller mapping has been created with a $T_{chillin}$ equal to 12°C.

The components of the HD unit in configuration (1) have been already sized (table 2-2), while the main assumption for the absorption chiller are shown in table 3-2. In order to investigate the effects on chiller performance and fresh water productivity, sea water flow rate has been varied in the range 2,6-7,6 kg/s.

Three sea water temperature levels have been considered (20-25-30°C) for the analysis shown in figure 3-9, while the chosen T_{heatin} was 90°C. Figure 3-9a and 3-9b show chiller performance vs. sea water flow rate at different temperatures. If flow rate is increased, the average temperature in the cooling circuit of the chiller decreases, producing a beneficial effect both on capacity (Q_{chill}) and *COP* accordingly with the chiller behavior documented in figure 3-6. A similar effect is given by sea water temperature: the warmer is the water, the lower is the chiller performance. Figure 3-9e shows that the productivity of fresh water (*D*) is strongly affected by the temperature of sea water. Moving from 20 to 30°C, *D* drops of about 30%, although the inlet temperature (T_3) is increasing (Figure 3-9c): this is due to the significant chiller capacity drop (up to 40%) that implies a dramatic reduction of rejected heat (Figure 3-9d). So it can be concluded that the major driver for fresh water production is the amount of thermal energy entering the desalinator, more than its temperature level. The augmentation of sea water flow rate produces a positive effect on fresh water productivity, even if there is an asymptotic trend. For higher sea water temperatures larger sea water flow rates are required.

The distilled water to cooling index I_d shows a decreasing trend (Figure 3-9f): at higher mass flow rates the cooling capacity grows more than the fresh water productivity. On the opposite, the specific energy increases with the sea water mass flow rate (Figure 3-9g), this because the rejected heat grows more than the productivity *D*. Looking at the overall system efficiency (Figure 3-9h), for each sea water temperature an optimum can be detected: the lower is the sea temperature, the lower is the optimal mass flow rate. At 20°C the best overall efficiency (1.03) takes place at about 3 kg/s, but at higher temperatures the optimal flow rate is much larger: about 6 kg/s for 30°C. It has to be pointed out that the optimal efficiency corresponds to a system design minimizing the solar collector field surface and hence the related costs.

Hot water temperature level has a strong influence on chiller behavior: higher values would be preferable as they lead to better performance in terms of capacity and *COP*. However it has to be reminded that the higher this temperature is, the lower the solar collector field efficiency will be. Therefore it is crucial to optimize the global plant efficiency taking into account also solar collector performance.

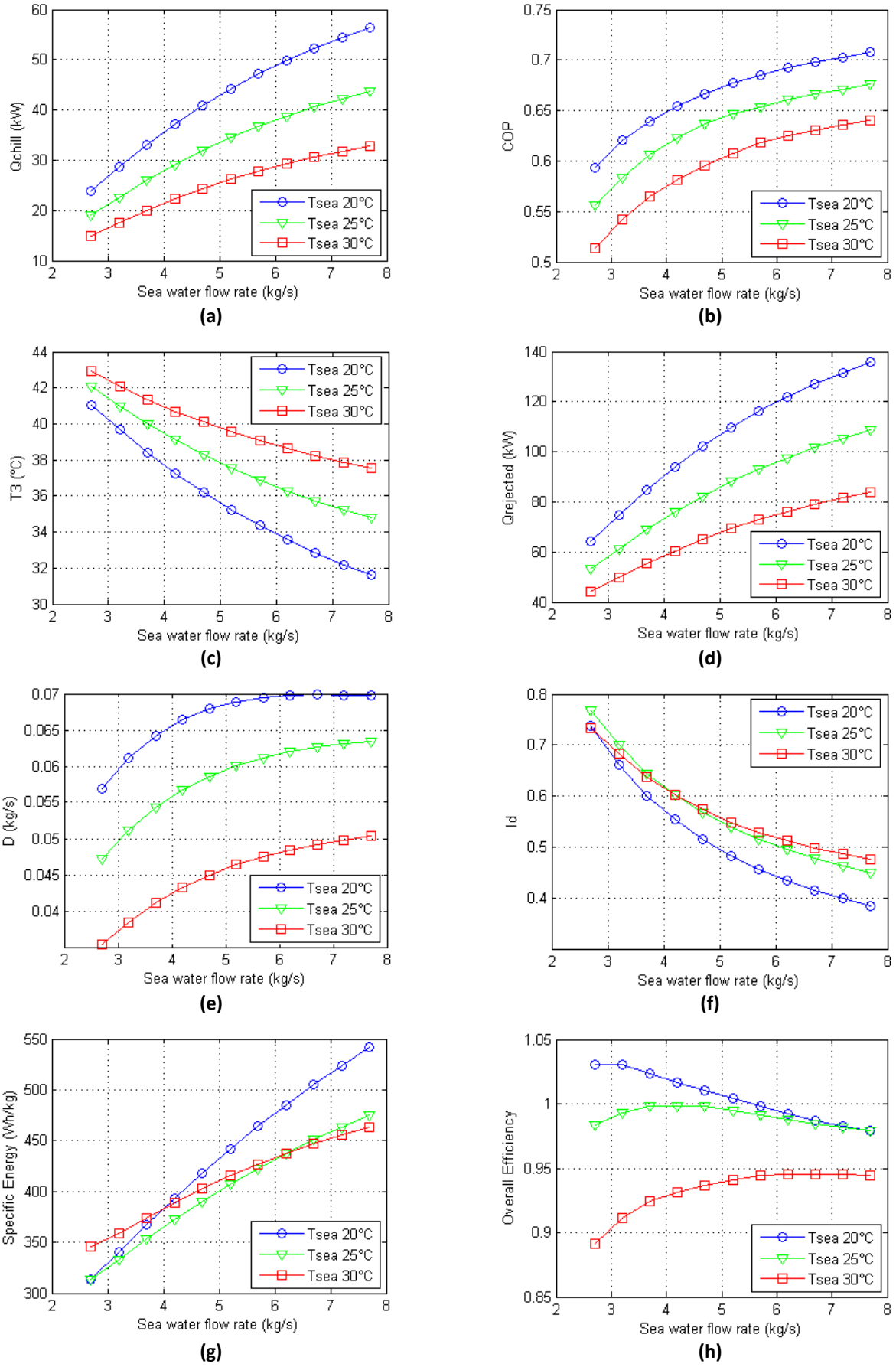

Figure 3-9: Performance for different sea water flow rates with HD unit in conf. (1)

To analyze the sensitivity of the chiller/desalinator system to inlet water temperature, additional simulations have been carried out. Figure 3-10 reports a comparison between the performance of the cogeneration system at 90°C and 110°C for different sea water flow rates and temperatures.

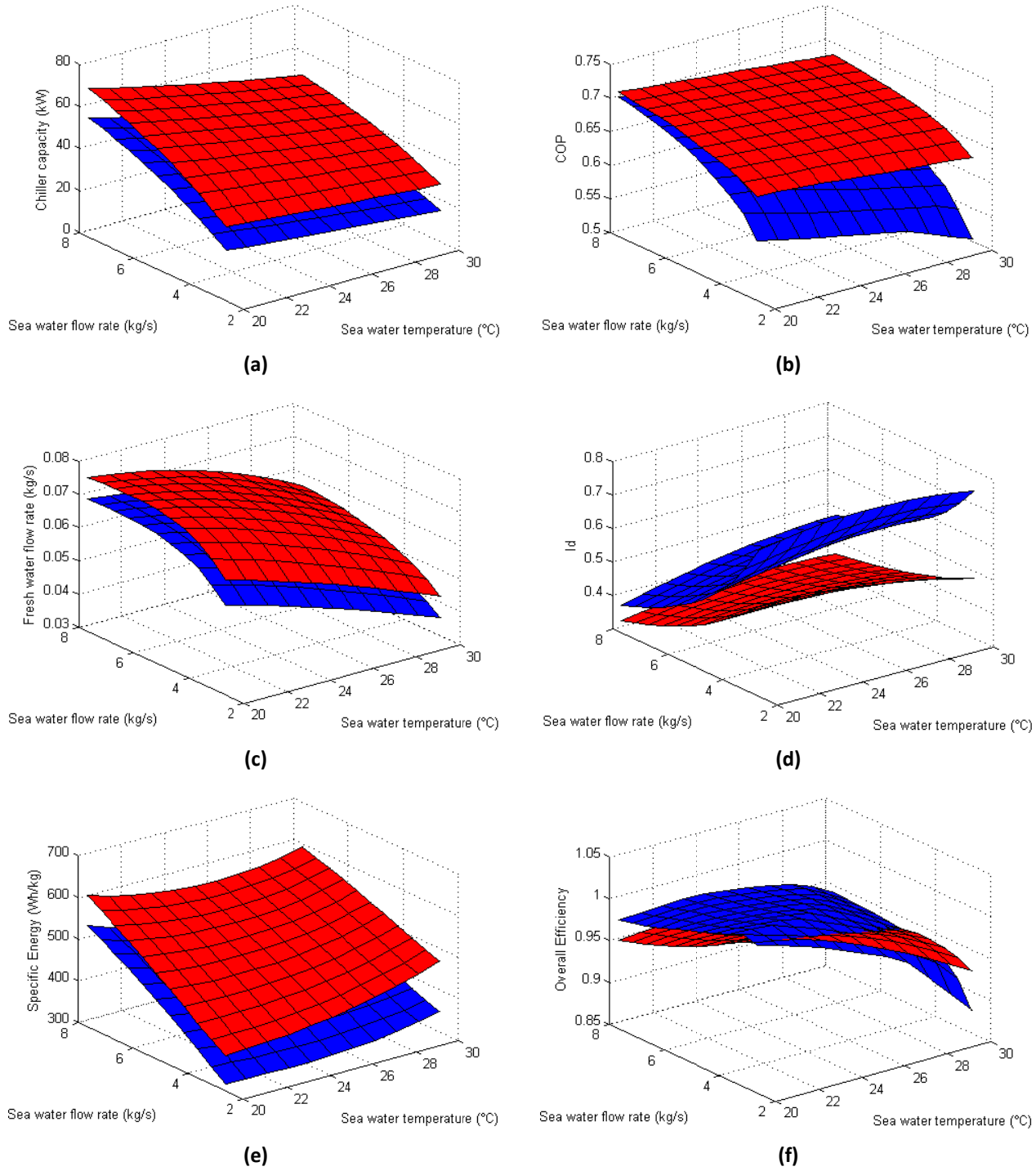

Figure 3-10: Performance for inlet heating temperature 90°C (blue) and 110°C (red) with HD unit in conf. (1)

Chiller capacity (Figure 3-10a) presents similar trends for the two considered temperature levels; however at 110°C the chiller provides about 20 kW more than for 90°. This roughly stands for all the considered sea water temperatures and mass flow rates. *COP* (Figure 3-10b) on the opposite, appears to be much more influenced by hot water temperature levels. At 110 °C chiller maintains almost stable values (in the range 0.62-0.70), while at 90°C *COP* undergoes a strong decrease either when the sea water flow is diminished or when the sea temperature is higher. Fresh water productivity (Figure 3-10c) at 110°C results to be generally greater (about 0.01 kg/s) because of the increased heat rejection. Nevertheless, I_d at 110°C (Figure 3-10d) is lower because the chiller capacity increases more than the fresh water productivity. Similarly, the required specific energy is always higher when the heat source is at 110°C (Figure 3-10e).

The overall system efficiency η_{ov} (Figure 3-10f) shows an interesting behavior: the case with inlet heating temperature at 90°C is generally more efficient, but with high sea water temperature (26-30°C) and low mass flow rate the system driven at 110°C performs better; in fact, under these conditions the absorption chiller *COP* at 90°C undergoes a major drop, down to 0.5 (Figure 3-10b). In conclusion, the use of an heat source at higher temperature appears to be a good strategy when the sea water temperature is high.

The same analysis has been carried out using desalinator in configuration (4) with design parameters shown in table 2-2. As we expect, the production of cooling power (figure 3-11a) is greater than the production of the cogeneration system in configuration (1), while the fresh water production is lower for sea water flow rate bigger than 3,5kg/s.

Figure 3-11a and 3-11b show chiller performance vs. sea water flow rate at different temperatures. If flow rate is increased, the average temperature in the cooling circuit of the chiller decreases, producing a beneficial effect both on capacity (Q_{chill}) and *COP* accordingly with the chiller behavior documented in figure 3-6. A similar effect is given by sea water temperature: the warmer is the water, the lower is the chiller performance. Thanks to the not preheated sea water, it is possible to obtain chiller capacity bigger than 50kW with sea water temperature of 20°C and 25°C, considering the complete range of sea water flow rates (2,6-7,6 kg/s), and with sea water temperature of 30°C with sea water flows bigger than 4,2kg/s.

The fresh water productivity (Figure 3-11e) is strongly affected by inlet sea water temperature, like in the previous configuration. Moving from 20 to 30°C, *D* drops of about 30%, although the inlet temperature (T_3) is increasing (Figure 3-11c): this is due to the significant chiller capacity drop (up to 40%) that implies a dramatic reduction of rejected heat (Figure 3-11d). However figure 3-11e shows that the fresh water productivity (*D*) decreases with increasing sea water flow rates. So it can be concluded that also the temperature water level is equally determinant to drive the fresh water production, and not only the rejected energy from the absorption chiller.

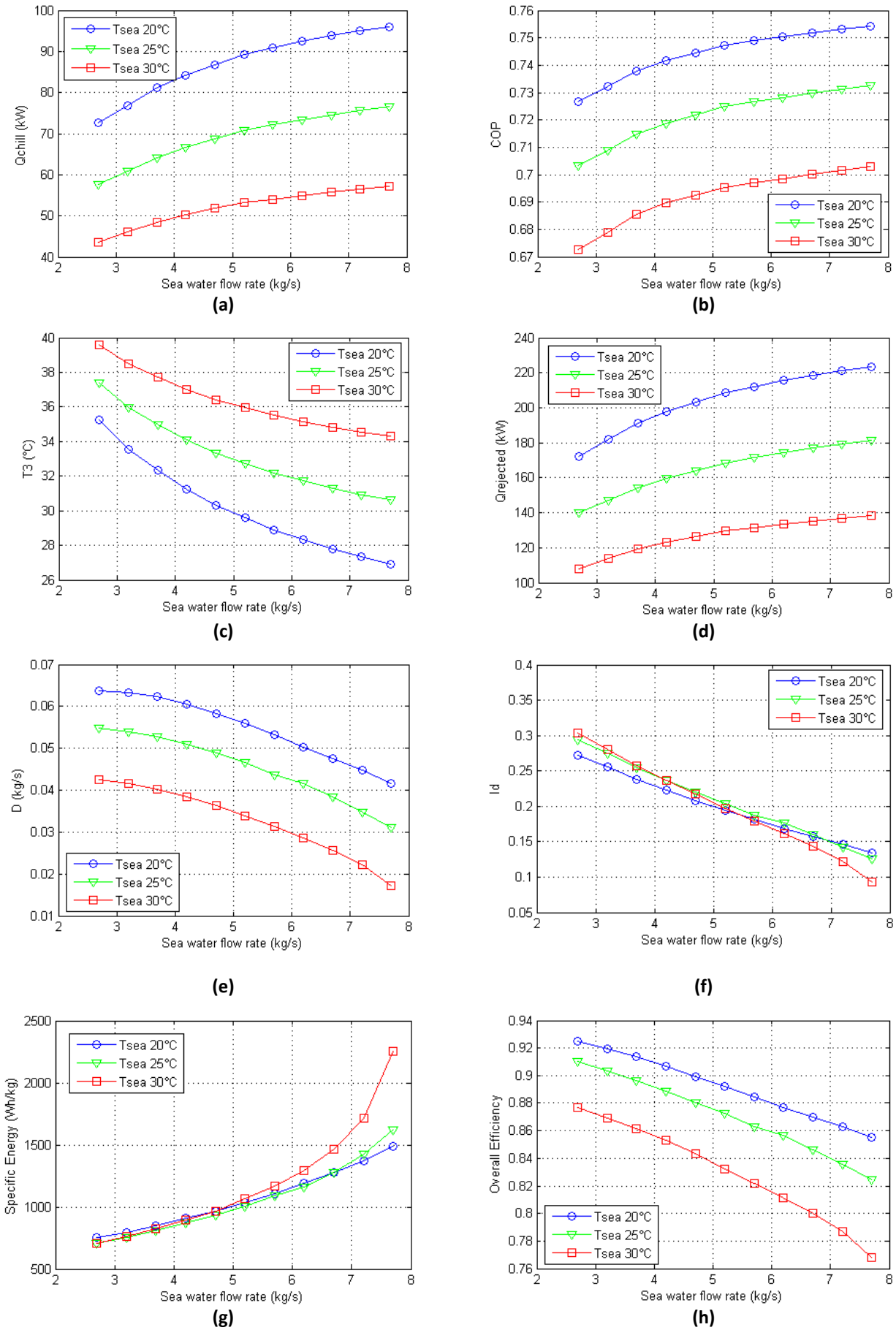

Figure 3-11: Performance for different sea water flow rates with HD unit in conf. (4)

The distilled water to cooling index I_d (Figure 3-11f) shows a complete imbalance toward the production of cooling energy: I_d values bigger than 0,25 are possible only for sea water flow rates lower than 3,5kg/s. Furthermore, as in the previous configuration, it is possible to observe a decreasing trend of I_d index: at higher mass flow rates the cooling capacity grows more than the fresh water productivity. On the opposite, the specific energy increases with the sea water mass flow rate (Figure 3-11g), this because the rejected heat grows more than the productivity *D*. The specific energy values for sea water flow rates bigger than 3,5kg/s are extraordinarily high.

Looking at the overall system efficiency (Figure 3-11h), for each sea water temperature a negative trend can be observed: the best overall efficiency value (0,925) is registered with the minimum value of sea water flow rate (2,6kg/s) and with a sea water temperature of 20°C.

Figure 3-12 reports a comparison between the performance of the cogeneration system at 90°C and 110°C for different sea water flow rates and temperatures. Chiller capacity (Figure 3-12a) presents similar trends for the two considered temperature levels; however at 110°C the chiller provides about 20 kW more than for 90°. This roughly stands for all the considered sea water temperatures and mass flow rates. *COP* (Figure 3-12b) on the opposite, appears to be much more influenced by hot water temperature levels. At 110 °C chiller maintains almost stable values (in the range 0.70-0.74), while *COP* at 90°C undergoes a strong decrease either when the sea water flow decreases or when the sea temperature is higher. In particular, COP at 90°C is higher than COP at 110°C with sea water temperatures lower than 25°C, while the opposite can be noticed for sea water temperatures higher than 25°C.

Fresh water productivity (Figure 3-12c) at 110°C results to be generally greater (about 0.005kg/s) because of the increased heat rejection. Nevertheless, I_d at 110°C (Figure 3-12d) is lower because the chiller capacity increases more than the fresh water productivity. Similarly, the required specific energy is always higher when the heat source is at 110°C (Figure 3-12e). The overall system efficiency η_{ov} (Figure 3-12f) shows an interesting behavior: the case with inlet heating temperature at 90°C is generally more efficient, but with high sea water temperature (26-30°C) the system driven at 110°C performs better; in fact, under these conditions the absorption chiller *COP* at 90°C undergoes a major drop (Figure 3-12b). Also in this configuration, the use of an heat source at higher temperature appears to be a good strategy when the sea water temperature is high.

In the next paragraphs, the cogeneration system with HD unit in configuration (1) was preferred to the system with HD unit in configuration (4), for the following reasons:

- Bigger fresh water productivity for a wide range of sea water flow rates;
- Better balance between fresh water and cooling energy production (I_d values between 0,4 and 0,8);
- Lower specific energy consumption for the fresh water production;
- Better overall efficiency of the system.

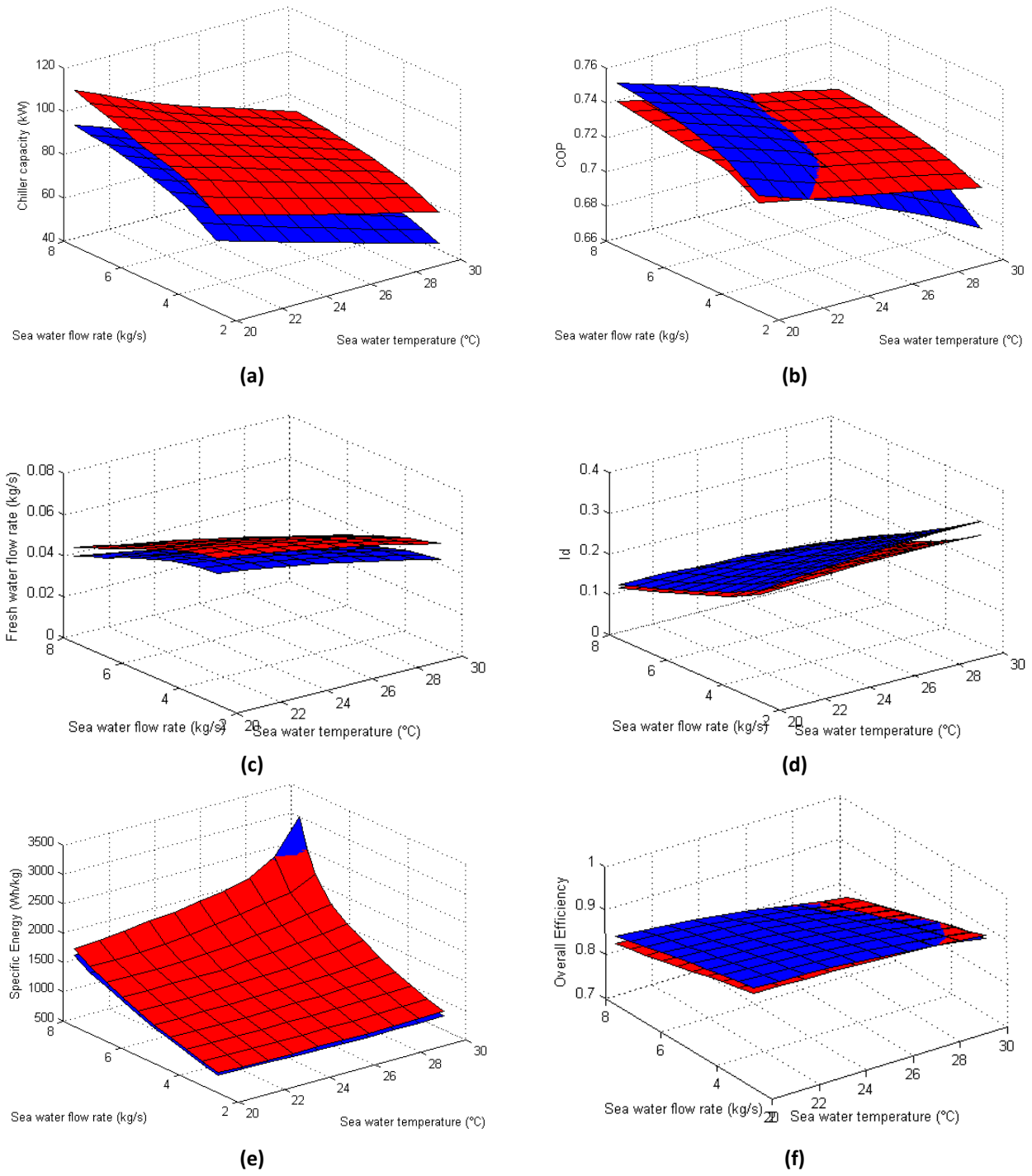

Figure 3-12: Performance for inlet heating temperature 90°C (blue) and 110°C (red) with HD unit in conf. (4)

3.4 *Off-design simulation*

The performance evaluation of the whole cogeneration system, including solar collectors, has been carried out by a simulation deck implemented in TRNSYS environment, shown in figure 3-13.

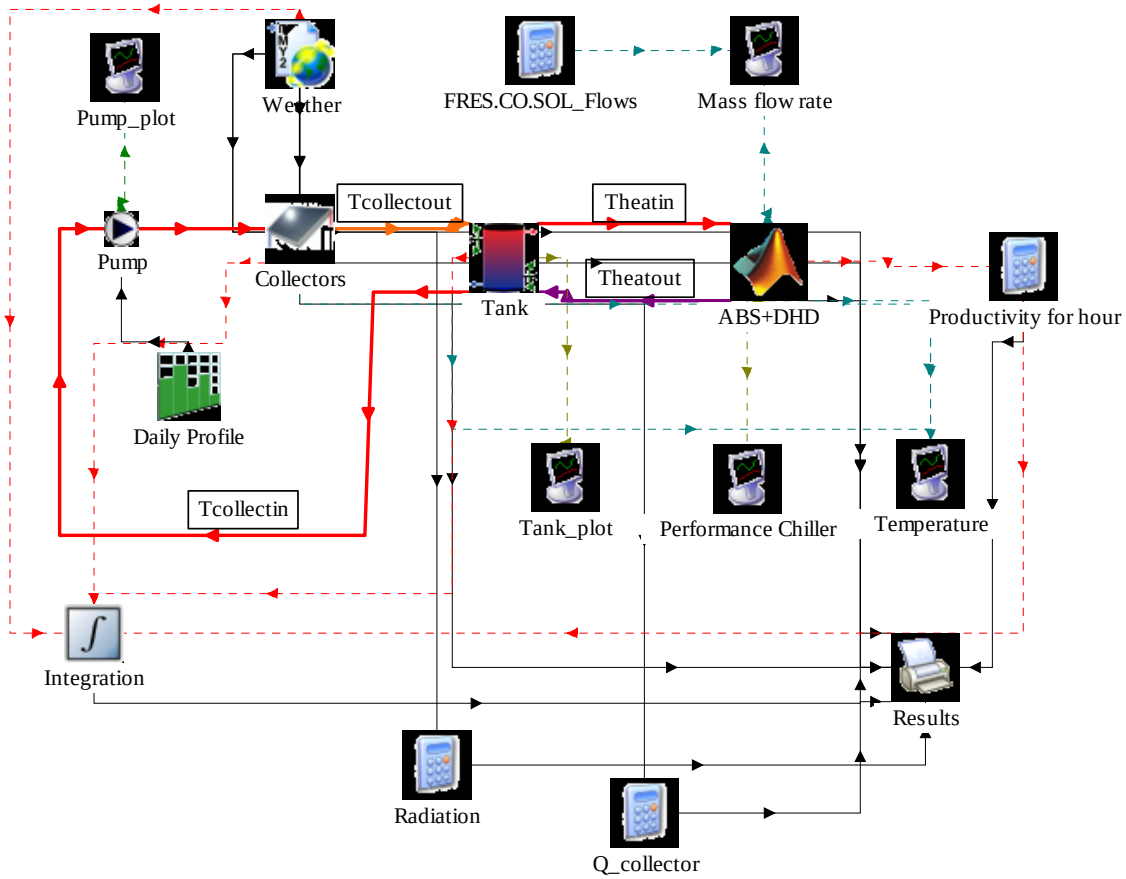

Figure 3-13: TRNSYS implementation of the cogeneration system for off-design simulation

The system is supposed to be located in a Mediterranean region characterized by hot climate. Sicily (38°11′65″N 13°36′33″E) meteorological conditions, taken from the global climatologic database METEONORM, were assumed for this study.

The considered collectors are evacuated tube type, with intercept efficiency, first and second order loss coefficients respectively equal to 0.75, 1.7 W/(m^{2}K) and 0.008 W/(m^{2}K^2). Slope and azimuth angles have been both set to 0°. Collector field has been sized with typical specifications of solar cooling plant: total solar collector area resulted to be 220 m^2. The water flows within solar collectors for 12 hours per day with a single speed pump. The thermal storage has been modeled with a TRNSYS standard component. The storage is divided in 6 fully mixed segments to take into account the thermal stratification,. The losses from the tank to the environment are calculated with an overall heat transfer coefficient equal to 0.7 W/(m^{2}K).

The heart of the simulation deck shown is the type 155, called ABS+DHD, which allows to interface TRNSYS with a MATLAB code, shown in Appendix B. Both absorption chiller and HD unit in

configuration (1) are represented by mappings which make leaner and faster the calculation code. The desalinator mapping contains the fresh water flow rates (D) and outlet temperature from condenser (T(2)) values corresponding to sea water flow rate (L), sea water temperature (T(1)) and inlet seawater temperature to the humidifier (T(3)) changes.

All subsequent daily simulations have been carried out with HD unit in configuration (1), sea water temperature of 20°C and mass flow rate of 3kg/s. The chilled water m_{chill} and the hot water m_{heat} mass flow rates are both kept to their nominal values: 2,39kg/s and 1,7kg/s respectively.

It has to be underlined that the system performance is significantly influenced both by tank volume and solar panels water flow rate; these two parameters, indeed, influence the temperature levels both at solar panels and chiller inlet, so they determine the overall amount of collected solar energy and the chiller performance as well. For this reason two different tank volumes have been considered: 2 m^3 and 10 m^3 with different solar panels water flow rates in the range 3000-15000 kg/h.

Figure 3-14 shows the results of three simulations over 24 hours (referred to a sunny June day). The left column (Figure 3-14a-c-e) shows the water temperature trends at collectors outlet ($T_{coll,out}$), hot water at chiller inlet ($T_{heat,in}$) and cooling sea water at chiller exit (i.e. desalinator inlet) ($T_{cool,out}$). The right column (Figure 3-14b-d-f) reports the heat collected by solar panels (Q_{coll}), the fresh water production (D) and the cooling power (Q_{chill}). The three cases differ in collector mass flow rate and hot storage volume. In the first simulation (Figure 3-14a-b) a flow rate of 9000 kg/h and a tank volume of 2 m^3 have been considered. When the sun rises, the outlet collector temperature increases up to a maximum about 110°C. The cogeneration system switches on when the temperature in the hot storage tank is high enough to drive the chiller (i.e. at 75°C). When the sun sets, the production of cooling and distilled water goes on for a couple of hours, even if at a reduced rate, thanks to the storage. Figure 3-14c-d show what happens if the collector mass flow rate is reduced at 3000 kg/h, with the same tank volume. As expected, the outlet collector temperature rises and exceeds 120°C. This temperature increase, that is detrimental for collector efficiency, doesn't produce beneficial effects on the cogeneration system. Indeed, cooling and freshwater production stops 3 hours in advance. Figure 3-14e-f reports on the effects of a different strategy: in this case a larger hot storage (10 m^3) has been used, with a collector flow rate of 9000 kg/h. It can be seen that the daily trend of outlet collector temperature is smoother: the temperature in the tank grows more slowly up to the maximum value, but it remains for a longer time above the threshold value (75°C) for the chiller operation. In such a way cooling and fresh water production may continue until late evening.

In order to compare the performance of the whole system for different collector flow rates and tank volumes, some integral values on a daily basis have been computed. Figure 3-15a and 3-15b respectively report the amounts of chilling energy and fresh water production. It has to be pointed that the daily production depends both on the efficiency and on the duration of the system operation. It is evident that the use of a larger storage is beneficial, because it allows to extend the operation time.

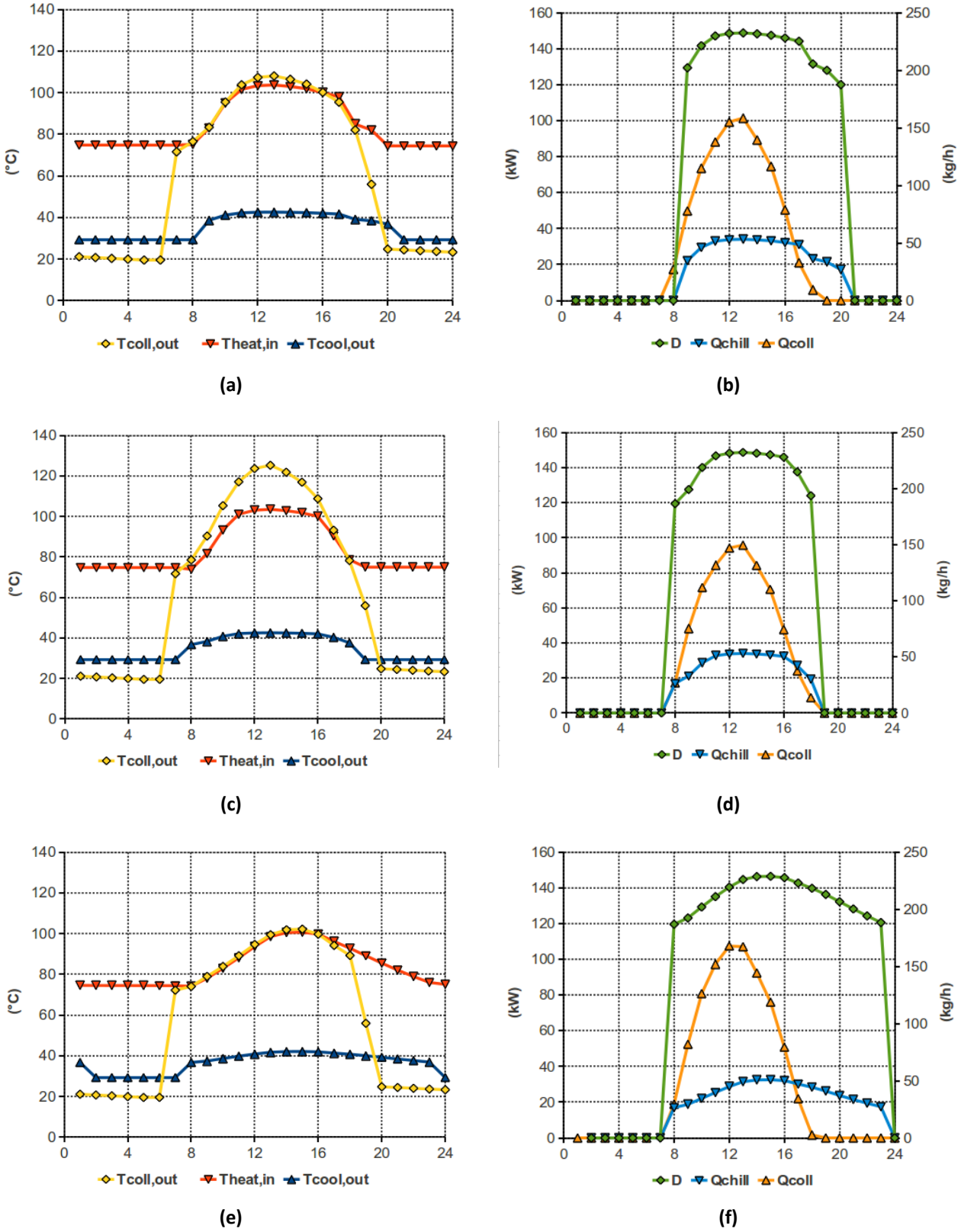

Figure 3-14: Results of a daily off-design simulation: a,b) collector mass flow rate 9000 kg/h, hot storage 2 m^3; c,d) collector mass flow rate 3000 kg/h, hot storage 2 m^3; e,f) collector mass flow rate 9000 kg/h, hot storage 10 m^3

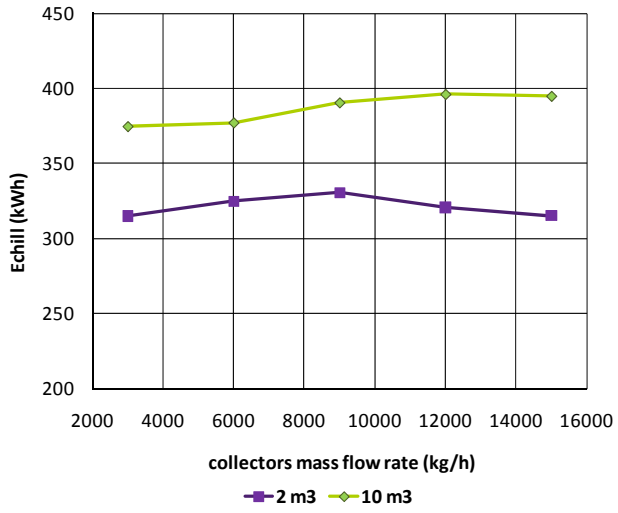

(a)

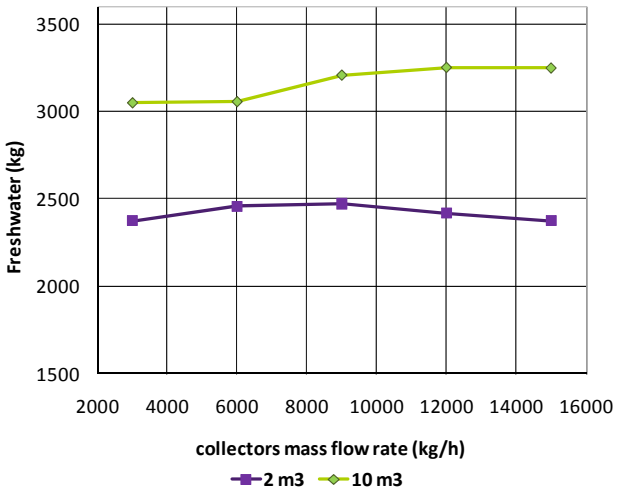

(b)

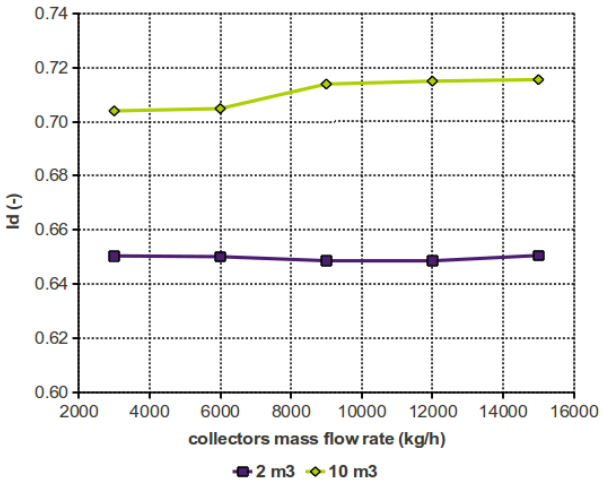

(c)

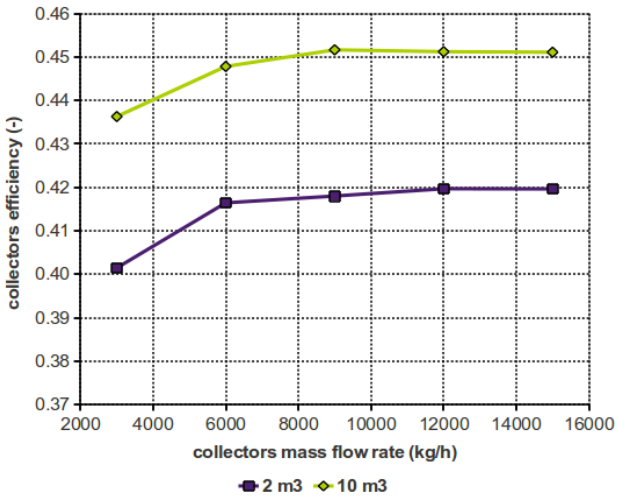

(d)

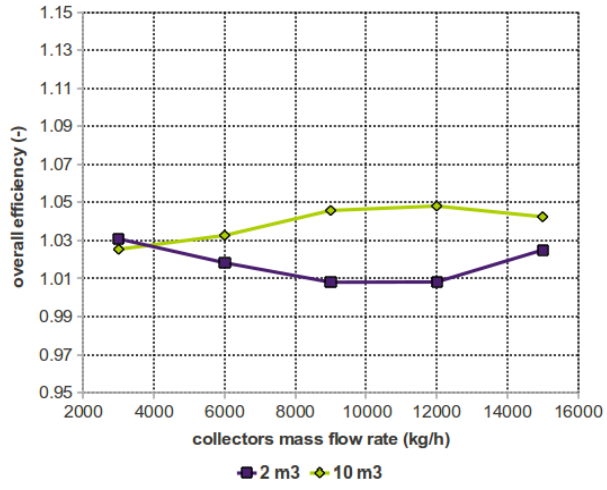

(e)

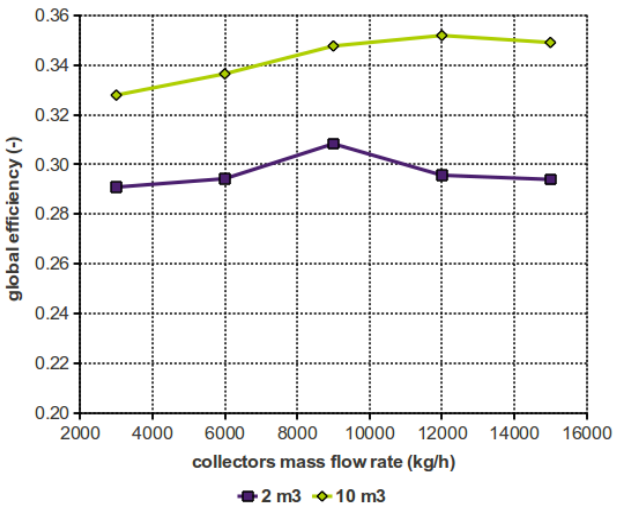

(f)

Figure 3-15: Daily integration results: a) chilling energy; b) freshwater production; c) I_d; d) collector efficiency; e) η_{ov}; f) η_{glob}

Ceteris paribus, an average overproduction of about 10% of chilling energy and 20% of freshwater takes place, independently on collector flow rate. For each tank volume an optimal collector flow rate can be identified: 9000 kg/h for the small storage, 12000 kg/h for the bigger one.

For flow rates smaller than the optimum, the higher water temperatures make the effect of reducing solar collector efficiency (see Figure 3-15d). For higher flow rates, on the contrary, tank water temperature remains too low and this is detrimental for chiller operation. Looking at the overall efficiency referred to chiller and desalinator (Figure 3-15e), there are only small differences, but cases with a larger storage appear to better perform. Global efficiency, including solar collector field efficiency, is presented in Figure 3-15f. Note that such parameter is representing cooling plus freshwater conversion efficiency of daily available solar energy (Q_{rad}):

$$\eta_{glob} = \left(\dot{Q}_{chill} + D \cdot E_{sp,ref}\right)/\dot{Q}_{rad} \tag{3.5}$$

Cases with the larger storage exhibit an average global efficiency 12-15% higher than the ones with a small tank: this confirms that the storage volume is a critical design parameter for these systems. One can note that the optima take place at the same collector flow rates corresponding to maximum chilling energy and freshwater production.

3.5 GenOpt optimization

The TRNSYS simulation revealed the main design variables on which to focus the optimization:

1) the storage volume (V_{tank}),
2) the water flow rate in the collector field (m_{coll})
3) the sea water flow rate (L)

The design variables are optimized changing the following parameters:

1) the surface area of condenser (A_{cond}) in the desalinator
2) the surface area of humidifier (A_{humid}) in the desalinator
3) the sea water on air flow rates ratio (L/G)

The collector field area (A_{coll}) was excluded from the optimization: in fact, to a greater area corresponds always a bigger amount of thermal energy provided to the storage tank, so the collector field area optimization would be trivial. The value of 220m^2 has been fixed for the collector field area. The chilled water m_{chill} and the hot water m_{heat} mass flow rates are both kept to their nominal values: 2,39kg/s and 1,7kg/s respectively.

3.5.1 GenOpt environment

GenOpt [18] was chosen as the generic optimization program to size the design parameters. This program minimizes an objective function with respect to multiple parameters. The objective function is evaluated by a simulation program that is iteratively called by GenOpt (like EnergyPlus,

SPARK, DOE-2, TRNSYS, or any user-written program). GenOpt allows coupling any simulation program with text-based I/O by simply modifying a configuration file, without requiring code modifications. Further, it has an open interface for easily adding custom minimization algorithms to its library. This allows using GenOpt as an environment for the development of optimization algorithms.

To perform the optimization GenOpt automatically generates input files for the simulation program. These files are based on input templates for the particular simulation program. GenOpt then launches the simulation program, reads the function value being minimized from the simulation result file, checks possible simulation errors and then determines a new set of input parameters for the next run. The whole process is repeated iteratively until a minimum of the function is found. If the simulation problem has some underlying constraints, they can be taken into account either by a default implementation or by modifying the function that has to be minimized.

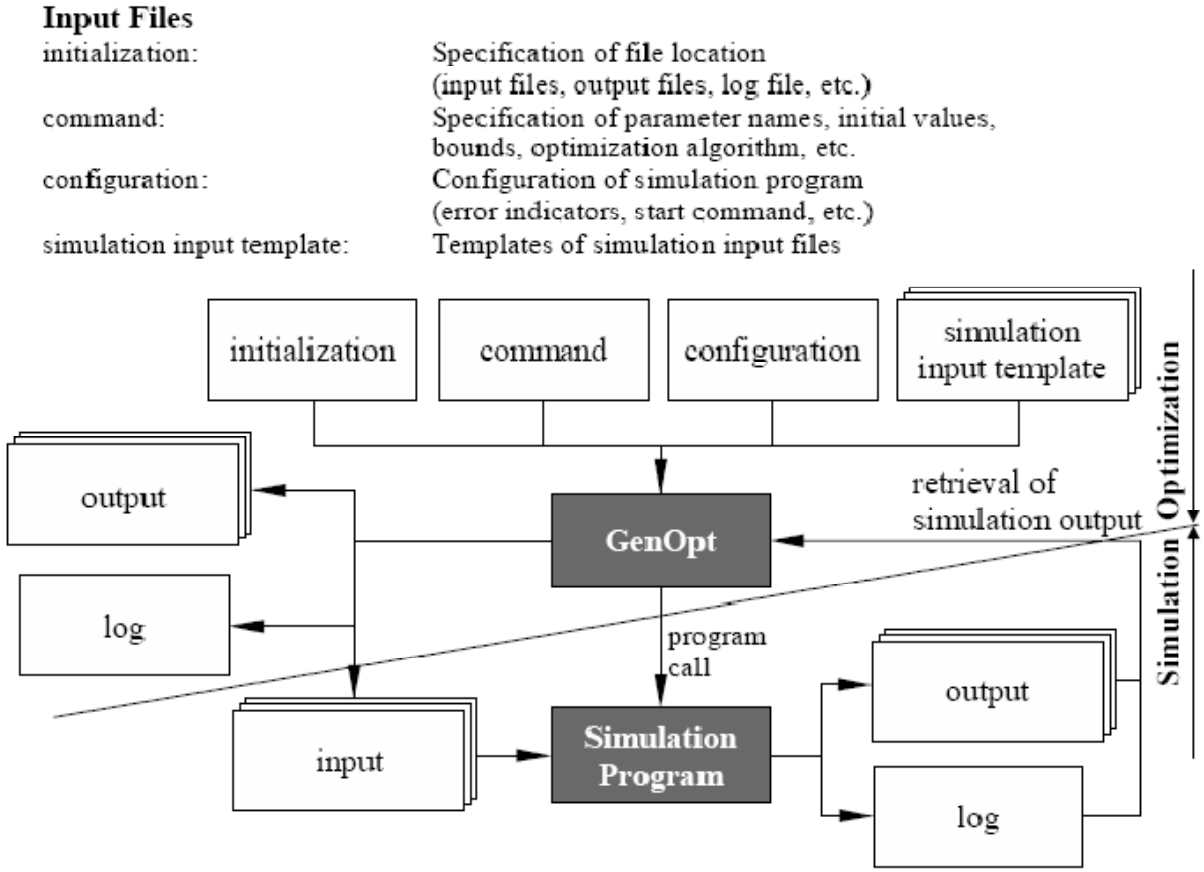

Figure 3-16: Interface between GenOpt and the simulation program

The data exchange between GenOpt and the external program is done with text files only (Figure 3-16). For performing the optimization, GenOpt, based on input template files, automatically generates new input files for the simulation program. To generate such templates, the user accesses the already-defined simulation input files and replaces the numerical values of the parameters to be modified with keywords. GenOpt then replaces these keywords with the

corresponding numerical values and writes the simulation input files. This approach makes GenOpt capable of writing text input files for any simulation program. In a configuration file, the user can specify how the simulation program is to be launched and where GenOpt can find the current value of the objective function to be minimized, as well as other values that may be processed by the optimization algorithm. This makes it possible to couple any external program to GenOpt without modifying and recompiling either program. The only requirement of the external program is that it must read its input from text files and write the function value to be minimized (plus any possible error messages) to text files.

When the objective function is evaluated by a simulation program like TRNSYS, computing the cost involves solving a system of partial and ordinary differential equations that are coupled to algebraic equations. In general, one cannot obtain an exact solution, but it is possible to obtain an approximate numerical solution. The best one can do in trying to solve optimization problems where the cost and constraint functions are evaluated by a simulation program that does not allow controlling the approximation error is to find points that are close to a local minimizer of the objective function. Numerical experiments show that by using tight enough precision and starting the optimization algorithm with coarse initial values, one often comes close to a minimizer of the objective function. Furthermore, by selecting different initial iterates for the optimization, or by using different optimization algorithms, one can increase the chance of finding a point that is close to a minimizer of the objective function. However, even if the optimization terminates at a point that is non-optimal, one may have obtained a better system performance compared to not doing any optimization. The authors of [18] recommend using the hybrid algorithm, the Generalized Pattern Search (GPS) implementation of the Hooke-Jeeves algorithm, possibly with multiple starting points, or a Particle Swarm Optimization algorithm. The algorithm chosen for this study is the GPS implementation of the Hooke-Jeeves algorithm.

3.5.2 Objective functions

The objective functions for the GenOpt optimization are the followings:

1) The amount of cooling energy provided by the absorption chiller: this function has to be maximized;
2) The amount of fresh water produced by the HD unit: this function has to be maximized;
3) The overall efficiency η_{ov} (Eq. 3.2): this function has to be maximized;
4) The global efficiency η_{glob} (Eq. 3.5): this function has to be maximized;
5) The specific energy needed to produce fresh water (Eq. 3.4): this function has to be minimized;
6) The index S (Eq. 3.6) related to an economic evaluation of the cogeneration system over 20 years: this function has to be maximized;

$$S = -\mathrm{Cinv} + \sum_{n=1}^{20} (-\mathrm{Cvar}_n + \mathrm{Rev}_n) \tag{3.6}$$

Cinv includes all the investment costs for the collector field, the storage tank, the absorption chiller, the HD unit, the pumps and the pipes. The table 3-3 shows the correlations to evaluate the investment cost: the known investment costs are 88.000€ for 220m^2 of the collector field, and 33.217€ for 50kW of the absorption chiller. The costs for the pumps and the pipes were not considered, so the annual cost for the electrical consumption ($Cvar_n$) was excluded. Rev_n is the annual revenue from the production of the cogeneration system: 0,067€/kWh$_{th}$ for cooling energy, and 1€/m^3 for the fresh water. The useful life of the system is 20 years: every year an interest rate of 5% has been kept for the production revenue.

Component	Component value
Collector field	400€/m^2 x Collector area
Storage tank	600€/m^3 x Tank volume
ABS chiller	(4396,2 x Capacity$^{(-0,48)}$)€/kW x Capacity
HD unit Condenser	285,304€/m^2 x $A_{cond}^{(0,2910878)}$
HD unit Humidifier	855,913€/m^2 x $A_{humid}^{(0,2910878)}$

Table 3-3: Correlations to evaluate the investment cost

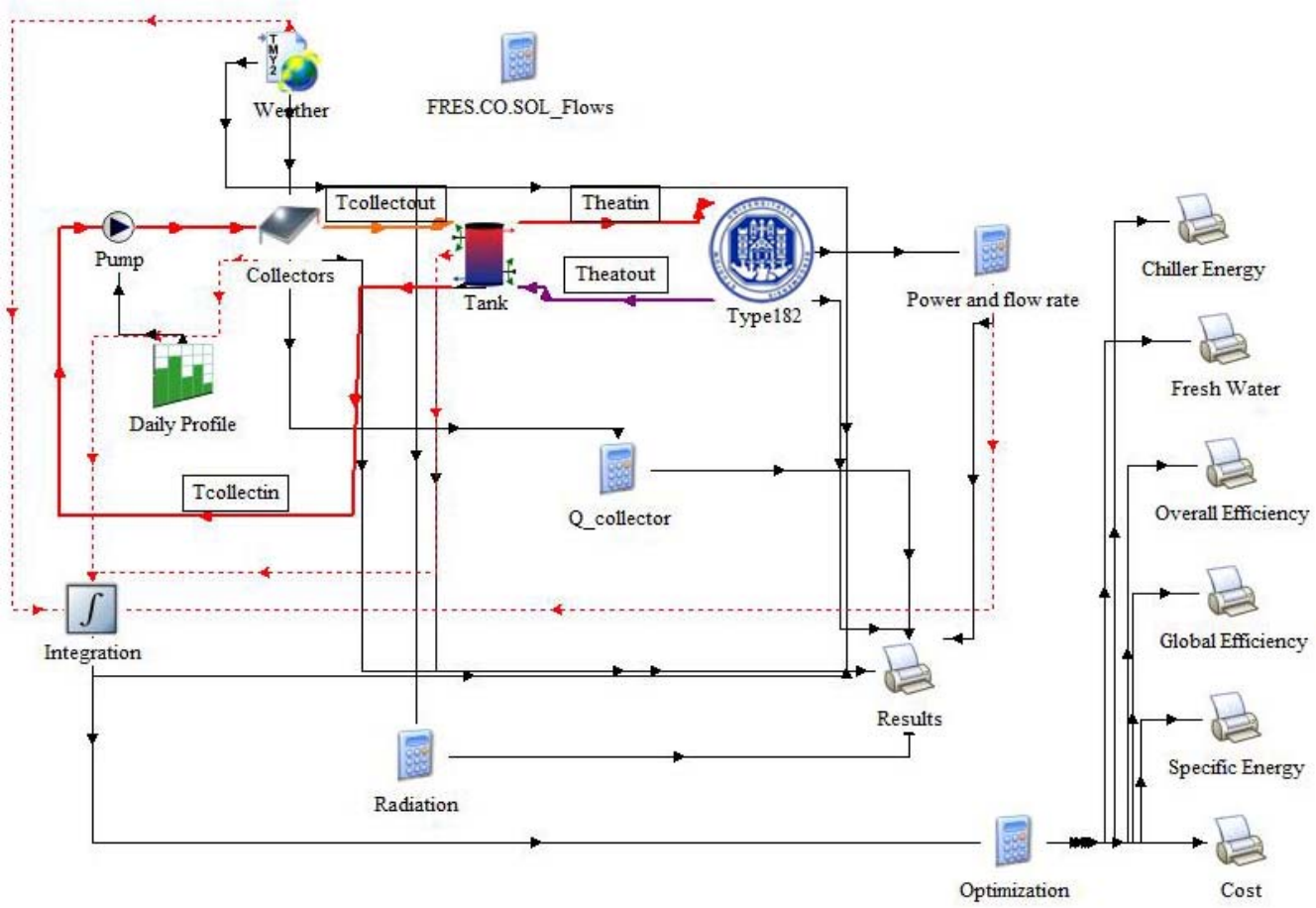

Figure 3-17: TRNSYS implementation of the cogeneration system for GenOpt optimization

Figure 3-17 shows the new TRNSYS deck used for the GenOpt optimization. On the right side of the deck, there are all the objective function plots creating the outputs for GenOpt. The presence of MATLAB code causes compatibility problems with GenOpt, so the old type ABS+DHD (shown in Figure 3-13) was replaced by the type 182, written in FORTRAN code. The FORTRAN code (presented in Appendix C) allows to build the library 182.dll, which is loaded every time that TRNSYS kernel finds the component in the simulation.

Like in off-design simulation, the system is supposed to be located in Sicily (38°11′65″N 13°36′33″E). The considered collectors are evacuated tube type, with intercept efficiency, first and second order loss coefficients respectively equal to 0.75, 1.7 W/(m^{2}K) and 0.008 W/(m^{2}K^2). Slope and azimuth angles have been both set to 0°. The water flows within solar collectors for 12 hours per day with a single speed pump. The thermal storage has been modeled with a TRNSYS standard component. The storage is divided in 6 fully mixed segments to take into account the thermal stratification. The losses from the tank to the environment are calculated with an overall heat transfer coefficient equal to 0.7 W/(m^{2}K).

3.5.3 Results

Figure 3-18 shows the optimization results using the objective function previously listed in paragraph 3.5.2. The results are subdivided in three surfaces corresponding to a different L/G ratio and are in function of condenser and humidifier surface areas of desalinator. The results were obtained from simulations over 72 hours (referred to sunny June days), except for the optimization of index S (Eq. 3.6), where simulations over 4 months each year were carried out.

Figure 3-18a,b,c,d show the results of fresh water, specific energy, overall and global efficiency optimizations respectively. The optimization of these four objective functions lead to the same result: to a wider surface area of condenser and humidifier corresponds an higher productivity and a greater efficiency of the cogeneration system.

Table 3-4 shows the objective function values and the corresponding design variables for A_{cond} = 2500m^2, A_{humid} = 500m^2 and L/G = 1, while the table 3-5 presents the reciprocal values of the objective functions.

Figure 3-18e,f show the results of chiller energy and index S optimization, and the interpretation is not so clear like in the previous cases. In fact, the configuration with A_{cond} = 2500m^2, A_{humid} = 500m^2 and L/G = 1 is no longer optimal. Table 3-5 confirms this result: the value of sea water flow L has been chosen higher than 5 kg/s to maximize the chiller energy production and the index S. With this flow rate, the sea water temperature T(3) from absorption chiller (entering the humidifier) is less than 30°C, so the production of fresh water is blocked.

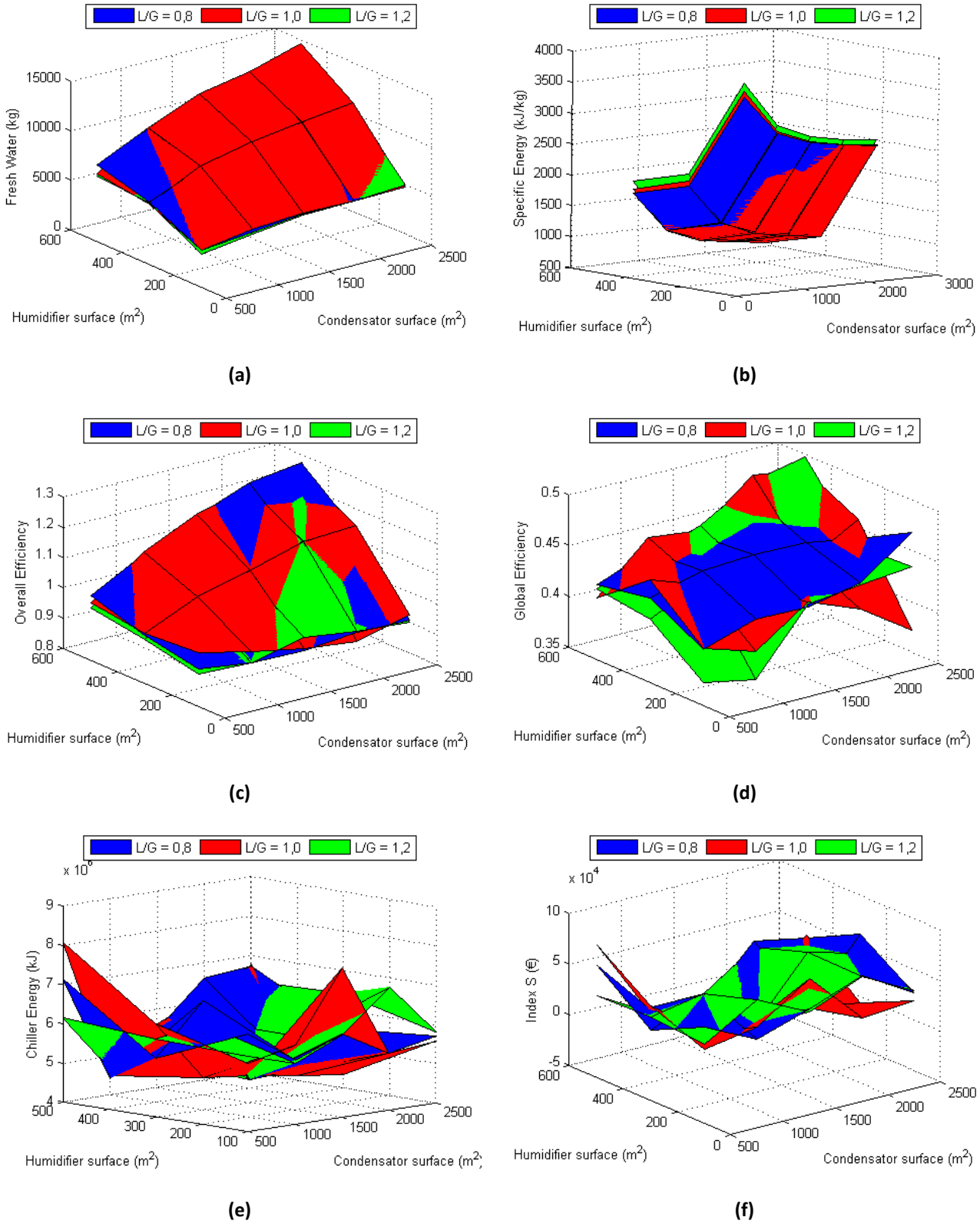

Figure 3-18: Results of GenOpt optimization

The observation of figure 3-18e-f allows to note how the two objective functions trends are very similar, with two peaks at A_{cond} = 500m^2, A_{humid} = 500m^2, and A_{cond} = 1500m^2, A_{humid} = 100m^2.

Objective function	Value	V_{tank} (m^3)	L (kg/s)	m_{coll} (kg/hr)
Fresh water (kg)	14687,4	11,00	3,80	5375
Specific Energy (kJ/kg)	683,2	16,00	2,60	3875
Overall Efficiency	1,248	13,88	3,00	4000
Global Efficiency	0,484	10,13	4,28	5815
Chiller Energy (MJ)	6768,7	16,00	5,26	4000
Index S (€)	38134,7	16,00	5,26	4000

Table 3-4: Objective function values and design variables with A_{cond} = 2500m^2, A_{humid} = 500m^2 and L/G = 1

Objective function	Fresh water (kg)	Spec. Energy (kJ/kg)	Overall Eff.	Global Eff	Chiller Energy (MJ)	Index S (€)
Fresh water (kg)	14687,4	802,9	1,244	0,452	4195,6	-6887,8
Specific Energy (kJ/kg)	13290,9	683,2	1,198	0,380	3012,8	-41600,8
Overall Efficiency	13895,8	719,1	1,248	0,417	3512,9	-26411,6
Global Efficiency	10496,7	1258,2	1,102	0,484	5279,6	17301,6
Chiller Energy (MJ)	0,0	-	0,937	0,361	6768,7	38134,7
Index S (€)	0,0	-	0,937	0,361	6768,7	38134,7

Table 3-5: Objective function values with A_{cond} = 2500m^2, A_{humid} = 500m^2 and L/G = 1

L/G	A_{cond} (m^2)	A_{humid} (m^2)	Index S (€)	Chill. Energy (MJ)	Fresh water (kg)	Spec. Energy (kJ/kg)	Overall Eff.	Global Eff.
1,0	500	500	80577,6	8077,0	0	-	0,858	0,430
1,0	1500	100	66926,0	7443,7	1373	12725	0,864	0,419
0,8	2500	300	62213,5	7432,6	0	-	0,850	0,396
0,8	500	500	60502,7	7073,2	4657	3633	0,899	0,454
1,2	2000	300	56839,4	7003,9	3211	5158	0,834	0,426
0,8	2000	100	56730,4	6984,7	3470	4831	0,914	0,429
1,2	2000	100	55914,3	7138,9	1709	9858	0,962	0,408
1,2	1000	100	49504,5	6700,1	3175	5060	0,928	0,409
0,8	2000	500	45273,0	6595,5	5683	2788	1,084	0,445
0,8	500	100	45222,3	6514,5	3520	4480	0,857	0,405
1,0	500	300	43773,9	6367,6	6778	2322	0,967	0,451
1,2	2500	300	42568,8	6452,5	4521	3411	0,954	0,418
1,2	1000	300	42344,5	6270,6	6991	2196	1,064	0,449
0,8	1000	300	42283,8	6783,1	0	-	0,880	0,361
1,2	2000	500	38667,6	6690,6	0	-	0,876	0,356
1,0	2500	500	38134,7	6768,7	0	-	0,937	0,361
0,8	1500	100	36962,8	6130,4	4305	3482	0,857	0,398
0,8	2500	500	35330,0	6148,5	7064	2123	1,093	0,444
1,2	1500	100	33733,1	6095,7	4145	3593	0,925	0,393
1,2	500	300	32695,9	5983,3	6145	2411	0,938	0,420

Table 3-6: Objective functions values of the top twenty configurations which maximize the Index S

L/G	A_{cond} (m^2)	A_{humid} (m^2)	Index S (€)	m_{coll} (kg/hr)	L (kg/s)	V_{tank} (m^3)
1,0	500	500	80577,6	8000	5,13	4,00
1,0	1500	100	66926,0	4000	4,60	4,50
0,8	2500	300	62213,5	6000	4,90	6,00
0,8	500	500	60502,7	7500	4,30	4,50
1,2	2000	300	56839,4	4000	4,60	4,00
0,8	2000	100	56730,4	5000	4,00	6,00
1,2	2000	100	55914,3	4000	4,25	10,00
1,2	1000	100	49504,5	6000	3,99	5,75
0,8	2000	500	45273,0	4125	4,35	10,00
0,8	500	100	45222,3	6125	3,60	6,25
1,0	500	300	43773,9	8250	3,58	7,75
1,2	2500	300	42568,8	3000	4,25	6,50
1,2	1000	300	42344,5	6000	3,90	5,75
0,8	1000	300	42283,8	5875	4,90	12,00
1,2	2000	500	38667,6	4000	4,81	12,00
1,0	2500	500	38134,7	4000	5,26	16,00
0,8	1500	100	36962,8	7875	3,43	4,00
0,8	2500	500	35330,0	4250	4,20	10,00
1,2	1500	100	33733,1	7750	3,43	7,50
1,2	500	300	32695,9	5750	3,40	8,00

Table 3-7: Design variables of the top twenty configurations which maximize the Index S

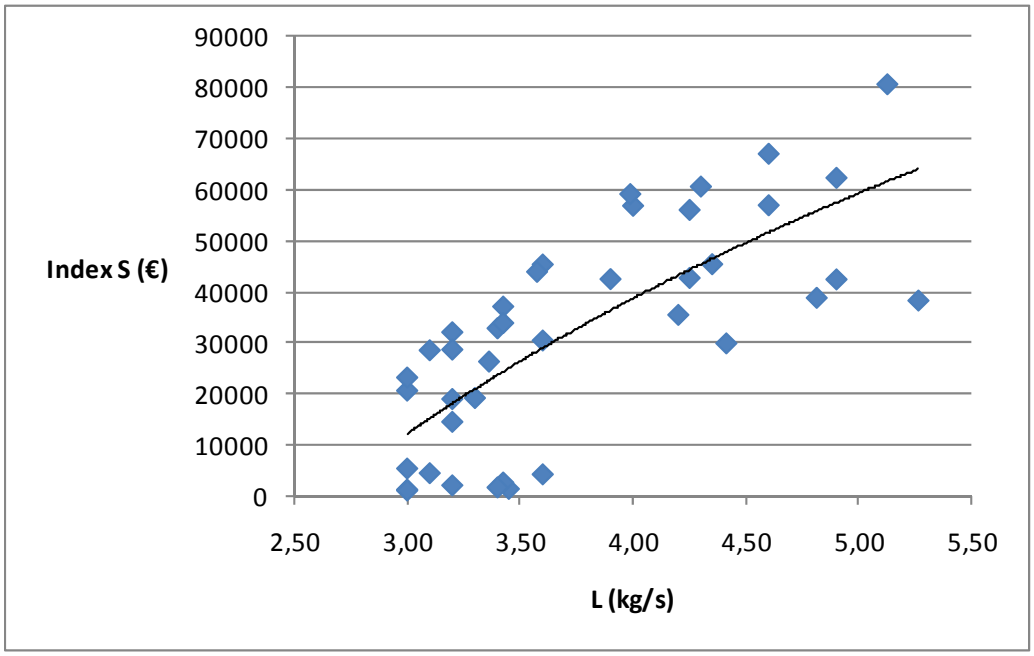

Figure 3-19: Correlation between L and index S

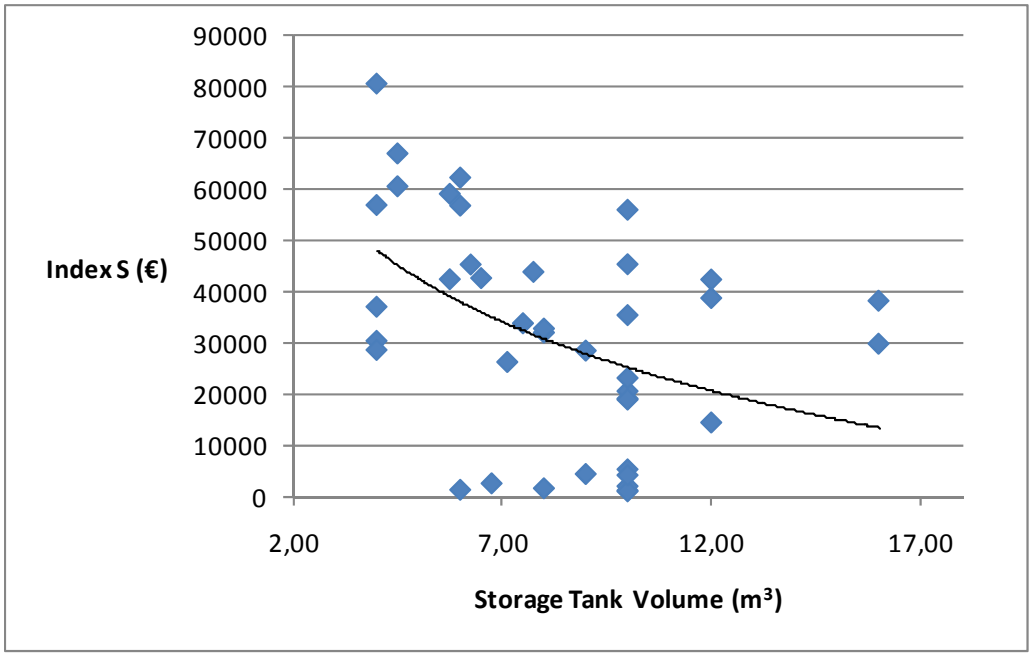

Figure 3-20: Correlation between storage tank volume and index S

This result clearly shows how the index S is related to the chiller energy production, and the maximization of the chiller energy sometimes involves the exclusion of the fresh water production. Table 3-6 and 3-7 shows the top twenty configurations which allows to maximize the index S. It is clear that the economic weight of the cooling energy is greater than fresh water's value.

Figure 3-19 shows the correlation between the sea water flow rate L and the index S, while figure 3-20 shows the correlation between the hot water storage tank volume and the index S: increasing the sea water flow rate L or decreasing the storage tank volume implies the increase of the revenue after 20 years.

Maximizing the production of cooling energy means damaging the fresh water production. A compromise solution has been chosen to balance the contrast between cooling energy and fresh water production: the global efficiency maximization. The configuration with A_{cond} = 2500m^2, A_{humid} = 500m^2 and L/G = 1,2 allows to obtain the best balance between the two outputs. Table 3-8 shows the optimization result.

Objective function	Value	Design Parameter	Value
Fresh water (kg)	11971,6	L/G	1,2
Specific Energy (kJ/kg)	1182,8	A_{cond} (m^2)	2500
Overall Efficiency	1,349	A_{humid}(m^2)	500
Global Efficiency	0,497	V_{tank} (m^3)	9,21
Chiller Energy (MJ)	5616,9	L (kg/s)	4,00
Index S (€)	28723,3	m_{coll} (kg/hr)	3336

Table 3-8: Objective functions and design parameters values at A_{cond} = 2500m^2, A_{humid} = 500m^2 and L/G = 1,2

The total cost of the cogeneration system is 134.750€, including 88.000€ for the collector field. Table 3-9 completes the table 3-3, showing the cost of the cogeneration system components, while Figure 3-21 highlights the payback time of the cogeneration system: 18 years, if the collector field is considered, 8 years without collector field.

Component	Component value	Size	Cost (€)
Collector field	400€/m^2 x Collector area	220m^2	€ 88.000
Storage tank	600€/m^3 x Tank volume	9,21m^3	€ 5.524
ABS chiller	(4396,2 x Capacity$^{(-0,48)}$)€/kW x Capacity	50kW	€ 33.217
HD unit Condenser	285,304€/m^2 x $A_{cond}^{(0,2910878)}$	2500m^2	€ 2.782
HD unit Humidifier	855,913€/m^2 x $A_{humid}^{(0,2910878)}$	500m^2	€ 5.225

Table 3-9: Cost of the cogeneration system components

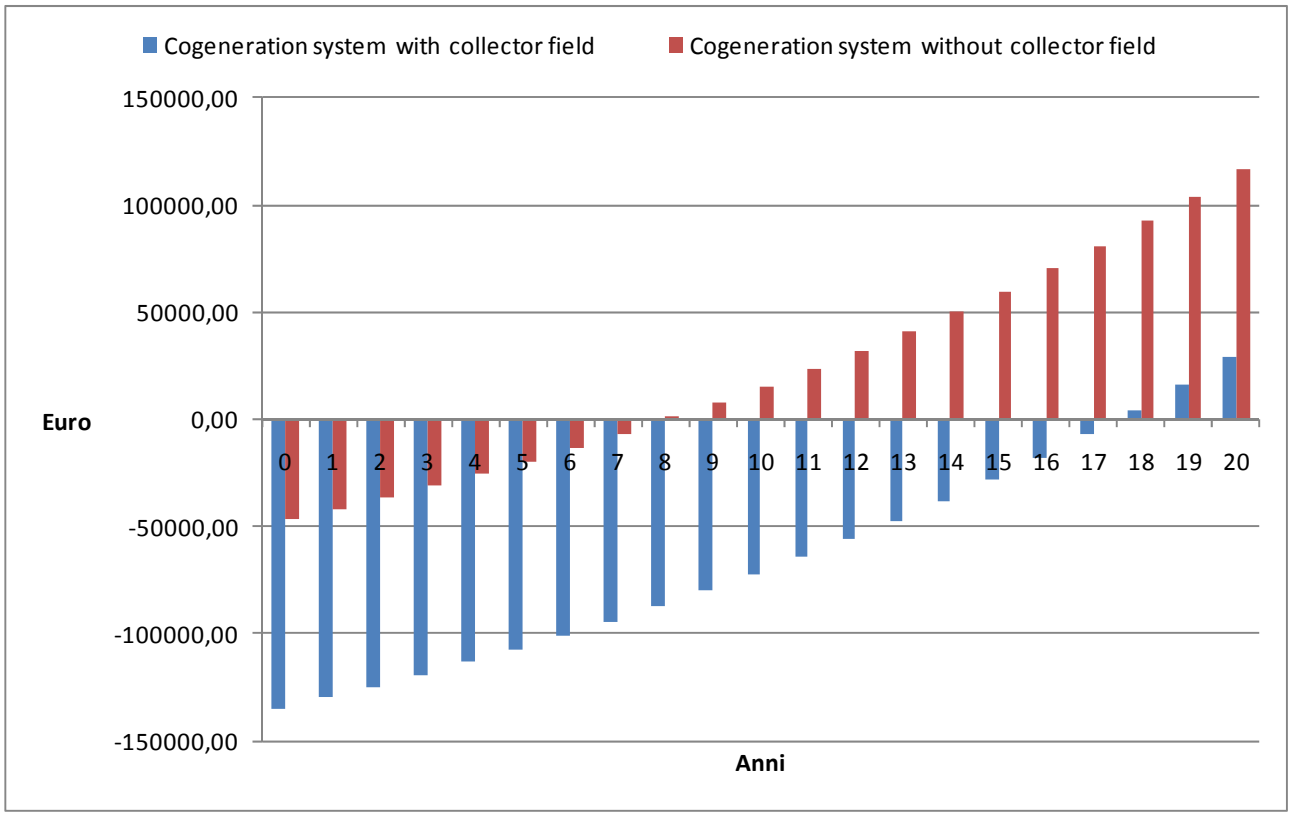

Figure 3-21: Payback time of the cogeneration system at A_{cond} = 2500m^2, A_{humid} = 500m^2 and L/G = 1,2

Chapter 4: Conclusions and future developments

In this study a cogeneration system producing cooling energy and fresh water was simulated and optimized. First of all, a research on the desalination techniques has been carried out to find the less energy-consuming techniques. Among the multiple effect distillation (MED), the natural vacuum distillation (NVD), the membrane distillation (MD), the solar distillation (SD), and the humidification and dehumidification technique (HD), the choice fell on the last one for these main reasons:

1) MED and NVD processes need a working pressure lower than atmospheric, while in HD distillation is possible to keep the atmospheric pressure, ensuring greater reliability and durability.

2) MD technique is really promising, but it's difficult to obtain membranes at reasonable prices with hydrophobic property, high porosity for the vapor phase, a high resistance to heat flow by conduction, a sufficient but not excessive thickness, and low moisture adsorptivity.

3) HD distillation produce desalinated water at higher rates than those usually obtained from solar stills under similar solar radiation.

4) HD distillation avoids the direct contact between the collector and the saline water, which may cause corrosion and scaling in the solar still.

The second step was the simulation of an HD unit, implementing the condenser and the humidifier models. The process used in this study is a closed air cycle type, in which air is circulated in the unit by forced draft between the humidifier and condenser. Four different configuration of the HD unit were considered, but only two of these were chosen for the integration in the cogeneration system, as shown in figure 3-7 and 3-8. The cogeneration system includes a field of evacuated tube solar collectors, an hot storage tank which feeds a single stage LiBr–H_2O absorption chiller, and the desalinator, which recovers the heat rejected from the chiller as heat source. The system produces cooling energy by the absorption chiller and then fresh water from the desalination unit. Sea water is used as cooling medium of the absorption machine. This kind of coupling between a low temperature desalination unit and a refrigeration unit powered by solar energy appears new and essentially unexplored.

A design simulation of the cogeneration system allowed to chose the best HD unit configuration, while a TRNSYS off-design simulation revealed the main design variables on which to focus the optimization: the hot storage tank volume, the water flow rate in the collector field, and the sea water flow rate to cool the absorption chiller and to feed the desalinator. The optimization study on the design variables was performed by GenOpt, a generic optimization program which minimizes an objective function with respect to multiple variables. This study has been carried out on different objective functions and reveals that maximizing the production of cooling energy means damaging the fresh water production. A compromise solution has been chosen to balance the contrast between cooling energy and fresh water production: the global efficiency maximization. This solution allows to obtain a positive economic evaluation.

This study is a starting point for many future developments:

a) An analytic determination of the mass transfer coefficient K_{humid} for the desalinator humidifier is necessary to establish the exact amount of the fresh water produced by the system. As anticipated in paragraph 2.2, an algorithm based on Poppe method could be developed.

b) In paragraph 3.3 the cogeneration system with the HD unit in configuration (1) was preferred to the system with HD unit in configuration (4), for different reasons: the bigger fresh water productivity for a wide range of sea water flow rates, the lower specific energy consumption for the fresh water production, the better balance between fresh water and cooling energy production (I_d values between 0,4 and 0,8), and the better overall efficiency of the system. On the other hand, the use of the HD unit in configuration (4) would allow to increment the cooling energy production, ensuring less payback time of the investment cost. Hence a TRNSYS off-design analysis and a GenOpt optimization could be performed for the cogeneration system with HD unit also in this last configuration, considering sea water flow rate smaller than 3,5kg/s.

c) An improvement of the cogeneration system could be represented by an hot water tapping from the chiller generator to increase the sea water temperature T(3) entering the desalinator humidifier.

d) The GenOpt optimization could be performed without mappings, but using FORTRAN code to simulate the desalinator and the absorption chiller: in this case the number of configurable variables would be greater.

e) The development of a desalinator model using other desalination techniques would be interesting to obtain a direct comparison among different desalinators. The three most suitable techniques for this kind of application could be MED, MD and NVD.

f) Finally, the experimental implementation of the cogeneration system would be necessary to verify the assumptions of the simulation model and to improve the optimization of the entire system.

Appendix A: Nomenclature

A	surface	$[m^2]$
a_{cond}	volume of condenser per unit surface area	$\left[\frac{m^3}{m^2}\right]$
a_{humid}	surface area of humidifier packing per unit volume	$\left[\frac{m^2}{m^3}\right]$
Cp	specific heat	$\left[\frac{kJ}{kg \cdot K}\right]$
d	diameter	$[m]$
D	fresh water mass flow rate	$\left[\frac{kg}{s}\right]$
Eu	Eulero Number	
G	dry air mass flow rate	$\left[\frac{kg}{s}\right]$
h	convective heat transfer coefficient	$\left[\frac{W}{m^2 \cdot K}\right]$
Ha	air enthalpy	$\left[\frac{kJ}{kg}\right]$
Hw	water enthalpy	$\left[\frac{kJ}{kg}\right]$
k	thermal conductibility	$\left[\frac{W}{m \cdot K}\right]$
K_{humid}	mass transfer coefficient	$\left[\frac{kg}{m^2 s}\right]$
L	feeding sea water mass flow rate	$\left[\frac{kg}{s}\right]$
lx	length of component along x direction	$[m]$
ly	length of component along y direction	$[m]$
lz	length of component along z direction	$[m]$
n_{comp}	number of components in the desalination unit	
n_{fin}	fin number	
ng	fin efficiency	
Nu	Nusselt Number	

nx	number of conduits (humidifier) along x direction	
ny	number of pipes (condenser) along y direction	
nz	number of pipes (condenser) or conduits (humidifier) along z direction	
p_a	ambient pressure	$[Pa]$
p_g	partial saturation vapor pressure	$[Pa]$
$pitch$	pitch between elements	$[m]$
Pr	Prandtl Number	
Re	Reynolds Number	
$speed$	velocity	$\left[\frac{m}{s}\right]$
T_{amb}	ambient temperature	$[T]$
Ta	air temperature	$[T]$
Tw	water temperature	$[T]$
$thick$	thickness of fins or sheets	$[m]$
U	global heat transfer coefficient	$\left[\frac{kW}{m^2 \cdot K}\right]$
V	volume	$[m^3]$
X	specific humidity	$\left[\frac{kg_{water}}{kg_{dry\ air.}}\right]$
Δp	pressure drop	$[Pa]$
η_{el}	electrical efficiency	
μ	cinematic viscosity	$\left[\frac{N \cdot s}{m^2}\right]$
ρ	density	$\left[\frac{kg}{m^3}\right]$

Subscript

a	air
alu	aluminum
cond	condenser

eq	equivalent
ext	external
fan	fan
fin	fin
fr	frontal
humid	humidifier
hydr	hydraulic
in	inlet
int	internal
loss	energetic loss
out	outlet
rec	recuperator
sheet	wooden sheet
tot	total
unit	unit of desalination
w	water
x	x direction
y	y direction
z	z direction

Appendix B: MATLAB code for type 155 in TRNSYS deck

```
% ABS+DHD.m
% --------------------------------------------------------------------------
%
% HD desalinator model with ABS chiller data base  (M-file called by TRNSYS type
155)
%
% Data passed from / to TRNSYS
% ----------------------------
%
% trnTime (1x1)        : simulation time
% trnInfo (15x1)       : TRNSYS info array
% trnInputs (nIx1)     : TRNSYS inputs
% trnStartTime (1x1)   : TRNSYS Simulation Start time
% trnStopTime (1x1)    : TRNSYS Simulation Stop time
% trnTimeStep (1x1)    : TRNSYS Simulation time step
% mFileErrorCode (1x1) : Error code for this m-file. It is set to 1 by TRNSYS
and the m-file should set it to 0 at the
%                         end to indicate that the call was successful. Any non-
zero value will stop the simulation
% trnOutputs (nOx1)    : TRNSYS outputs
%
% trnInputs
% ---------
%
% trnInputs(1) : Qevanom , nominal power of ABS chiller [kW]
% trnInputs(2) : COPnom , nominal COP of ABS chiller [-]
% trnInputs(3) : Theatin, input hot water temperature [°C]
% trnInputs(4) : Tchillin, input chilled water temperature [°C]
% trnInputs(5) : mchill, chilled water flow rate [kg/s]
% trnInputs(6) : Tamb , ambient temperature [°C]
% trnInputs(7) : T1 , input sea water temperature [°C]
% trnInputs(8) : mheat, hot water flow rate [kg/s]
% trnInputs(9) : mcool (L), cooling water flow rate [kg/s]
%
% trnOutputs
% ----------
%
% trnOutputs(1) : Qevaeff, effective power of ABS chiller [kW]
% trnOutputs(2) : COPeff, effective COP of ABS chiller [-]
% trnOutputs(3) : Qcool (Qheater), power from ABS chiller [kW]
% trnOutputs(4) : Theatout, output hot water temperature [°C]
% trnOutputs(5) : Tcoolin (T2), input cooling water temperature [°C]
% trnOutputs(6) : Tcoolout (T3), output cooling water temperature [°C]
% trnOutputs(7) : Tbrine (T4), brine temperature [°C]
% trnOutputs(8) : Tfresh (T5), fresh water temperature [°C]
% trnOutputs(9) : D, fresh water flow rate [kg/s]
% trnOutputs(10) : Tchillout, output chilled water temperature [°C]
% trnOutputs(11) : indice1;
% trnOutputs(12) : indice2;
% trnOutputs(13) : Spec_energy;
%
% Dalmine (BG), July 2009
% --------------------------------------------------------------------------

% TRNSYS sets mFileErrorCode = 1 at the beginning of the M-File for error
detection
% This file increments mFileErrorCode at different places. If an error occurs in
the m-file the last succesful step will
```

```
% be indicated by mFileErrorCode, which is displayed in the TRNSYS error message
% At the very end, the m-file sets mFileErrorCode to 0 to indicate that
everything was OK

mFileErrorCode = 100    % Beginning of the m-file

% Desalinator parameters
% ------------------------------------------------------------------------

% Specific heat capacity of water [kJ/(kg*k)]
Cpw=4.186;
% Tolerance to exit from iteration
tol=1e-5;
% Maximum number of iteration
MaxIter=101;

mFileErrorCode = 110    % After setting parameters


% --- Process Inputs ------------------------------------------------------
---------------------------------------
% ------------------------------------------------------------------------------
---------------------------------------

Qevanom = trnInputs(1);
COPnom = trnInputs(2);
Theatin = trnInputs(3);
Tchillin = trnInputs(4);
mchill = trnInputs(5);
Tamb = trnInputs(6);
T1 = trnInputs(7);
mheat = trnInputs(8);
mcool = trnInputs(9);

mFileErrorCode = 120    % After processing inputs

% --- First call of the simulation: initial time step (no iterations) ----------
---------------------------------------
% ------------------------------------------------------------------------------
---------------------------------------
% (note that Matlab is initialized before this at the info(7) = -1 call, but the
m-file is not called)

if ( (trnInfo(7) == 0) & (trnTime-trnStartTime < 1e-6) )

    % This is the first call (Counter will be incremented later for this very
first call)
    nCall = 0;

    % This is the first time step
    nStep = 1;

    % Initialize history of the variables for plotting at the end of the
simulation
    nTimeSteps = (trnStopTime-trnStartTime)/trnTimeStep + 1;
    history.Qevanom = zeros(nTimeSteps,1);
    history.COPnom = zeros(nTimeSteps,1);
    history.Theatin = zeros(nTimeSteps,1);
    history.Tchillin = zeros(nTimeSteps,1);
    history.mchill = zeros(nTimeSteps,1);
    history.Tamb = zeros(nTimeSteps,1);
    history.T1 = zeros(nTimeSteps,1);
    history.mheat = zeros(nTimeSteps,1);
```

```
    history.mcool = zeros(nTimeSteps,1);

    % No return, we will calculate the solar collector performance during this
call
    mFileErrorCode = 130    % After initialization

end

% --- Very last call of the simulation (after the user clicks "OK"): Do nothing
---------------------------------------
% ------------------------------------------------------------------------------
---------------------------------------

if ( trnInfo(8) == -1 )

    mFileErrorCode = 0; % Tell TRNSYS that we reached the end of the m-file
without errors
    return

end


% --- Post convergence calls: store values ----------------------------------
---------------------------------------
% ------------------------------------------------------------------------------
---------------------------------------

if (trnInfo(13) == 1)

    mFileErrorCode = 140;   % Beginning of a post-convergence call

    history.Qevanom(nStep) = Qevanom;
    history.COPnom(nStep) = COPnom;
    history.Theatin(nStep) = Theatin;
    history.Tchillin(nStep) = Tchillin;
    history.mchill(nStep) = mchill;
    history.Tamb(nStep) = Tamb;
    history.T1(nStep) = T1;
    history.mheat(nStep) = mheat;
    history.mcool(nStep) = mcool;

    mFileErrorCode = 0; % Tell TRNSYS that we reached the end of the m-file
without errors
    return  % Do not update outputs at this call

end


% --- All iterative calls ---------------------------------------------------
---------------------------------------
% ------------------------------------------------------------------------------
---------------------------------------

% --- If this is a first call in the time step, increment counter ---

if ( trnInfo(7) == 0 )
    nStep = nStep+1;
end

% --- Get TRNSYS Inputs ---

nI = trnInfo(3);     % For bookkeeping
nO = trnInfo(6);   % For bookkeeping
```

```
Qevanom = trnInputs(1);
COPnom = trnInputs(2);
Theatin = trnInputs(3);
Tchillin = trnInputs(4);
mchill = trnInputs(5);
Tamb = trnInputs(6);
T1 = trnInputs(7);
mheat = trnInputs(8);
mcool = trnInputs(9);

mFileErrorCode = 150;   % After reading inputs

%%%%%%%%%%%%%%%%%%%%%%%%%%%%%%%%%%%%%%%%%%%%%%%%%%%%%%%%%%%%%%%%%%%%%%%%%%%%%%%
% --- Calculate desalinator outputs ---
%%%%%%%%%%%%%%%%%%%%%%%%%%%%%%%%%%%%%%%%%%%%%%%%%%%%%%%%%%%%%%%%%%%%%%%%%%%%%%%

L=mcool;                    % seawater flow rate [kg/s]
D=0.03;                     % fresh water flow rate (first attempt) [kg/s]

%%%%%%%%%%%% Initial temperatures %%%%%%%%%%%%

T=[];

T(1)=T1;                    % inlet seawater temperature [°C]
T(2)=30;                    % outlet seawater from condenser [°C]
T(3)=45;                    % outlet seawater from absorption chiller [°C]
% T(4)=38;
% T(5)=30;
% T(6)=33;

%%%%%%%%%%%%%%%%%%%%%%%%%%%%%%%%%%%%%%%%%%%%%%%%%%%%%%%%%%%%%%%%%%%%%%%%%%%%%%%
%%%%%%%%%%%%%%%%%%%%%%%%%%%%%%%%%%%%%%%%%%%%%%%%%%%%%%%%%%%%%%%%%%%%%%%%%%%%%%%

fin = fopen('mappa_ABS.txt','rt');    % 'rt' means "read text"
if (fin < 0)
    error('could not open file "mappa_ABS.txt"');
end

line=fgetl(fin);                            % get a line
n_line=1;
input=[];

while (ischar(line))                        % while not end of file
    switch (n_line)
        case(1)
            [portata,n1]=sscanf(line,'%f');
        case(2)
            [theatin,n2]=sscanf(line,'%f');
        case(3)
            [tcoolin,n3]=sscanf(line,'%f');
        otherwise
            input=[input, sscanf(line,'%f')];
    end

    line=fgetl(fin);                        % get next line
    n_line=n_line+1;
end

fclose(fin);
input=input';

Qevat=input(:,1);
```

```
COPt=input(:,2);

m=1;
for i=1:n1
    for j=1:n2
        for k=1:n3
            Q(j,k,i)=Qevat(m);
            COPa(j,k,i)=COPt(m);
            m=m+1;
        end
    end
end

portata=portata';
theatin=theatin';
tcoolin=tcoolin';

Qcool=Qevanom/COPnom+Qevanom;       % Qheater for desalination process [kW]
Lnom=(Qcool*191)/3575;                 % Nominal mass flow rate for ABS chiller
[kg/s]
Lratio=L/Lnom;

%%%%%%%%%%%%%%%%%%%%%%%%%%%%%%%%              Reading              mappa_HD.txt
%%%%%%%%%%%%%%%%%%%%%%%%%%%%%

fin = fopen('mappa_HD.txt','rt');    % 'rt' means "read text"
if (fin < 0)
    error('could not open file "mappa_HD.txt"');
end

line=fgetl(fin);                            % get a line
n_line=1;
input=[];

while (ischar(line))                        % while not end of file
    switch (n_line)
        case(1)
            [flusso_L,m1]=sscanf(line,'%f');
        case(2)
            [TfromABS,m2]=sscanf(line,'%f');
        case(3)
            [Tsea,m3]=sscanf(line,'%f');
        otherwise
            input=[input, sscanf(line,'%f')];
    end

    line=fgetl(fin);                        % get next line
    n_line=n_line+1;
end

fclose(fin);
input=input';

Dt=input(:,1);
T2t=input(:,2);

m=1;
for i=1:m1
    for j=1:m2
        for k=1:m3
            Da(j,k,i)=Dt(m);
            T2a(j,k,i)=T2t(m);
            m=m+1;
```

```
        end
    end
end

flusso_L=flusso_L';
TfromABS=TfromABS';
Tsea=Tsea';

%%%%%%%%%%%%% Iterative system resolution %%%%%%%%%%%%%

err=1;
NIter=0;
Tnew=T;
Qfan=0;

while (err>=tol && NIter<MaxIter)

    %%%%%%%%%%%% Desalinator %%%%%%%%%%%%

    deltaD=1;
    while (deltaD>0.01)
        if(T(3)==T(2))
            D=0;
            T(2)=T(1);
            deltaD=0;
        else
            Dold=D;
            if(T(3)<TfromABS(1) | T(3)>TfromABS(m2))
                D=0;
                T(2)=T(1);
                deltaD=0;
            else
                D=interp3(Tsea,TfromABS,flusso_L,Da,T(1),T(3),L);
                T(2)=interp3(Tsea,TfromABS,flusso_L,T2a,T(1),T(3),L);
                deltaD=abs((Dold-D)/Dold);
            end
        end
    end

    T3old=T(3);

    %%%%%%%%%%%% Chiller %%%%%%%%%%%%

    deltaQ=1;
    while (deltaQ>0.01)
        if(Theatin<theatin(1))
            T(3)=T(2);
            Qevaeff=0;
            COPeff=0;
            Qcool=0;
            Qin=0;
            deltaQ=0;
            D=0;
        else
            if(Theatin>theatin(n2))
                Theatin=theatin(n2);
            end
            if(T(2)<tcoolin(1) | T(2)>tcoolin(n3))
                T(3)=T(2);
                Qevaeff=0;
                COPeff=0;
                Qcool=0;
                Qin=0;
```

```
                deltaQ=0;
                D=0;
            else
                Qcoolold=Qcool;
                Qevaeff=interp3(tcoolin,theatin,portata,Q,T(2),Theatin,Lratio);
                Qevaeff=Qevaeff*Qevanom;

COPeff=interp3(tcoolin,theatin,portata,COPa,T(2),Theatin,Lratio);
                Qcool=Qevaeff/COPeff+Qevaeff;
                T(3)=T(2)+Qcool/(L*Cpw);
                Qin=Qcool/(1+COPeff);
                deltaQ=abs((Qcoolold-Qcool)/Qcoolold);
            end
        end
    end

    err=abs(T3old-T(3));
    NIter=NIter+1
end

Theatout=Theatin-Qin/(Cpw*mheat);
Tchillout=Tchillin-Qevaeff/(Cpw*mchill);
indice1=(D*310)/Qevaeff;
indice2=(Qevaeff+D*310)/Qin;
Spec_energy=Qcool/(D*3.6);

%%%%%%%%%%%%%%%%%%%%%%%%%%%%%%%%%%%%%%%%%%%%%%%%%%%%%%%%%%%%%%%%%%%%%%%%%%%%%%%
% --- Set outputs ---
%%%%%%%%%%%%%%%%%%%%%%%%%%%%%%%%%%%%%%%%%%%%%%%%%%%%%%%%%%%%%%%%%%%%%%%%%%%%%%%

trnOutputs(1) = Qevaeff;
trnOutputs(2) = COPeff;
trnOutputs(3) = Qcool;
trnOutputs(4) = Theatout;
trnOutputs(5) = T(2);
trnOutputs(6) = T(3);
trnOutputs(7) = 0;
trnOutputs(8) = 0;
trnOutputs(9) = D;
trnOutputs(10) = Tchillout;
trnOutputs(11) = indice1;
trnOutputs(12) = indice2;
trnOutputs(13) = Spec_energy;

mFileErrorCode = 0; % Tell TRNSYS that we reached the end of the m-file without
errors
return
```

Appendix C: FORTRAN code for type 182 in TRNSYS deck

```
                  SUBROUTINE TYPE182 (TIME,XIN,OUT,T,DTDT,PAR,INFO,ICNTRL,*)
!************************************************************************
! Object: ABS+DHD
! Simulation Studio Model: Type182
!
! Author: Alberto Picinardi
! Editor:
! Date:      July 21, 2010 last modified: July 21, 2010
!
!
! ***
! *** Model Parameters
! ***
!                 Cpw   kJ/kg.K [-Inf;+Inf]
!                 tol   - [-Inf;+Inf]
!                 MaxIter     - [-Inf;+Inf]

! ***
! *** Model Inputs
! ***
!                 Qevanom     kW [-Inf;+Inf]
!                 COPnom      - [-Inf;+Inf]
!                 Theatin     C [-Inf;+Inf]
!                 Tchillin    C [-Inf;+Inf]
!                 Tamb  C [-Inf;+Inf]
!                 Tsea  C [-Inf;+Inf]
!                 mheat kg/s [-Inf;+Inf]
!                 mcool kg/s [-Inf;+Inf]
!                 mchill      kg/s [-Inf;+Inf]

! ***
! *** Model Outputs
! ***
!                 Qevaeff     kW [-Inf;+Inf]
!                 COPeff      - [-Inf;+Inf]
!                 Qcool kW [-Inf;+Inf]
!                 Theatout    C [-Inf;+Inf]
!                 Tcoolin     C [-Inf;+Inf]
!                 Tcoolout    C [-Inf;+Inf]
!                 Tchillout   C [-Inf;+Inf]
!                 FreshWater  kg/s [-Inf;+Inf]
!                 Id    - [-Inf;+Inf]
!                 Overalleff  - [-Inf;+Inf]
!                 SpecEnergy  - [-Inf;+Inf]
!
! ***
! *** Model Derivatives
! ***

! (Comments and routine interface generated by TRNSYS Studio)
!************************************************************************

!    TRNSYS acess functions (allow to acess TIME etc.)
      USE TrnsysConstants
      USE TrnsysFunctions

!-------------------------------------------------------------------------------
---------------------------------------
```

```
!    REQUIRED BY THE MULTI-DLL VERSION OF TRNSYS
      !DEC$ATTRIBUTES DLLEXPORT :: TYPE182                        !SET THE
CORRECT TYPE NUMBER HERE
!------------------------------------------------------------------------------
--------------------------------------
!------------------------------------------------------------------------------
--------------------------------------
!    TRNSYS DECLARATIONS
      IMPLICIT NONE                !REQUIRES THE USER TO DEFINE ALL VARIABLES
BEFORE USING THEM

      DOUBLE PRECISION XIN    !THE ARRAY FROM WHICH THE INPUTS TO THIS TYPE WILL
BE RETRIEVED
      DOUBLE PRECISION OUT    !THE ARRAY WHICH WILL BE USED TO STORE THE OUTPUTS
FROM THIS TYPE
      DOUBLE PRECISION TIME   !THE CURRENT SIMULATION TIME - YOU MAY USE THIS
VARIABLE BUT DO NOT SET IT!
      DOUBLE PRECISION PAR    !THE ARRAY FROM WHICH THE PARAMETERS FOR THIS TYPE
WILL BE RETRIEVED
      DOUBLE PRECISION STORED !THE STORAGE ARRAY FOR HOLDING VARIABLES FROM
TIMESTEP TO TIMESTEP
      DOUBLE PRECISION T           !AN ARRAY CONTAINING THE RESULTS FROM THE
DIFFERENTIAL EQUATION SOLVER
      DOUBLE PRECISION DTDT   !AN ARRAY CONTAINING THE DERIVATIVES TO BE PASSED
TO THE DIFF.EQ. SOLVER
      INTEGER*4 INFO(15)           !THE INFO ARRAY STORES AND PASSES VALUABLE
INFORMATION TO AND FROM THIS TYPE
      INTEGER*4 NP,NI,NOUT,ND !VARIABLES FOR THE MAXIMUM NUMBER OF
PARAMETERS,INPUTS,OUTPUTS AND DERIVATIVES
      INTEGER*4 NPAR,NIN,NDER !VARIABLES FOR THE CORRECT NUMBER OF
PARAMETERS,INPUTS,OUTPUTS AND DERIVATIVES
      INTEGER*4 IUNIT,ITYPE   !THE UNIT NUMBER AND TYPE NUMBER FOR THIS
COMPONENT
      INTEGER*4 ICNTRL        !AN ARRAY FOR HOLDING VALUES OF CONTROL FUNCTIONS
WITH THE NEW SOLVER
      INTEGER*4 NSTORED       !THE NUMBER OF VARIABLES THAT WILL BE PASSED INTO
AND OUT OF STORAGE
      CHARACTER*3 OCHECK           !AN ARRAY TO BE FILLED WITH THE CORRECT
VARIABLE TYPES FOR THE OUTPUTS
      CHARACTER*3 YCHECK           !AN ARRAY TO BE FILLED WITH THE CORRECT
VARIABLE TYPES FOR THE INPUTS
!------------------------------------------------------------------------------
--------------------------------------

!------------------------------------------------------------------------------
--------------------------------------
!    USER DECLARATIONS - SET THE MAXIMUM NUMBER OF PARAMETERS (NP), INPUTS (NI),
!    OUTPUTS (NOUT), AND DERIVATIVES (ND) THAT MAY BE SUPPLIED FOR THIS TYPE
      PARAMETER (NP=3,NI=9,NOUT=11,ND=0,NSTORED=0)
!------------------------------------------------------------------------------
--------------------------------------

!------------------------------------------------------------------------------
--------------------------------------
!    REQUIRED TRNSYS DIMENSIONS
      DIMENSION
XIN(NI),OUT(NOUT),PAR(NP),YCHECK(NI),OCHECK(NOUT),STORED(NSTORED),T(ND),DTDT(ND)
      INTEGER NITEMS
!------------------------------------------------------------------------------
--------------------------------------
!------------------------------------------------------------------------------
--------------------------------------
!    ADD DECLARATIONS AND DEFINITIONS FOR THE USER-VARIABLES HERE
```

```
!    PARAMETERS
      DOUBLE PRECISION Cpw
      DOUBLE PRECISION tol
      DOUBLE PRECISION MaxIter

!    INPUTS
      DOUBLE PRECISION Qevanom
      DOUBLE PRECISION COPnom
      DOUBLE PRECISION Theatin
      DOUBLE PRECISION Tchillin
      DOUBLE PRECISION Tamb
      DOUBLE PRECISION Tsea
      DOUBLE PRECISION mheat
      DOUBLE PRECISION mcool
      DOUBLE PRECISION mchill

!    Other Parameters

      CHARACTER(70), PARAMETER :: mappaABS ='mappa_ABS.txt'
      CHARACTER(70), PARAMETER :: mappaHD ='mappa_HD.txt'

      INTEGER i
      INTEGER j
      INTEGER k
      INTEGER m

      INTEGER n1
      INTEGER n2
      INTEGER n3
      INTEGER m1
      INTEGER m2
      INTEGER m3

      INTEGER NIter
      INTEGER istatus

      DOUBLE PRECISION, DIMENSION(:), ALLOCATABLE, SAVE :: flowrate_ratio
      DOUBLE PRECISION, DIMENSION(:), ALLOCATABLE, SAVE :: theatin_range
      DOUBLE PRECISION, DIMENSION(:), ALLOCATABLE, SAVE :: tcoolin_range
      DOUBLE PRECISION, DIMENSION(:), ALLOCATABLE, SAVE :: flowrate
      DOUBLE PRECISION, DIMENSION(:), ALLOCATABLE, SAVE :: tcoolout_range
      DOUBLE PRECISION, DIMENSION(:), ALLOCATABLE, SAVE :: tsea_range

      DOUBLE PRECISION, DIMENSION(:,:), ALLOCATABLE, SAVE :: input

      DOUBLE PRECISION, DIMENSION(:,:,:), ALLOCATABLE, SAVE :: Qmatrix
      DOUBLE PRECISION, DIMENSION(:,:,:), ALLOCATABLE, SAVE :: COPmatrix
      DOUBLE PRECISION, DIMENSION(:,:,:), ALLOCATABLE, SAVE :: Dmatrix
      DOUBLE PRECISION, DIMENSION(:,:,:), ALLOCATABLE, SAVE :: T2matrix

      DOUBLE PRECISION Qevaeff
      DOUBLE PRECISION COPeff
      DOUBLE PRECISION Qcool
      DOUBLE PRECISION Qin
      DOUBLE PRECISION Lnom
      DOUBLE PRECISION Lratio

      DOUBLE PRECISION err
      DOUBLE PRECISION deltaD
      DOUBLE PRECISION deltaQ
      DOUBLE PRECISION FreshWater_old
```

```
      DOUBLE PRECISION Tcoolout_old
      DOUBLE PRECISION Qcool_old

      DOUBLE PRECISION :: FreshWater = 0.03
      DOUBLE PRECISION :: Tcoolin = 30
      DOUBLE PRECISION :: Tcoolout = 45

!      DOUBLE PRECISION, EXTERNAL :: LINT3

!------------------------------------------------------------------------------
----------------------------------------
!       READ IN THE VALUES OF THE PARAMETERS IN SEQUENTIAL ORDER
      Cpw=PAR(1)
      tol=PAR(2)
      MaxIter=PAR(3)

!------------------------------------------------------------------------------
----------------------------------------
!    RETRIEVE THE CURRENT VALUES OF THE INPUTS TO THIS MODEL FROM THE XIN ARRAY
IN SEQUENTIAL ORDER

      Qevanom=XIN(1)
      COPnom=XIN(2)
      Theatin=XIN(3)
      Tchillin=XIN(4)
      Tamb=XIN(5)
      Tsea=XIN(6)
      mheat=XIN(7)
      mcool=XIN(8)
      mchill=XIN(9)
         IUNIT=INFO(1)
         ITYPE=INFO(2)

!------------------------------------------------------------------------------
----------------------------------------
!    SET THE VERSION INFORMATION FOR TRNSYS
      IF(INFO(7).EQ.-2) THEN
         INFO(12)=16
         RETURN 1
      END IF
!------------------------------------------------------------------------------
----------------------------------------

!------------------------------------------------------------------------------
----------------------------------------
!    DO ALL THE VERY LAST CALL OF THE SIMULATION MANIPULATIONS HERE
      IF (INFO(8).EQ.-1) THEN
         RETURN 1
      END IF
!------------------------------------------------------------------------------
----------------------------------------

!------------------------------------------------------------------------------
----------------------------------------
!    PERFORM ANY 'AFTER-ITERATION' MANIPULATIONS THAT ARE REQUIRED HERE
!    e.g. save variables to storage array for the next timestep
      IF (INFO(13).GT.0) THEN
         NITEMS=0
!        STORED(1)=... (if NITEMS > 0)
!        CALL setStorageVars(STORED,NITEMS,INFO)
         RETURN 1
      END IF
!
```

```
!------------------------------------------------------------------------------
----------------------------------------

!------------------------------------------------------------------------------
----------------------------------------
!    DO ALL THE VERY FIRST CALL OF THE SIMULATION MANIPULATIONS HERE
      IF (INFO(7).EQ.-1) THEN

!       SET SOME INFO ARRAY VARIABLES TO TELL THE TRNSYS ENGINE HOW THIS TYPE IS
TO WORK
         INFO(6)=NOUT
         INFO(9)=1
         INFO(10)=0     !STORAGE FOR VERSION 16 HAS BEEN CHANGED


!       SET THE REQUIRED NUMBER OF INPUTS, PARAMETERS AND DERIVATIVES THAT THE
USER SHOULD SUPPLY IN THE INPUT FILE
!       IN SOME CASES, THE NUMBER OF VARIABLES MAY DEPEND ON THE VALUE OF
PARAMETERS TO THIS MODEL....
         NIN=NI
         NPAR=NP
         NDER=ND

!       CALL THE TYPE CHECK SUBROUTINE TO COMPARE WHAT THIS COMPONENT REQUIRES
TO WHAT IS SUPPLIED IN
!       THE TRNSYS INPUT FILE
         CALL TYPECK(1,INFO,NIN,NPAR,NDER)

!       SET THE NUMBER OF STORAGE SPOTS NEEDED FOR THIS COMPONENT
         NITEMS=0
!        CALL setStorageSize(NITEMS,INFO)

!       RETURN TO THE CALLING PROGRAM
         RETURN 1

      END IF
!------------------------------------------------------------------------------
----------------------------------------

!------------------------------------------------------------------------------
----------------------------------------
!    DO ALL OF THE INITIAL TIMESTEP MANIPULATIONS HERE - THERE ARE NO ITERATIONS
AT THE INTIAL TIME
      IF (TIME .LT. (getSimulationStartTime() + getSimulationTimeStep()/2.D0))
THEN

!       SET THE UNIT NUMBER FOR FUTURE CALLS
         IUNIT=INFO(1)
         ITYPE=INFO(2)

!       CHECK THE PARAMETERS FOR PROBLEMS AND RETURN FROM THE SUBROUTINE IF AN
ERROR IS FOUND
!         IF(...) CALL TYPECK(-4,INFO,0,"BAD PARAMETER #",0)

!       PERFORM ANY REQUIRED CALCULATIONS TO SET THE INITIAL VALUES OF THE
OUTPUTS HERE
!            Qevaeff
                OUT(1)=0
!            COPeff
                OUT(2)=0
!            Qcool
                OUT(3)=0
!            Theatout
```

```
                OUT(4)=0
!            Tcoolin
                OUT(5)=0
!            Tcoolout
                OUT(6)=0
!            Tchillout
                OUT(7)=0
!            FreshWater
                OUT(8)=0
!            Id
                OUT(9)=0
!            Overalleff
                OUT(10)=0
!            SpecEnergy
                OUT(11)=0

!       PERFORM ANY REQUIRED CALCULATIONS TO SET THE INITIAL STORAGE VARIABLES
HERE
         NITEMS=0
!        STORED(1)=...

!       PUT THE STORED ARRAY IN THE GLOBAL STORED ARRAY
!         CALL setStorageVars(STORED,NITEMS,INFO)

!       RETURN TO THE CALLING PROGRAM
         RETURN 1

      END IF
!-------------------------------------------------------------------------------
-------------------------------------

!-------------------------------------------------------------------------------
-------------------------------------
!    *** ITS AN ITERATIVE CALL TO THIS COMPONENT ***
!-------------------------------------------------------------------------------
-------------------------------------


!-------------------------------------------------------------------------------
-------------------------------------
!    RETRIEVE THE VALUES IN THE STORAGE ARRAY FOR THIS ITERATION
!      NITEMS=
!     CALL getStorageVars(STORED,NITEMS,INFO)
!      STORED(1)=
!-------------------------------------------------------------------------------
-------------------------------------
!-------------------------------------------------------------------------------
-------------------------------------
!    CHECK THE INPUTS FOR PROBLEMS
!      IF(...) CALL TYPECK(-3,INFO,'BAD INPUT #',0,0)
!     IF(IERROR.GT.0) RETURN 1
!-------------------------------------------------------------------------------
-------------------------------------
!-------------------------------------------------------------------------------
-------------------------------------
!    *** PERFORM ALL THE CALCULATION HERE FOR THIS MODEL. ***
!-------------------------------------------------------------------------------
-------------------------------------

!           ADD YOUR COMPONENT EQUATIONS HERE; BASICALLY THE EQUATIONS THAT WILL
!           CALCULATE THE OUTPUTS BASED ON THE PARAMETERS AND THE INPUTS.
      REFER TO
!           CHAPTER 3 OF THE TRNSYS VOLUME 1 MANUAL FOR DETAILED INFORMATION ON
```

```
!           WRITING TRNSYS COMPONENTS.

!       Reading from mappa_ABS.txt

        OPEN(1,FILE=mappaABS,STATUS='OLD',ACTION='READ',IOSTAT=istatus)

        IF(istatus==0) THEN     ! the file is open correctly

            READ(1,*,IOSTAT=istatus)n1,n2,n3

            ALLOCATE(flowrate_ratio(n1))
            ALLOCATE(theatin_range(n2))
            ALLOCATE(tcoolin_range(n3))
            ALLOCATE(input(n1*n2*n3,2))

            i=1

            DO WHILE(i<(n1*n2*n3)+3)
                SELECT CASE(i)
                    CASE(1)
                        READ(1,*,IOSTAT=istatus)flowrate_ratio(:)
                        i=i+1
                    CASE(2)
                        READ(1,*,IOSTAT=istatus)theatin_range(:)
                        i=i+1
                    CASE(3)
                        READ(1,*,IOSTAT=istatus)tcoolin_range(:)
                        i=i+1
                    CASE DEFAULT
                        READ(1,*,IOSTAT=istatus)input(i-3,:)
                        IF(istatus/=0) THEN
                            WRITE(*,*) 'The file ', mappaABS, ' is not complete'
                            EXIT
                        END IF
                        i=i+1
                END SELECT
            END DO
            CLOSE(1)
        ELSE
            WRITE(*,*) 'The file ', mappaABS, ' does not exist'
        END IF

        ALLOCATE(Qmatrix(n2,n3,n1))
        ALLOCATE(COPmatrix(n2,n3,n1))

        m=1;
        DO i=1,n1
              DO j=1,n2
                    DO k=1,n3
                        Qmatrix(j,k,i)=input(m,1)
                        COPmatrix(j,k,i)=input(m,2)
                        m=m+1
                    END DO
              END DO
        END DO

        DEALLOCATE(input)

        Qcool=Qevanom/COPnom+Qevanom
        Lnom=(Qcool*191)/3575
        Lratio=mcool/Lnom
```

```
!       Reading from mappa_HD.txt

        OPEN(1,FILE=mappaHD,STATUS='OLD',ACTION='READ',IOSTAT=istatus)

        IF(istatus==0) THEN     ! the file is open correctly

            READ(1,*,IOSTAT=istatus)m1,m2,m3

            ALLOCATE(flowrate(m1))
            ALLOCATE(tcoolout_range(m2))
            ALLOCATE(tsea_range(m3))
            ALLOCATE(input(m1*m2*m3,2))

            i=1

            DO WHILE(i<(m1*m2*m3)+3)
                SELECT CASE(i)
                    CASE(1)
                        READ(1,*,IOSTAT=istatus)flowrate(:)
                        i=i+1
                    CASE(2)
                        READ(1,*,IOSTAT=istatus)tcoolout_range(:)
                        i=i+1
                    CASE(3)
                        READ(1,*,IOSTAT=istatus)tsea_range(:)
                        i=i+1
                    CASE DEFAULT
                        READ(1,*,IOSTAT=istatus)input(i-3,:)
                        IF(istatus/=0) THEN
                            WRITE(*,*) 'The file ', mappaHD, ' is not complete'
                            EXIT
                        END IF
                        i=i+1
                END SELECT
            END DO
            CLOSE(1)
        ELSE
            WRITE(*,*) 'The file ', mappaHD, ' does not exist'
        END IF

        ALLOCATE(Dmatrix(m2,m3,m1))
        ALLOCATE(T2matrix(m2,m3,m1))

        m=1;
        DO i=1,m1
              DO j=1,m2
                    DO k=1,m3
                        Dmatrix(j,k,i)=input(m,1)
                        T2matrix(j,k,i)=input(m,2)
                        m=m+1
                    END DO
              END DO
        END DO

        DEALLOCATE(input)


!       Resolution of the System

        err=1;
        NIter=0;

        DO WHILE(err>=tol.AND.NIter<MaxIter)
```

```
!       Desalinator

            deltaD=1;
            DO WHILE(deltaD>0.01)
                IF(Tcoolout==Tcoolin) THEN
                    FreshWater=0
                    Tcoolin=Tsea
                    deltaD=0
                ELSE

IF(Tcoolout<tcoolout_range(1).OR.Tcoolout>tcoolout_range(m2)) THEN
                        FreshWater=0
                        Tcoolin=Tsea
                        deltaD=0
                    ELSE
                        FreshWater_old=FreshWater

FreshWater=LINT3(m2,m3,m1,tcoolout_range,tsea_range,flowrate,Dmatrix,Tcoolout,Ts
ea,mcool)

Tcoolin=lint3(m2,m3,m1,tcoolout_range,tsea_range,flowrate,T2matrix,Tcoolout,Tsea
,mcool)

                        deltaD=ABS((FreshWater_old-FreshWater)/FreshWater_old)
                    END IF
                END IF
            END DO

            Tcoolout_old=Tcoolout

!       Chiller

            deltaQ=1
            DO WHILE(deltaQ>0.01)
                IF(Theatin<theatin_range(1)) THEN
                    Tcoolout=Tcoolin
                    Qevaeff=0
                    COPeff=0
                    Qcool=0
                    Qin=0
                    deltaQ=0
                    FreshWater=0
                ELSE
                    IF(Theatin>theatin_range(n2)) THEN
                        Theatin=theatin_range(n2)
                    END IF
                    IF(Tcoolin<tcoolin_range(1).OR.Tcoolin>tcoolin_range(n3))
THEN
                        Tcoolout=Tcoolin
                        Qevaeff=0
                        COPeff=0
                        Qcool=0
                        Qin=0
                        deltaQ=0
                        FreshWater=0
                    ELSE
                        Qcool_old=Qcool

Qevaeff=lint3(n2,n3,n1,theatin_range,tcoolin_range,flowrate_ratio,Qmatrix,Theati
n,Tcoolin,Lratio)
                        Qevaeff=Qevaeff*Qevanom
```

```
COPeff=lint3(n2,n3,n1,theatin_range,tcoolin_range,flowrate_ratio,COPmatrix,Theat
in,Tcoolin,Lratio)
                        Qcool=Qevaeff/COPeff+Qevaeff
                        Tcoolout=Tcoolin+Qcool/(mcool*Cpw)
                        Qin=Qcool/(1+COPeff)
                        deltaQ=ABS((Qcool_old-Qcool)/Qcool_old)
                    END IF
                END IF
            END DO

            err=ABS(Tcoolout_old-Tcoolout)
            NIter=NIter+1

        END DO

        DEALLOCATE(flowrate_ratio)
        DEALLOCATE(theatin_range)
        DEALLOCATE(tcoolin_range)
        DEALLOCATE(Qmatrix)
        DEALLOCATE(COPmatrix)
        DEALLOCATE(flowrate)
        DEALLOCATE(tcoolout_range)
        DEALLOCATE(tsea_range)
        DEALLOCATE(Dmatrix)
        DEALLOCATE(T2matrix)


!-------------------------------------------------------------------------------
---------------------------------------

!-------------------------------------------------------------------------------
---------------------------------------
!-------------------------------------------------------------------------------
---------------------------------------
!    SET THE STORAGE ARRAY AT THE END OF THIS ITERATION IF NECESSARY
!      NITEMS=
!      STORED(1)=
!     CALL setStorageVars(STORED,NITEMS,INFO)
!-------------------------------------------------------------------------------
---------------------------------------
!-------------------------------------------------------------------------------
---------------------------------------
!    REPORT ANY PROBLEMS THAT HAVE BEEN FOUND USING CALLS LIKE THIS:
!      CALL MESSAGES(-1,'put your message here','MESSAGE',IUNIT,ITYPE)
!      CALL MESSAGES(-1,'put your message here','WARNING',IUNIT,ITYPE)
!      CALL MESSAGES(-1,'put your message here','SEVERE',IUNIT,ITYPE)
!      CALL MESSAGES(-1,'put your message here','FATAL',IUNIT,ITYPE)
!-------------------------------------------------------------------------------
---------------------------------------
!-------------------------------------------------------------------------------
---------------------------------------
!    SET THE OUTPUTS FROM THIS MODEL IN SEQUENTIAL ORDER AND GET OUT

!            Qevaeff
                 OUT(1)=Qevaeff
!            COPeff
                 OUT(2)=COPeff
!            Qcool
                 OUT(3)=Qcool
!            Theatout
                 OUT(4)=Theatin-Qin/(Cpw*mheat)
!            Tcoolin
```

```
                OUT(5)=Tcoolin
!               Tcoolout
                OUT(6)=Tcoolout
!               Tchillout
                OUT(7)=Tchillin-Qevaeff/(Cpw*mchill)
!               FreshWater
                OUT(8)=FreshWater
!               Id
                OUT(9)=(FreshWater*310)/Qevaeff
!               Overalleff
                OUT(10)=(Qevaeff+FreshWater*310)/Qin
!               SpecEnergy
                OUT(11)=Qcool/(FreshWater*3.6)

!-------------------------------------------------------------------------------
---------------------------------------
!    EVERYTHING IS DONE - RETURN FROM THIS SUBROUTINE AND MOVE ON
      RETURN 1

      CONTAINS
            DOUBLE PRECISION FUNCTION LINT3(NX,NY,NZ,X,Y,Z,W,X1,Y1,Z1)

            INTEGER :: NX,NY,NZ          !dimensioni dei vettori X, Y, Z
            DOUBLE PRECISION,DIMENSION(NX) :: X!vettore ascisse della griglia
            DOUBLE PRECISION,DIMENSION(NY) :: Y!vettore ordinate della griglia
            DOUBLE PRECISION,DIMENSION(NZ) :: Z!vettore ordinata complessa della
griglia
            DOUBLE PRECISION,DIMENSION(NX,NY,NZ):: W !iper-superficie da
interpolare
            DOUBLE PRECISION :: X1,Y1,Z1       !coordinate di interpolazione
            INTEGER :: IMIN,JMIN,KMIN    !valori coordinate estremo inferiore di
interpolazione

            INTEGER :: I

            !valori di interpolazione parziale
            DOUBLE PRECISION :: w11,w12,w21,w22
            DOUBLE PRECISION :: w1,w2

            IMIN=0
            JMIN=0
            KMIN=0

            !individuazione dell'estremo inferiore
            !(le ascisse e le ordinate siano vettori di elementi a valore
crescente)
            IF (IMIN==0) THEN
                  DO I=1,NX
                        IF (X(I)>X1) THEN
                        IMIN=I-1
                        EXIT
                        END IF
                  END DO
            END IF

            IF (X(NX)==X1) THEN
                IMIN=NX-1
            END IF

            IF (JMIN==0) THEN
                  DO I=1,NY
                        IF(Y(I)>Y1) THEN
                        JMIN=I-1
```

```
                        EXIT
                        END IF
                  END DO
            END IF

            IF (Y(NY)==Y1) THEN
                JMIN=NY-1
            END IF

            IF (KMIN==0) THEN
                  DO I=1,NZ
                        IF(Z(I)>Z1) THEN
                        KMIN=I-1
                        EXIT
                        END IF
                  END DO
            END IF

            IF (Z(NZ)==Z1) THEN
                KMIN=NZ-1
            END IF

            IF (IMIN*JMIN*KMIN==0)THEN
            WRITE(*,*)"Out of boundary"
            LINT3=-111.111
            RETURN
            END IF

            !interpolazioni parziali
            w11=W(IMIN,JMIN,KMIN)+(X1-X(IMIN))*(W(IMIN+1,JMIN,KMIN)-
W(IMIN,JMIN,KMIN))/(X(IMIN+1)-X(IMIN))
            w12=W(IMIN,JMIN+1,KMIN)+(X1-X(IMIN))*(W(IMIN+1,JMIN+1,KMIN)-
W(IMIN,JMIN+1,KMIN))/(X(IMIN+1)-X(IMIN))

            w1=w11+(Y1-Y(JMIN))*(w12-w11)/(Y(JMIN+1)-Y(JMIN))

            w21=W(IMIN,JMIN,KMIN+1)+(X1-X(IMIN))*(W(IMIN+1,JMIN,KMIN+1)-
W(IMIN,JMIN,KMIN+1))/(X(IMIN+1)-X(IMIN))
            w22=W(IMIN,JMIN+1,KMIN+1)+(X1-X(IMIN))*(W(IMIN+1,JMIN+1,KMIN+1)-
W(IMIN,JMIN+1,KMIN+1))/(X(IMIN+1)-X(IMIN))

            w2=w21+(Y1-Y(JMIN))*(w22-w21)/(Y(JMIN+1)-Y(JMIN))


            LINT3=w1+(Z1-Z(KMIN))*(w2-w1)/(Z(KMIN+1)-Z(KMIN))

            RETURN
            END FUNCTION

      END
!-------------------------------------------------------------------------------
---------------------------------------
```

Appendix D: Bibliography

Introduction

[1] German Aerospace Center (DLR), Institute of Technical Thermodynamics, Section Systems Analysis and Technology Assessment “Concentrating Solar Power for Seawater Desalination”, Stuttgart, November 2007

Chapter 1

[1] IDA Desalting Inventory 2004: Desalination Business Stabilized on a High Level, Int. Desal. Water reuse, 14 (2) (2004) 14–17.

[2] E.D. Howe, Fundamentals of Water Desalination, Marcel Dekker, New York, 1974. [4] O.K. Buros, The U.S.A.I.D. Desalination Manual, International Desalination and Environmental Association, 1980.

[3] O.K. Buros, The U.S.A.I.D. Desalination Manual, International Desalination and Environmental Association, 1980.

[4] K.S Spiegler and A.D.K. Laird, Principles of Desalination, 2nd edn., Academic Press, New York, 1980.

[5] A. Porteous, Desalination Technology, Applied Science Publishers, London, 1983.

[6] H.G. Heitmann, Saline Water Processing, VCH Verlagsgesellschaft, Germany, 1990.

[7] K.S. Spiegler and Y.M. El-Sayed, A Desalination Primer, Balaban Desalination Publications, Santa Maria Imbaro, Italy, 1994.

[8] B. Van der Bruggen, Desalination by distillation and by reverse osmosis — trends towards the future, Membr. Tech., 2003 (2) (2003) 6–9.

[9] Global Water Intelligence, Market Profile: Desalination Markets 2007 Preview, October 2006, p. 27.

[10] A.D. Khawaji, T. Khan and J.M. Wie, Gas Turbine Operating Experience in a Power/Seawater Desalination Cogeneration Mode, ASME ASIA ‘97 Congress & Exhibition, Paper Reprint No 97-AA-120, Singapore, September 30–October 2, 1997.

[11] B.A. Kamaluddin, S. Khan and B.M. Ahmed, Selection of optimally matched cogeneration plants, Desalination, 93 (1993) 311–321.

[12] A.M. El-Nashar, Cogeneration for power and desalination-state of the art review, Desalination, 134 (2001) 7–28.

[13] F.I. Jambi and J.M. Wie, The Royal Commission Gas Turbine/HRSG/Desalination Cogeneration Plant, 1989 ASME COGEN-TURBO, 3rd International Symposium on

Turbomachinery, Combined-Cycle and Cogeneration, American Society of Mechanical Engineers, New York, 1989, pp. 275–280.

[14] A.M. Al Mudaiheem and H. Miyamura, Construction and Commissioning of Al Jobail Phase II Desalination Plant, in: Proceedings of the Second IDA World Congress on Desalination and Water Re-use, Bermuda, Vol. II, November 17–22, 1985, pp. 1–11.

[15] M.F. Al Ghamdi, C.H. Hughes and S. Kotake, The Makkah-Taif MSF desalination plant, Desalination, 66 (1987) 3–10.

[16] M.A.K. Al-Sofi, M.A. Al-Hussain, A.A.Z. Al-Omran and K.M. Farran, A Full Decade of Operating Experience on Al-Khobar-II Multi Stage Flash (MSF) Evaporators (1982–1992), in: Proceedings of the IDA and WRPC World Conference on Desalination and Water Treatment, Yokohama, Japan, November 3–6, 1993, pp. 271–279.

[17] The 12 MIGD Multistage Flash Desalination Units, Mod. Power Sys., 15 (7) (1995) 11–14.

[18] C. Sommariva, The 72 MIGD multi-stage flash distillation plant at Al Taweelah, Abu Dhabi, UAE, Desal. Water Reuse, 6 (1) (1996) 30–36.

[19] A.D. Khawaji, J.M. Wie and T. Khan, Operating Experience of the Royal Commission Acid-Dosed MSF Seawater Desalination Plant, in: Proceedings of IDA World Congress on Desalination and Water Reuse, Vol. II, Madrid, Spain, October 6–9, 1997, pp. 3–19.

[20] A. Harris, Seawater Chemistry and Scale Control, Desalination Technology Development and Practice, in: A. Porteous (Ed.), Applied Science Publishers, London, UK, 1983, 31–56.

[21] S.A. Al-Saleh and A.R. Khan, Evaluation of Belgard EV 2000 as Antiscalant Control Additive in MSF Plant, in: Proceedings of the IDA and WRPC World Conference on Desalination and Water Treatment, Yokohama, Japan, November 3–6, 1993, pp. 483–490.

[22] F. Pujadas, Y. Fukumoto and K. Isobe, Performance Test of Antiscalant AQUAKREEN KC-550 under a Wide Range of Temperature Conditions at the MSF Desalination Plant in Abu-Dhabi, in: Proceedings of IDA World Congress on Desalination and Water Reuse, Vol. II, Washington, DC, August 1991, pp. 25–29.

[23] American Cyanamid Company, Performance of CYANAMER P-80 on an MSF Seawater Distillation Unit Operating at 112°C Top Temperature, Ras Abu Fontas Power and Water Station, Qatar, 29 October 1986–24 January 1987, 1987.

[24] G.F. Casini, The application of a high temperature scale control additive in a Middle East MSF plant, Desalination, 47 (1983) 19–22.

[25] J.C. Bernard and E. Demolins, Scale Control Additive-Practical Experiences in Multistage Flash Plants, in: Proceedings of the Second IDA World Congress on Desalination and Water Re-use, Vol. I, Bermuda, November 17–22, 1985, pp. 301–305.

[26] H.G. Heitmann, Chemical Problems and Chemical Conditioning in Seawater Desalination, Saline Water Processing, in: H.G. Heitmann (Ed.), VCH Verlagsgesellschaft, Germany, 1990, pp. 55–66.

[27] M. Al-Ahmad and F.A.A. Aleem, Scale formation and fouling problems effect on the performance of MSF and RO desalination plants in Saudi Arabia, Desalination, 93 (1–3) (1993) 287–310.

[28] I. Barthelmes and H. Bohmer, Fouling and scaling control in MSF desalination units by on-load tube cleaning, Desal. Water Reuse, 7 (2) (1997), 27–33.

[29] S. Patel and M.A. Finan, New antifoulants for deposit control in MSF and MED plants, Desal. Water Reuse, 9 (2) (1999) 61–69.

[30] A.I. Dabbour, J.M. Wie and S. Sheikh, Removal of Calcium Sulfate Scale by EDTA, in: Proceedings of the IDA World Congress on Desalination and Water Reuse, San Diego, August 29–September 3, 1999.

[31] D.P. Logan and S.P. Rey, Scale Control in Multi Stage Flash Evaporators, Materials Performance, June 1986, pp. 38–44.

[32] IDA Desalination Yearbook 2006–2007, Water Desalination Report, Global Water Intelligence and International Desalination Association, Topsfield, MA, USA.

[33] T. Michels, Recent achievements of low-temperature multiple effect desalination in the western area of Abu Dhabi, UAE, Desalination, 93 (1993) 111–118.

[34] A. Ophir, A. Gendel and G. Kronenberg, The LT-MED process for SW Cogen Plants, Desal. Water Reuse, 4 (1) (1994) 28–31.

[35] M.A. Darwish, Desalination Process: A Technical Comparison, in: Proceedings of IDA World Congress on Desalination and Water Sciences, Abu Dhabi, United Arab Emirates, Vol. I, November 18–24, 1995, pp. 149–173.

[36] L.A. Awerbuch, Vision for Desalination–Challenges and Opportunities, in: Proceedings of the IDA World Congress and Water Reuse, Manama, Bahrain, March 8–13, 2002.

[37] O.K. Buros, The Desalting ABC, International Desalination Association, Topsfield, MA, USA, 1990.

[38] K. Bourouni, M.T. Chaibi, L. Tadrist, Water desalination by humidification and dehumidification of air: state of the art, Desalination 137 (2001) 167–176

[39] K. Bourouni, R. Martin, L. Tadrist and H. Tadrist, Experimental investigation of evaporation performances of a desalination prototype using the aeroevapo- condensation process. Desalination, 114 (1997) 111–128.

[40] N.K. Nawayseh, M.M. Farid, A.A. Omar, S.M. Al- Hallaj and A.R. Tamimi, A simulation study to improve the performance of a solar humidification–dehumidification desalination unit constructed in Jordan. Desalination, 109 (1997) 277–284.

[41] Y.J. Dai and H.F. Zhang, Experimental investigation of a solar desalination unit with humidification– dehumidification. Desalination, 130 (2000) 169–175.

[42] Said Al-Hallaj, Mohammed Mehdi arid, Abdul Rahrnan Tamirni, Solar desalination with a humidification-dehumidification cycle: performance of the unit, Desalination I20 (1998) 273-280

[43] K. Bourouni, M. Chaibi, R. Martin and L. Tadrist, Appl. Energy, 64 (1999) 129.

[44] M. Vlachogiannis, V. Bontzoglou, C. Georgalas and G. Litinas, Desalination, 122 (1999) 35.

[45] Efat Chafik, A new seawater desalination process using solar energy, Desalination 153 (2002) 25-37

[46] Adnan Midilli, Wastewater distillation via natural vacuum technique. Ph.D. Thesis, Karadeniz Technical University, Turkey (2001)

[47] Adnan Midilli, Teoman Ayhan, Natural vacuum distillation technique, Int. J. Energy Res. 2004; 28:355–389

[48] Veera Gnaneswar Gude, Nagamany Nirmalakhandan, Combined desalination and solar-assisted air-conditioning system, Energy Conversion and Management 49 (2008) 3326–3330

[49] Teoman Ayhan, Hussain Al Madani, Feasibilty study of renewable energy powered seawater desalination technology using natural vacuum technique, Renewable Energy 35 (2010) 506–514

[50] L. Garzia-Rodriguez, Seawater desalination driven by renewable energies: a review, Desalination, 143 (2002) 103–113.

[51] G. Mink, M. Aboabbous and E. Karmazsin, Design parameters, performance testing and analysis of a double-glazed, air-blown solar still with heat recycling, Solar Energy, 62 (1998) 309–317.

[52] G. Zaki, A. Radhwan and A. Balbeid, Analysis of assisted coupled solar stills, Solar Energy, 51 (1993) 277–288.

[53] M. Malik, G. Tiwari, A. Kumar and M. Sodha, Solar Distillation: A Practical Study of a Wide Range of Stills and their Optimum Design Construction and Performance, Pergamon Press, 1996.

[54] O. Haddad, M. Al-Nimer and A. Maqableh, Enhanced solar still performance using a radiative cooling system, Renewable Energy, 21 (2000) 459–469.

[55] H. Fath, Solar distillation: a promising alternative for water provision with free energy, a simple technology and a clean environment, Desalination, 116 (1998) 45–56.

[56] T. Tanaka, A. Yamashita and K. Watanabe, Proc. International Solar Energy Congress, Brighton, England, Vol. 2, 1981, p. 1087.

[57] M. Sodha, A. Kumar, G. Tiwari and R. Tyagi, Simple multiple wick solar still: analysis and performance, Solar Energy, 26 (1981) 127–131.

[58] F. Graeter, M. Duerrbeck and J. Rheinlaender, Multi-effect still for hybrid solar/fossil desalination of sea and brackish water, Desalination, 138 (2001) 111–119.

[59] J. Rheinlaender and F. Graeter, Technologies for desalination of typically 10 m_3 of water per day, Desalination, 139 (2001) 393–397.

[60] M. Chaibi, Greenhouse systems with integrated water desalination for arid areas based on solar energy, Doctoral thesis, Swedish University of Agricultural Sciences, Alnarp, 2003.

[61] King Abdulaziz City for Science and Technology, Solar Energy Water Desalination Engineering Test Facility, Riyadh, Saudi Arabia, 1986.

[62] John Walton, Huanmin Lu, Charles Turner, Sergio Solis, Herbert Hein, Solar and Heat desalination by membrane distillation, College of Engineering University of Texas at El Paso El Paso, TX 79968, Program Report N. 81, April 2004

[63] A.M. Alklaibi, Noam Lior, Membrane-distillation desalination: status and potential, Desalination 171 (2004) 111-131

[64] K.W. Lawson and D.R. Lloyd, Membrane distillation. II. Direct contact MD, J. Membr. Sci., 120 (1996) 123.

[65] L. Martinez-Diez and F.J. Florido-Diaz, Theoretical and experimental studies on membrane distillation, Desalination, 139 (2001) 373-379.

[66] J. Phattaranawik and R. Jiraratananon, Direct contact membrane distillation: effect of mass transfer on heat transfer, J. Membr. Sci., 188 (2001) 137.

[67] S. Bandini, C. Gostoli and G.C. Sarti, Separation efficiency in vacuum membrane distillation, J. Membr. Sci., 73 (1992) 217-229.

[68] G.C. Sarti, C. Gostoli and S. Bandini, Extraction of organic components from aqueous streams by vacuum membrane distillation, J. Membr. Sci., 80 (1993) 21-33.

[69] A.S. Jonsson, R. Wimmerstedt and A.C. Harrysson, Membrane distillation -- A theoretical study of evaporation through microporous membranes, Desalination, 56 (1985) 237-249.

[70] F.A. Banat, Membrane distillation for desalination and removal of volatile organic compounds from water, Ph.D. Thesis, McGill University, 1994.

[71] L. Basini, G. D'Angelo, M. Gobbi, G.C. Sarti and C. Gostoli, A desalination process through sweeping gas membrane distillation, Desalination, 64 (1987) 245-257.

[72] M. Khayet, P. Godino andJ. I. Mengual, Theory and experiments on sweeping gas membrane distillation, J. Membr. Sci., 165 (2000) 261-272.

[73] M. Khayet, P. Godino and J.I. Mengual, Nature of flow on sweeping gas membrane distillation, J. Membr. Sei., 170 (2000) 243-255.

[74] C.A. Rivier, M.C. Garcia-Payo, I.W Marison and U. von Stocker, Separation of binary mixtures by thermostatic sweeping gas membrane distillation I. Theory and simulations, J. Membr. Sci., 201 (2002) 1-16.

[75] M.C. Garcia-Payo, C.A. Rivier, I.W. Marison and U. yon Stocker, Separation of binary mixtures by thermostatic sweeping gas membrane distillation II. Experimental results with aqueous formic acid solutions, J. Membr Sci., 198 (2002) 197-210.

[76] Y. Ayyash, H. Imai, T. Yamada, T. Fukuda and T. Taniyama, Performance of reverse osmosis membrane in Jeddah Phase I Plant, Desalination, 98 (1994) 215–224.

[77] A.R. Al-Badawi, S.S. Al-Harthi, H. Imai, H. Iwahashi, M. Katsube and N. Fujiwara, Operation and Analysis of Jeddah 1-Phase II Plant, in: Proceedings of the IDA and World Congress on Desalination and Water Sciences, Abu Dhabi, United Arab Emirates, Vol. III, November 18–24, 1995, pp. 41–54.

[78] N. Nada, Y. Yanaga and K. Tanaka, Design Features of the Largest SWRO Plant in the World — 33.8 MGD in Madina and Yanbu, in: Proceedings of the IDA and World Congress on Desalination and Water Sciences, Abu Dhabi, United Arab Emirates, Vol. V, November 18–24, 1995, pp. 3–15.

[79] M.B. Baig and A. Al Kutbi, Design features of 20 MIGD SWRO seawater plant, Al Jubail, Saudi Arabia, Water Supply, 17 (1999) 127–134.

[80] A.H.H. Al-Sheikh, Seawater reverse osmosis pretreatment with an emphasis on the Jeddah Plant operating experience, Desalination, 110 (1–2) (1997) 183–192.

[81] S. Bou-Hamad, M. Abdel-Jawad, S. Ebrahim, M. Al-Mansour and A. Al-Hijji, Performance evaluation of three different pretreatment systems for seawater reverse osmosis technique, Desalination, 110 (1–2) (1997) 85–92.

[82] B. Durham and A. Walton, Membrane pretreatment of reverse osmosis: long-term experience on difficult waters, Desalination, 122 (2) (1999) 157–170.

[83] S.H. Ebrahim, M.M. Abdel-Jawad and M. Safar, Conventional pretreatment system for the Doha reverse osmosis plant: technical and economic assessment, Desalination, 110 (1–3) (1995) 179–187.

[84] R. Rautenbach, T. Linn and D.M.K. Al-Gobaisi, Present and future pretreatment concept-strategies for reliable and low-maintenance reverse osmosis seawater desalination, Desalination, 110 (1–2) (1997) 97–106.

[85] Z. Amjad, RO systems current fouling problems & solutions, Desal. Water Reuse, 6 (4) (1997) 55–60.

[86] J.W. Oldfield and R.M. Kain, Economic Material Selection for Reverse Osmosis Desalination Plants, in: Proceedings of the 12th International Symposium on Desalination & Water Re-Use, Malta, April 15–18, 1991.

[87] A. Abu-Safiah, Material selection for the high pressure section of seawater RO plants, Desalination, 84 (1991) 279–308.

[88] M. Jasner, Application of of austenitic nitrogenalloyed 6MO stainless steel for seawater desalination (RO) and waste water treatment, Desalination, 84 (1991) 335–348.

[89] S.A. Shumway, The work exchanger for SWRO energy recovery, Desal. Water Reuse, 8 (4) (1999) 27–33.

[90] S.J. Duranceau, J. Foster, H.J. Losch, R.E. Weis, J.A. Harn and J. Nemeth, Interstage turbine, Desal. Water Reuse, 8 (4) (1999) 34–40.

[91] W. Childs and A. Dabiri, Hydraulic driven RO pump & energy recovery system, Desal. Water Reuse, 9 (2) (1999) 21–29.

[92] A. Gruendisch, Re-engineering of the Pelton tuirbine for SW & brackish water energy recovery, Desal. Water Reuse, 9 (3) (1999) 16–23.

[93] J.P. MacHarg, Exchanger tests verify 2.0 kW h/m^3 SWRO energy use, Desal. Water Reuse, 11 (1) (2001) 42–45.

[94] Davis, T.A., "Electrodialysis", in Handbook of Industrial Membrane Technology, M.C. Porter, ed., Noyes Publications, New Jersey (1990)

[95] Strathmann, H., "Electrodialysis", in Membrane Handbook, W.S.W. Ho and K.K. Sirkar, eds., Van Nostrand Reinhold, New York (1992)

[96] Mulder, M., Basic Principles of Membrane Technology, Kluwer, Dordrecht (1996)

[97] Sata, T., Ion Exchange Membranes: Preparation, Characterization, Modification and Application, Royal Society of Chemistry, London (2004)

[98] Strathmann, H., Ion-Exchange Membrane Separation Processes, Elsevier, New York (2004)

Chapter 2

[1] Naser Kh. Nawayseh, Mohammed Mehdi Farid, Said Al-Hallaj, Abdul Rahman Al-Timim, Solar desalination based on humidification process. Evaluating the heat and mass transfer coefficients, Energy Conversion & Management 40 (1999) 1423-1439

[2] D. Negrini, V. Redondi, "Implementazione di un modello di calcolo per un dissalatore HD", Master Thesis, University of Bergamo, 2009

[3] F. P. Incropera, D.P Witt, Fundamentals of Heat and Mass Transfer

[4] C. Bougriou, R. Bessaih, Determination of apparent heat transfer coefficient by condensation in an industrial finned-tube heat exchangers, Applied Thermal Engineering 25 (2005) 1863–1870

[5] Hewitt, Heat exchangers design handbook vol.2

[6] D. G. Kroger, J. C. Kloppers, Cooling Tower Performance Evaluation: Merkel, Poppe and e.NTU Methods of Analysis, Journal of Engineering for Gas Turbines and Power, ASME, 2005

[7] F. Besana, Heat Rejection Problematic in Solar Combi+ System, PhD Thesis, University of Bergamo, 2009

[8] C. Bourillot, On the hypothesis of calculating the water flowrate evaporated in a wet cooling tower, EPRI Report CS-3144-SR, August 1983.

Chapter 3

[1] J. Gunzbourg and D. Larger, Desalination, 125 (1999) 203–208.

[2] S.E. Aly, Desalination, 78 (1990) 363–379.

[3] S.E. Aly, Desalination, 82 (1991) 245.

[4] V.V. Slesarenko, Desalination, 126 (1999) 281–285.

[5] V.V. Slesarenko, Heat pumps as a source of heat energy for desalination of seawater, Desalination 139 (2001) 405-410

[6] F. Al-Juwayhel, H. El-Dessouky and H. Ettouney, Desalination, 114 (1997) 253–275.

[7] S. Elshamarka. Appl. Energy, 40 (1991) 31–40.

[8] M. Nguyen, S.B. Riffat and D. Whitman, Appl. Therm. Eng., 16 (1996) 347–356.

[9] Huicochea, J. Siqueiros and R.J. Romero, Desalination, 165 (2004) 385–391.

[10] F. Mandani, H. Ettouney and H. El-Dessouky, Desalination, 128 (2000) 161–176.

[11] J. Siqueiros, F.A. Holland, Water desalination using heat pumps, Energy 25 (2000) 717–729

[12] D.C.A. Padilla, L. G. Rodríguez, Application of absorption heat pumps to multi-effect distillation: a case study of solar desalination, Desalination 212 (2007) 294–302

[13] D.C.A. Padilla, L. G. Rodríguez, Assessment of an absorption heat pump coupled to a multi-effect distillation unit within AQUASOL project, Desalination 212 (2007) 303–310

[14] V.G. Gude, N. Nirmalakhandan, Combined desalination and solar-assisted air-conditioning system, Energy Conversion and Management 49 (2008) 3326–3330

[15] R. Borsani, R. Rebagliati , Fundamentals and costing of MSF desalination plants and comparison with other technologies, Desalination, 182 (2005), 29–37.

[16] G. Franchini, A. Perdichizzi, Freshwater and cooling cogeneration by solar energy, presented at ISES Solar World Congress 2009, Johannesburg, South Africa, October 11-14, 2009.

[17] G. Franchini, A. Perdichizzi, A. Picinardi, HD desalination by heat rejected from solar cooling system, presented at Energycon 2010, Manama, Bahrain, December 18-22, 2010

[18] Michael Wetter, GenOpt Generic Optimization Program User Manual version 3.0.0, Simulation Research Group Building Technologies Department Environmental Energy Technologies Division Lawrence Berkeley National Laboratory Berkeley, CA 94720, May 11, 2009

[19] Hooke, R., Jeeves, T.: Direct search solutions of numerical and statistical problems. Journal of the Association for Computing Machinery 8 (1961), 212–229